The influence of granulation methods and particle size on pharmaceutical granules flowability using ring shear tester and particle image velocimetry

Saleh Saeed Al-Zahrani

Submitted in the accordance with the requirements of the degree of

Master of Science (Eng) by Research

The University of Leeds

School of Chemical and Process Engineering

September 2014

The candidate confirms that the work submitted is his own and that appropriate credit has been given where reference has been made to the work of others.

Executive abstract

Good powder flowability is required in many industrial applications, particularly drug manufacturing. Pharmaceutical production processes strongly rely on powder flowability because the flowability of the powder ingredients a affects the quality and integrity of the final product (Prescott and Barnum, 2000). Many characteristics of particles and their surrounding environment are influenced by powder flowability (Antony**,** 2007), including: particle size, shape, particle size distribution, moisture content and chemical composition (Bodhmage, 2006). In spite of the extensive amount of research reported so far, powder flow behaviour still remains difficult to predict accurately (Ganesan et al., 2008). To enhance the flowability of powder industries use the granulation method to improve the flow behaviour of powder.

The main aim of this project is to study the flowability improvement of the granules prepared by wet and melt granulation in pharmaceutical industries, in addition to the flowability enhancement using different binding ratios, particle size ranges and storage geometries.

In this research, two granulation methods were applied (i.e. melt and wet) to examine the improvements of physiomechanical properties of the granules. Different variables were considered for the prepared granules: granulation method, binding ratios (5%-15%-25% w/w), particle size ranges (very fine 45-106μm, moderately coarse 250-355μm and coarse 600-710μm), and different hopper geometries. Granular flowability was measured qualitatively using different conventional methods such as, angle of repose, bulk and tapped density, Carr's index and Hausner Ratio. Schulze (2002) developed a fully automated ring shear cell RST-XS to measure the powder flow quantitatively using different loads which is used in this study. The output results were used to measure granules flowability, cohesivity and wall friction. These parameters are important for designing the silo and hopper geometries with proper internal hopper angles and outlet dimensions to produce uniform flow of powders. Silo design is performed for achieving better flowability for two geometries (i.e. conical and wedge-shaped hopper) which were designed using the data obtained from the ring shear test results. A new non-invasive and advanced flow dynamic method called digital particle image velocimetry (DPIV)

was used to understand the velocity distribution of the granular flow inside a typical case of silo with internal angles of 45° and 70°. The starch granules prepared by wet granulation showed better flowability than that prepared using melt granulation. This trend is in agreement with the outcomes of applying shear cell test stated earlier. Additionally, particle size has a significant influence on the flowability of granules, relatively stronger than the binding ratios. Also, PEG granules prepared using melt granulation required a relatively small internal hopper angle compared to starch granules prepared using wet granulation. In addition, starch granules moderately coarse and coarse were able to produce a symmetric flow trend within the flow champers when compared with the PEG granules.

New insights are provided on the flow behaviour of granules in terms of different granulation methods, single-particle characteristics and geometrical conditions. The integrated approach adopted here viz., designing the flow geometries based on using classical shear cells and DPIV provides a holistic and better pathway for designing powder flow geometries.

Acknowledgements

I am thankful to almighty Allah, most Gracious, who in his infinite mercy has guided me to complete this MSc project. May the peace and blessing of Allah be upon his prophet Mohammed, and peace be upon him.

I am grateful to my father Saeed Al-Zahrani for his continuous prayers and support. I would like to thank my wife and children for their patience, understanding and support during the last twelve months.

I am thankful to my supervisor Dr. Joseph Antony who gave me the opportunity to work under his supervision; also, I would like to express my gratitude and appreciation for his guidance during the research project.

My special thanks to Mr. Saeed Al-Baraki for his support and help during the lab works and Digital Particle Image Velocimetry analysis. And I wish him all the best of luck to obtain his PhD degree.

I am thankful to our research group especially Dr. George Okeake for his time, advice and support.

Finally, I would like to thank Dr. Umair Zafar for his training and induction in the use of lab machines, especially the ring shear cell tester. I would also like to thank Mr. Jabbar Gardy for his support in DSC and SEM analysis.

Table of Contents

List of Figures

List of Tables

Nomenclatures

(σ_c)	[Pa]	Unconfined yield strength and known as (f_c)
(σ_1)	[Pa]	Major Principal stress (consolidation stress)
(σ_1')	[Pa]	Major stress in an arch
(φ_x)	[°]	Kinematic angle of wall friction
(φ_e)	[°]	Effective angle of internal friction
(ff)		Flow factor (depending on flow properties and hopper geometry)
(b_{crit})	[m]	Critical outlet width for rectangular outlet
(d_{crit})	[m]	Critical outlet diameter for conical to avoid arching
(Θ)	[°]	Inclination of a hopper wall to the vertical
(Θ_c)	[°]	Inclination of the conical hopper wall to the vertical
(Θ_p)	[°]	Inclination of the wall of the wedge-shaped hopper wall to the vertical
(H)		Hausner Ratio
(g)	[m/s^2]	Acceleration due to gravity ($9.81 m/s^2$)
(ρ_b)	[kg/m^3]	Bulk density
(τ_w)	[Pa]	Wall shear stress
(σ_w)	[Pa]	Wall normal stress
(ff_c)		Flowability calculated from the ratio of consolidation stress to the compressive strength.
(PEG 6000)		Polyethylene glycol 6000
(PIV)		Particle image velocimetry
(DPIV)		Digital particle image velocimetry
(V_b)	[kg/m^3]	Bulk density
(V_t)	[kg/m^3]	Tapped density
(I)		Carr's Index
(μ)		Wall friction coefficient
(τ_{sh})	[Pa]	Maximum shear stress at shear to failure
(τ)	[Pa]	Shear force
(τ_{if})	[Pa]	Shear stress at incipient flow

(σ_{sh})	[Pa]	Normal stress at shear to failure
(σ_{pre})	[Pa]	Normal stress at the end of pre-shear
(τ_{pre})	[Pa]	Shear stress at the end of pre-shear

Chapter 1 Introduction

1.1 Introduction to research project

Powders are available in many industrial fields and are considered the primary component in the production of a wide range of commercial products. These fields include manufacturing of pharmaceutical products, detergents, foods and various engineering industries.

Powder flowability is one of the most important factors in many manufacturing processes. Poor flowability behaviour leads to an increase in the cost of production and seriously alters the quality of the final product. In general, it is a complex phenomenon in which physical, chemical, mechanical and particle properties, influence the behaviour of bulk powder flow (Freeman, 2000). It may be difficult to identify which factor has more influence than the other; however, they all play individual roles.

Some researchers have indicated that there is no clear, substantial link between powder properties and their bulk flow trend, which gives an insight into the complex behaviour of the bulk powders (Fitzpatrick et al., 2004). Moreover, Prescott and Barnum (2000), have reported that the pharmaceutical industry is still heavily reliant on powder flow properties, even though these properties are not well understood.

One of the most important indicators of powder flowability is particle size. Small particles show a cohesive property due to the presence of inter particle forces (van der Waals' force) which lead to a significant decrease in powder flowability (Winterton, 1970). It has been reported that if the particle diameters are less than 10 microns, the strong van der Waals cohesive forces might be equal to the gravitational force magnitude (Fitzpatrick et al., 2004). On the other hand, the influence of the inter-particle forces in larger particles is smaller than gravity and inertia, therefore they are normally classified as freely flowing (Li et al., 2004) .

To overcome the influence of the small particle size on bulk flowability and cohesivity, granulation is simply defined as a size enlargement technique applied

industrially to improve the cohesive powder flow. Multiple granulation techniques are commonly applied for multiple industrial purposes, depending on the raw material properties and the aim of the granulation. Further details about these techniques will be discussed in detail in Chapter 2. In this research project and among various granulation techniques available, wet and melt granulation methods have been selected as they are commonly applied in pharmaceutical industries due to their multiple advantages. Both techniques were able to modify the starting cohesive raw material to obtain a wider granular material range (45 - 710µm) using different binding materials in ratios of (5%, 15% and 25%).

Proper equipment geometry has a strong influence on powder flow behaviour during storage, handling, feeding and transferring. The most common flow problems that occur in inappropriate geometry design are arching, flooding, and ratholing. Powder discharge from silos and hoppers are mainly classified as funnel or mass flow trend (Schulze, 2008). To achieve the required flow trend (i.e., funnel or mass flow) from any silo or hopper, many parameters need to be determined to meet the requirements of proper dimensions and design. These parameters include bulk density, angle of internal friction, flowability factors and angle of wall friction (Schulze, 2006).

In the late 1960s a pioneer engineer, Jenike, developed and introduced a quantitative method and tool to design a silo and hopper by utilizing the aforementioned parameters in the mathematical calculation and design procedure (Jenike, 1967). This developed, mathematical method was easily applied to determine the proper minimum silo angle and the required outlet dimensions for mass or funnel flow both for conical and wedge-shaped hoppers. The tool is known as the Jenike shear tester which is a translational tester with a cylindrical cell. It consists of two closed rings, having the same diameter, lying above each other (Qiu et al., 2009). The Jenike cell tester can be operated manually, and the main advantage of this type of shear cell tester is the enhanced shearing uniformity of its powder bed. On the other hand, the main disadvantages are the increased time and large powder requirement for the test.

Based on Jenike's invention, Schulze developed the most recent ring shear tester in 1992. The Schulze ring shear tester is available as an annular or rotational shear tester. Two types of ring shear tester are available: RST-01.Pc and RST-XS; the main difference between these is the cell capacity which ranges between 85 - 900

ml, and 30 - 70ml, respectively. Depending on the particle size distribution, very small powder specimens (up to 10 ml) can be used for RST-XS, allowing powder saving. The main advantages of the ring shear tester are the following: it is an internationally recognised device with automated results; it is easy to operate with minimal training and skills; it is time saving as the time required to test materials and conduct analysis is short; and it can be used as a multipurpose tester in which a variety of materials can be tested by applying a wide range of stresses. Ring shear testers are the most widely accepted industry standards for the measuring and assessing of powder flowability and bulk characteristics (Fitzpatrick et al., 2004).

Non-invasive visual techniques, such as digital particle image velocimetry (DPIV), are considered to be a new technique able to show the granular material's flow trend in multiple geometrical storage bins. Most of the recent DPIV applications have been adapted for agricultural industries as both silo discharge and geometry design are crucial (Willert et al., 2007). DPIV can display and analyse granular flow trend via the clear illustration of spatial and temporal locations of particle velocity vectors (Sielamowicz et al., 2006).

The length of the velocity vector within the map is an indicator of the particle velocity magnitude at a particular position. In this research project, two silo angles are selected to evaluate granular flow trend in a 2D set-up.

1.2 **Motivation for Research**

Granulation techniques are covered in most literatures in terms of efficacy and efficiency by using many chemical or active pharmaceutical ingredients (APIs). There are several studies that investigate powder and granular flowability for different mixtures. However, few of them compare the two most common granulation techniques (i.e. wet and melt) using different variables. In this research, the wet and melt granulation methods were applied to investigate the influence of multiple variables, such as particle size distribution, binding ratio and the storage bin geometries on granular flow behaviour. The physiomechanical properties of the prepared granules, including static angle of repose, bulk and tapped density, Hausner Ratio and Carr's index, were used to evaluate the prepared granules. The influence

of granulation methods on flowability was conducted using the ring shear tester to predict the proper silo design and outlet dimension, and silo internal angle.

1.3 **Research objectives**

The aim of this work is an assessment of pharmaceutical excipients' granules flowability as a function of the granulation method, binding ratio and particle size. The following objectives are identified for the current research project:

1- Evaluation of wet and melt granulation methods on flowability of different pharmaceutical excipients' granules.
2- Evaluation of flow properties for selected ranges of granules using ring shear tester RST-XS having a 30 ml stainless steel cell.
3- Calculation of internal hopper angle and outlet dimensions for both conical and wedge-shaped hoppers for mass flow trend.
4- Application of DPIV in 2D to visualize the dynamic flow trend inside the silo and hopper through analysing the mean resultant velocity vectors map.

1.4 **Structure of Thesis**

This thesis consists of five chapters. **Chapter 1** gives a general introduction to the research project. **Chapter 2** is the literature review which covers the advantages of granules over powder, also the most common granulation methods are discussed from many aspects. In addition, the flowability measurement using different methods is covered. Furthermore, designing of silo and hopper using the ring shear cell tester is explained. The last part of this chapter is about DPIV and its recent applications in granular flow. In **Chapter 3** the used materials are mentioned in more detail and followed by the methodologies used. Granulation methods used for granules preparation are also explained in detail. Different methods are used to evaluate granules flowability. The qualitative methods include: static angle of repose, Compressibility Index, Hausner Ratio, and tapped and bulk density, the quantitative method uses the ring shear cell tester. The DPIV experimental set-up and procedure are shown. **Chapter 4** provides the results obtained from the methods used in Chapter 3. The results obtained for both granulation techniques using the mechanical properties, scanning electron microscope (SEM) and differential

scanning calorimetry (DSC) for the prepared granules, are discussed. The ring shear results (i.e. yield locus and wall yield locus) are analysed to measure flowability, cohesivity and to design the proper internal hopper angle and outlet dimension. **Chapter 5** reports the qualitative flow trend analysis of selected granules inside multiple silos geometries using digital particle image velocimetry. The last chapter is **Chapter 6** which concludes the research project and suggests future plans.

Chapter 2 Literature review

2.1 Introduction

The solid dosage form is regarded nowadays as being the most practical method of medication provision for patients (Andrews, 2007). Tablets and capsules, for example, are considered to be easy to handle and stable, both chemically and physically (Aulton and Wells, 2002). Such oral medications combine pharmaceutical excipients and APIs and, to meet high manufacturing standards, must be mixed and/or granulated correctly. Solid dosage now accounts for almost 80% of pharmaceutical products (Bodhmage, 2006). Solid dosage forms are also prepared from powder (Emery, 2008).

2.2 Powder

Powder can be defined as a mixture of fine drugs and/or chemicals in dry form that can be administered internally or externally (Kunii and Chisaki, 2007). Dry powders can be taken orally by patients who are unable to swallow other solid dosage forms, such as capsules and tablets. Powders can also be used by such individuals as asthmatic patients when a quick response to a medical condition is deemed important (Edwards, 2010). Powdered drugs can be combined with other materials, such as excipients and APIs to produce solid dosage forms such as tablets, ointments, creams, pastes and suppositories, among others (Kimura, 2012).

2.2.1 Powder Characteristics

There are two types of property that characterise powders (Mittal, 1999):

1. Primary properties: A particle is considered to be the smallest component of a powder that cannot be subdivided. Particle size, shape, surface area, chemical composition, density, and porosity determine the primary properties of the powder system (Bodhmage, 2006).

2. Secondary properties: Particle distribution, cohesion, angle of internal friction, bulk porosity, bulk density, moisture content, and specific surface area of bulk are key secondary properties (Bodhmage, 2006, Parikh, 2009, Pandeya, 2009).

Powder properties relevant to pharmaceutical formulations (Pandeya, 2009) are single particle and bulk properties, particle to particle interactions, powder morphology (particle size, specific surface area, porosity, and particle shape) as well as mixing and blending properties.

Particle size is an important physical characteristic of the raw material used in pharmaceutical granulation and also other engineering industries (Chan and Heng, 2005). Particle size has a significant influence on drug dissolution and drug bioavailability, flowability, packing, and compaction behaviour of the bulk powder in granule production (Patel et al., 2007).

Particle shape is another significant factor of the bulk properties of powders (Tang and Puri, 2007). More spherical particles will have better flowability, better packing and a lower surface area to volume ratio compared to non-spherical particles (Chan and Heng, 2005, Parikh, 2009). Recently, marked attention has been given to the particle surface area as it has an obvious impact on drug-carrier interaction, especially for dry inhalant powders (Tang and Puri, 2007, Parikh, 2009). All the above factors, i.e. particle size, particle shape and surface area, significantly influence the granulation process and properties of granules (Chan and Heng, 2005, Parikh, 2009).

The particle size of powders is standardised according to United States Pharmacopeia (USP) descriptive terms, such as, very fine, fine, moderately coarse, coarse, and very coarse (Usp, 2012) as shown in Table 2.1.

Table 2.1 Powder classification according to USP.

Categories	Maximum Diameter
Very Fine	≤ 125 μm (≤ 0.125 mm)
Fine	≤ 180 μm (≤ 0.180 mm)
Moderately coarse	≤ 425 μm (≤ 0.425 mm)
Coarse	≤ 850 μm (≤ 0.850 mm)

Particle size analysis can be determined using different techniques: sieving; gravitational sedimentation; microscopy-based; optical and electrical sensing zone; and laser light diffraction (Jillavenkatesa et al., 2001, Li et al., 2005).

Sieve analysis involves the use of a stack of graded sieves with each lower sieve having a smaller opening size than the one above.

Sieves can be referred to either by their size of opening size or by their mesh size (or sieve number).The mesh size equates to the number of wires per linear inch.

There are two common standards: Tyler standard and US standard (ASTM E11-70) as shown in Table 2.2. The two standards differ slightly but can be used interchangeably (Allen, 1990, Jillavenkatesa et al., 2001).

Table 2.2 Opening of standard sieves (Jillavenkatesa et al., 2001).

ASTM Sieve No. (mesh/inch)	Sieve opening	ASTM Sieve No. (mesh/inch)	Sieve opening
400 (µm)	38	70	212 (µm)
325 (µm)	45	60	250 (µm)
270 (µm)	53	50	300 (µm)
230 (µm)	63	45	355 (µm)
200 (µm)	75	40	425 (µm)
170 (µm)	90	35	500 (µm)
140 (µm)	106	30	600 (µm)
120 (µm)	125	25	710 (µm)
100 (µm)	150	20	850 (µm)
80 (µm)	180	8	2,360 (mm)

2.2.2 Disadvantages of the powder dosage form

Powders are not commonly used in therapeutics. They have several disadvantages in dosage form (Remington et al., 2006, Kunii and Chisaki, 2007), as listed below:

1. Patients might misunderstand the correct method of administration; for example, some patients might inhale powder intended for oral administration;

2. Most powders have a bitter or unpleasant taste and the old adage “bitter medicine is better medicine” does not always hold true (Skinner, 1862);

3. Powders are susceptible to decomposition due to various factors, including temperature and humidity;

4. Powders might come in sachets – a packaging method that can add to industrial costs and lead to inaccurate dosage amounts being delivered;

5. The therapeutic effect of a drug might be influenced by particle size, especially in dissolution; however, particle size must be a homogeneous blend of all components.

For the above reasons, powders are not commonly used as a dosage model, the preference being to modify the product into more stable, granule form.

2.3 **Granules**

The simplest definition of granular materials is the assembly of solid particles that have contact with each other but are surrounded by air voids (Duran, 2000). The mechanical behaviour of such an assembly is very complex at both macro and micro levels (Jaeger et al., 1996, Antony, 2007). The main reason for this complex behaviour is the ability of such materials to build up a network-like structure known as a force transmission chain (Radjai et al., 1999, Antony, 2000, Antony, 2007).

The term "granulated" is derived from the Latin word "granulatum," (Ennis, 2005, Parikh, 2009) meaning grained. For many centuries the practice of preparing medicinal powder was performed by hand rolling into a pill, using a sweetener such as honey or sugar to mask the unpleasant taste, especially in herbal and alternative medicines. Such methods are still practised in some countries. Thomas Skinner described an earlier mention of granulating medicine, cited in 1773 in Duncan's *Elements of Therapeutics*, as follows: "by the application of art, it is intended that medicines should be made more pleasant, more convenient, safer and more efficacious than they are in their natural state. To obtain these ends is the intention of pharmacy" (Skinner, 1862).

The early practice of preparing granules was carried out by French pharmacists who produced a form of medication they called "poudres granulés" (Parikh, 2009). The granules were usually prepared by mixing particles of medicine in syrup, enveloping them by heating and constant stirring. This method was later modified to produce granules using less heat and moisture.

The granulation process has been defined as "any process whereby small particles are gathered into larger, permanent masses in which the original particles can still be identified." (Ennis and Litster, 1997).

In other words, granulation is a size enlargement operation in which a fine powder is agglomerated into larger granules to provide a specific size and shape, improving flowability and appearance and, in general, producing a powder with specific properties such as dissolution rates, granule strength and apparent bulk density (Ennis, 2005). Granulation is practised in various industries, including the preparation of detergents, foods, agricultural chemicals and pharmaceutical products (Tardos et al., 1997).

Granulation technology has been extensively used in a wide range of industries, such as chemical, coal mining, metallurgy, ceramic, and agrochemical (Parikh, 2009). These industries employ agglomeration techniques to reduce dust, provide ease of handling, and enhance the material's ultimate utility (Hassanpour et al., 2009).

In 1843, William Brockedon invented the tablet press machine, leading to the development of pharmaceutical granulation (Ennis, 2005). Consecutive progresses in tablet-making machines were patented in the United States by J. A. McFerran (1874), T. J. Young (1874), and J. Dunton (1876) (Parikh, 2009). Granulation properties were further enhanced in the 1970s with the advent of automated high-speed tablet- and capsule-filling machines.

2.3.1 Advantages of Granules

Granules have many advantages over powders (Kunii and Chisaki, 2007, Pandeya, 2009, Agrawal and Naveen, 2011, Saikh, 2013) as follows:

1. Granules have better flowability than powders, especially in hoppers or silos and help to reduce dust.

2. Granules enhance compressibility, especially for the tableting process.

3. Granules are more stable physically and chemically because they have less surface area. Moreover, caking is less likely, compared to powder.

4. Granules are preferred for formulating pharmaceutical solutions. Solvents easily wet the granules and help to reconstitute them prior to use, whereas some powders are unstable in aqueous solution. In addition, granules also contain pharmaceutical

excipients, so the resulting solution or suspension has all the desired medical and pharmaceutical characteristics of the pharmaceutical product.

5. Granules enable particle-size uniformity and therefore content uniformity.

Granules are most widely used in the production of pharmaceutical oral dosage forms. New improvements in granulation technology have revolutionised this sphere and resulted in the development of several processes. Each individual process has many advantages, disadvantages and/or limitations. Extensive knowledge and background about granulation technology is essential and is required to formulate and achieve the desired product parameters.

2.3.2 Classification of Granulation Technologies

Based on the type of processing involved (Kristensen and Schaefer, 1987, Ennis, 2005, Agrawal and Naveen, 2011, Saikh, 2013) granulation technology can be classified as follows:

i. Conventional methods

Dry and wet granulations are the most common techniques in the industry.

1- Dry granulation is commonly used for very cohesive particles with very small particle size. The fine particles agglomerate and form granules without a binder by applying pressure on them.

2- Wet granulation:

Wet granulation is defined as a size enlargement process using liquid binder enabling powder particles to stick together to produce granules. It can be sub-classified into two types according to the mixer used for granulation;

A. High shear wet granulation:

Wet granulation techniques using high shear granulators or mixer include continuous pin and plow shear type mixers which have blades rotating at high speed, also batch high shear pharmaceutical mixers (Gokhale and Trivedi, 2010).

B. Low-shear wet granulation:

Wet granulation techniques using a low shear granulator or mixer produce less shear than high shear granulators, because of either sweep volume, agitator speed, or bed pressures on the powder bed (Gokhale and Trivedi, 2010).

ii. Novel/advanced methods:

1- Moisture activated dry granulation:

A process of adding granulating fluid to dry powder particles without a drying step. This method is a very efficient, cost effective and less time-consuming process (Christensen et al., 1994).

2- Thermal adhesion granulation:

The thermal adhesion method is a process to produce granules by using a minimal solvent to moisturize the mixture, followed by exposing the mixture in sealed container to temperatures based on the type of solvent. The moist powder is mixed under continuous flip for 3-20 minutes until the granules are formed, then instantly sifted through a suitable sieve (Lin et al., 2008).

3- Pneumatic dry granulation:

The novel dry granulation method has a similar technique to roller compaction which is characterised by using a very low compaction force to compact materials, followed by milling process. Milled and fractionated granules are separated using a fractionater device. The main advantage of this method is to produce porous granules with good flowability and compressibility properties (Sandler and Lammens, 2011).

4- Melt or thermoplastic granulation:

A granulation method to produce granules by adding either a solid binder, which has a relatively low melting point, or a molten binder during the granulation process (Parikh, 2009).

5- Fluidized bed granulation:

The fluidized bed method is known as a one step process, because all ingredients are mixed, granulated and dried in the same container. It is time-consuming but decreases the material handling (Srivastava and Mishra, 2010).

6- Extrusion-Spheronization granulation:

A multiple step process which includes the extrusion of wet mass and spheronization of produced filaments in order to produce free flowing spherical granules. The main advantage of this method is to combine high levels of active ingredients to form pellets or granules in small scales (Breitenbach, 2002, Trivedi et al., 2007).

7- Spray drying granulation:

Spray drying is a process of making granules in a fluidized powder bed by spraying binder solution within the passage of air followed by a drying process using hot air (Heinrich and Mörl, 1999, Saikh, 2013).

8- Freeze granulation:

A granulation method to obtain homogeneous granules by spraying homogeneous powder mixtures concurrently with liquid nitrogen; the obtained granules are instantly frozen (Wisniewski, 1999).

9- Foam binder granulation:

A granulation method to produce consistent foam by incorporating air into conventional, water soluble, polymeric binder excipients (Sheskey et al., 2007).

10- Steam granulation:

A modified wet granulation, where the steam is used as a binding agent instead of water. The steam produces overheating and excessive wetting of the particles to form granules (Hampel et al., 2006, Srivastava and Mishra, 2010, Saikh, 2013).

11- Seeded granulation:

This technique is a novel granulation method and has a strong potential to be used in the food and pharmaceutical industries and in multiple engineering applications. This method is modified to produce large particles surrounded by fine particles having good content uniformity. This occurs by wetting the fine particles then the large particles adhere to each other forming a core-like structure at the granules' centre. Multiple factors influence seeded granulation, including particle size distribution, speed of impeller tip, binder viscosity and the ratio of binder to powder mass (Rahmanian and Ghadiri, 2011, Rahmanian et al., 2011, Rahmanian et al., 2013, Hassanpour et al., 2013, Rahmanian and Ghadiri, 2013).

2.4 Wet granulation

2.4.1 Principle of wet granulation

Wet granulation is considered to be a subdivision of size enlargement which involves any process whereby small particles are agglomerated, compacted, or brought together into larger, semi-permanent structures but the original particles can still be recognised (Liu et al., 2000, Litster, 2003). In the wet granulation process, liquid, with or without binder, needs to be added to the powder mix and distributed and then the powder agglomerated to form a wet bulk before subsequent drying and sizing yields (Saikh, 2013).

The main purpose of the wet granulation technique in pharmaceutical production is to obtain granules with the desired physiomechanical properties (Faure et al., 2001). Granules must be free-flowable with no segregating, and mixtures of ingredients of controlled strength, which may be reproducibly metered in subsequent tableting or for vial or capsule filling processes (Ennis, 2005, Parikh, 2009). In addition, granulation improves the particle size and shape which enhance the particles' flow with increased void fraction without segregation (Shimoska et al., 2013).

2.4.2 Advantages

The main advantages of the wet granulation technique are listed below (Parikh, 2009, Srivastava and Mishra, 2010, Agrawal and Naveen, 2011):

- Improved flowability and compressibility and increased density of granular materials (Miyamoto et al., 1998);
- Increased bioavailability as the hydrophobic surface of the active ingredients becomes more hydrophilic by adding a hydrophilic binder. This method enhances the wettability of sparingly soluble or non-soluble compound;
- The uniformity of dosage forms;
- Quick method for preparing control released granules (Albertini et al., 2008);
- Minimisation of the risk of dust.

2.4.3 Disadvantages

Wet granulation also has some disadvantages (Parikh, 2009, Agrawal and Naveen, 2011, Saikh, 2013):

- Wet granulation is a quite expensive process requiring particular equipment, energy, space, time and labour;
- It is a complex technique involving several steps in the process;
- It is inappropriate for moisture sensitive and thermolabile materials;
- The formulation components must be compatible to avoid aggravation during the process;
- Material loss during numerous stages of processing.

2.4.4 Wet agglomeration behaviour

According to Iveson et al. (2001) there are three main stages of the process, as shown in Figure 2.1, which determine the wet agglomeration behaviour:

- Wetting and nucleation: wetting is the first stage of the process involving spraying the granulation liquid into a dry powder bed to form granule nuclei.

- Consolidation and growth: where collisions are occurring between two granules, granules and feed powder, or a granule and the equipment, leading to the liquid being forced towards the surface, allowing granules to grow then coalesce.
- Attrition and breakage: the granules will break if not strong enough to withstand the agitation or compaction in the granulator during process.

These three stages are occurring all together and will determine the final properties of the produced granules (Lee, 2013).

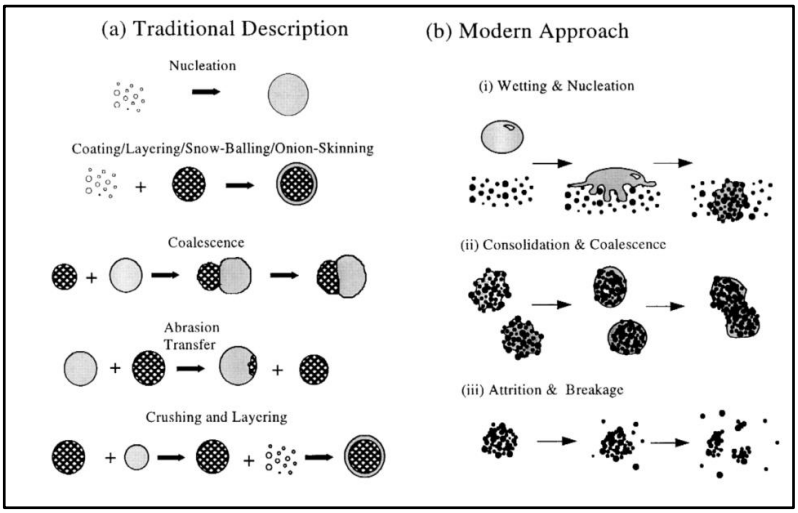

Figure 2.1 Schematic of granulation processes (a) Traditional view (b) Modern approach (Iveson et al., 2001).

Wetting of the particles is necessary for nucleation, i.e. the formation of initial agglomerates. As per (Iveson et al., 2001), the nucleation rate is governed by the following:

2.4.4.1 Wetting and nucleation

This is the process of bringing a liquid binder into contact with dry powder and endeavouring to distribute this liquid consistently throughout the dry powder (Litster et al., 2004). The binder dispersion process will focus on the nucleation zone where the liquid powder and powder surface make contact to form the initial nuclei (Iveson et al., 2001). In this zone, two processes are important: firstly, nuclei formation which is the function of wetting thermodynamics and kinetics; secondly, binder dispersion or effective mixing between powder and binder (Pandeya, 2009).

2.4.4.2 Granular growth

Granular growth takes place when materials of granular collision stick together, this process being called coalescence (Iveson et al., 2001, Litster et al., 2004). If fine materials are sticking to large granules this is frequently called layering (Ennis, 2005, Pandeya, 2009).

It starts when liquid is added to the agitated bulk powder, acting concurrently with the wetting and nucleation process, as shown in Figure 2.2. The size of the granules is determined by the nucleation condition (Ennis, 2005).

Permanent collision between two granules depends on the granular mechanical properties and availability of the liquid binder at or near the granule surface (Litster et al., 2004, Parikh, 2009).

During agitation, granules increasingly consolidate which increases the saturation of liquid pores and changes their mechanical properties (Ennis, 2005). Therefore, consolidation often has an impact on granule growth behaviour and must be considered in conjunction with it (Iveson et al., 2001).

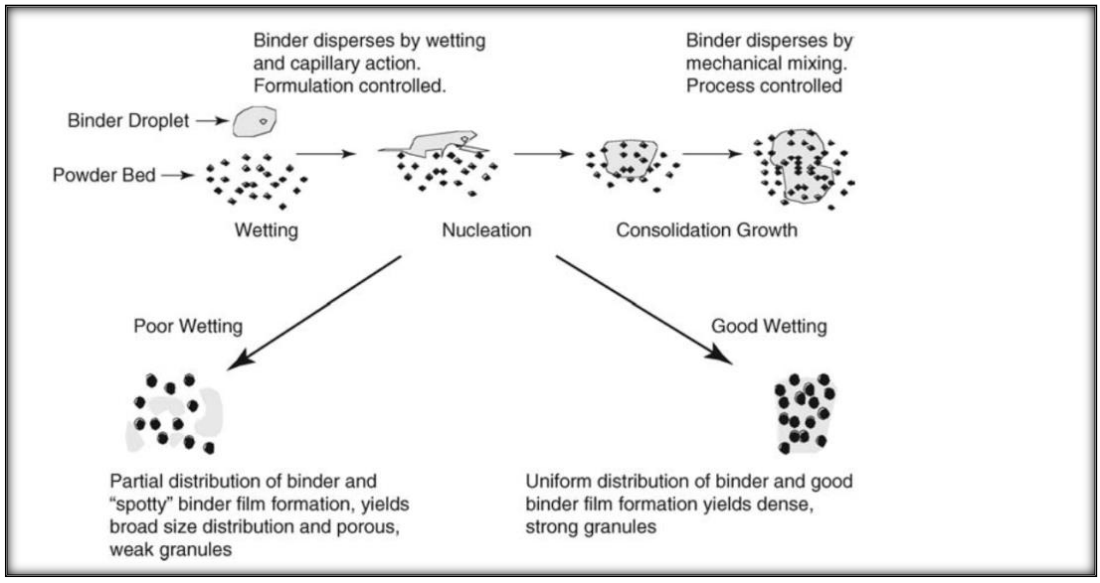

Figure 2.2 Schematic showing wetting, nucleation, consolidation, and granule growth processes (Parikh, 2009)

Granules can exist in different states of liquid saturation. These states were first described by Newitt and Conway-Jones (1958), and are shown in Figure 2.3:

- Pendular state: particles are held together with binding liquid, which forms a liquid bridge between the particles' contact points (Pendular bond).

- Funicular state: with an increasing quantity of liquid, the liquid bridges coalesce. Nevertheless, empty spaces are still not saturated and filled by air.

- Capillary state: occurs when a granule is saturated and all the spaces between the particles are filled with liquid and the surface liquid is drawn back into the pores under capillary action.

- Droplet state: the particles are suspended inside or at the surface of a liquid drop.

- Pseudo-droplet state: where empty spaces remain surrounded inside the droplet. This occurs in poor wetting systems.

Liquid-bound granule strength is governed by two types of force: liquid bridge and inter-particle friction. The liquid bridges can create both static surface tension forces and dynamic forces due to the liquid viscosity (Iveson et al., 2001).

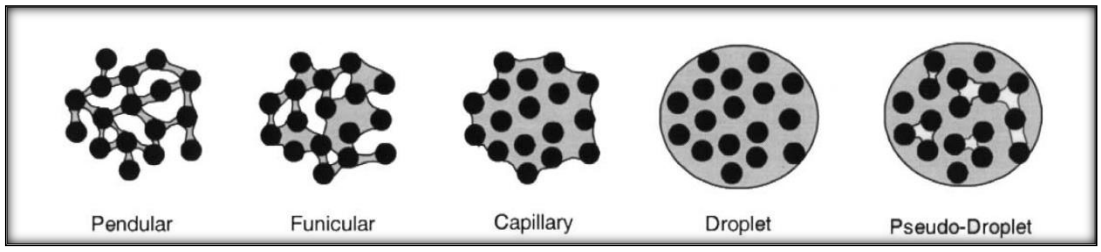

Figure 2.3 The different states of saturation liquid-bound granules (Iveson et al., 2001)

2.4.4.3 Breakage and attrition

There are two phenomena that describe the breakage and attrition of granules (Iveson et al., 2001) to be considered: firstly, breakage of the wet granules inside the

granulator during the process; secondly, attrition or breakage of dried granules inside the granulator, drier or through handling.

Breakage has a significant influence on the granule-size distribution and it may be used to limit the maximum granule size or to help distribute a viscous binder, otherwise attrition leads to the creation of dust which represents a hazard to employees (Saikh, 2013).

2.5 Melt granulation

Melt granulation or the thermoplastic granulation process is widely used in the pharmaceutical manufacturing process (Walker et al., 2006). It is similar to wet granulation but the molten binder acts as a granulation fluid to form the liquid bridge between particles in the heated powder bed followed by agglomeration and consolidation (Schæfer, 2001). Granules must be left to cool at room temperature. At the end of the process, solidified binder forms bridges between the particles to produce a solid product with a granular structure (Parikh, 2009). The active ingredients should have a high melting point compared to the molten binder (Saikh, 2013).

2.5.1 Advantages

The melt granulation technique has several advantages over conventional wet granulation (Walker et al., 2006, Halle et al., 2013, Saikh, 2013):

- No solvent is involved in the process, thereby negating problems associated with in-process hydrolysis and water removal via heating;
- It is very efficient for moisture-sensitive materials, so granules can be formed without solvent;
- The process is time efficient and thereby less energy is required;
- All steps, including mixing, agglomeration and formation of solid bridges are completed in a single pot which reduces loss of materials that might otherwise occur in transferring operations;
- The process enhances the stability of hydrophilic substances which are highly degradable in the presence of moisture. The lipophilic binder coats the particles to be protected from water;

- The process improves the dissolution rate and bioavailability, especially for poor water soluble ingredients, by forming solid dispersion (Onoue et al., 2010).

2.5.2 Disadvantages

- Heat-sensitive materials are not suitable as thermal degradation might occur during the heating process (Schæfer, 2001).
- Only a meltable binder can be used for those with a relatively low range melting point of between 50ºC-70ºC (Saikh, 2013).

2.5.3 Mechanism of melt granulation

Melt granulation is similar to the wet granulation technique and the molten binder in solid or liquid form used as granulation liquid to form a liquid bridge between powder particles (Parikh, 2009). Granules can be obtained either by spraying on the liquid molten binder over the powder bed or by mixing solid molten with the powder bed and heating it over its melting point using a high shear mixer or heating jackets (Kidokoro et al., 2003). Granules are dried by a cooling step at room temperature and followed by the milling process (Saikh, 2013).

The melting granulation process involves three mechanisms (Breitenbach, 2002, Kidokoro et al., 2003, Heng and Wong, 2003):

- Wetting and nucleation;
- Coalescence;
- Attrition and breakage.

2.5.3.1 Wetting and nucleation

Through the nucleation step, the binder is introduced to the powder bed and some liquid bridges are formed, leading to the creation of small agglomerates (Parikh and Mogavero, 2005) .

Two nucleation mechanisms (Figure 2.4), have been explained by Schæfer (2001):

- Distribution
- Immersion

Distribution: In this phase, molten binding liquid is distributed onto the surface of fine solid particles leading to nuclei formation due to collision between the wetted particles, as shown in Figure 2.4(a). Generally, the optimum conditions for using the distribution method are when the size of the binder droplet is small and there is low binder viscosity and high shearing forces.

Immersion: Nucleation by the immersion process occurs when the droplet size of the molten binder is larger than the fine solid particles (Schæfer and Mathiesen, 1996) as shown in Figure 2.4(b). The process starts with deposition of fine solid particles onto the surfaces of molten binder droplets.

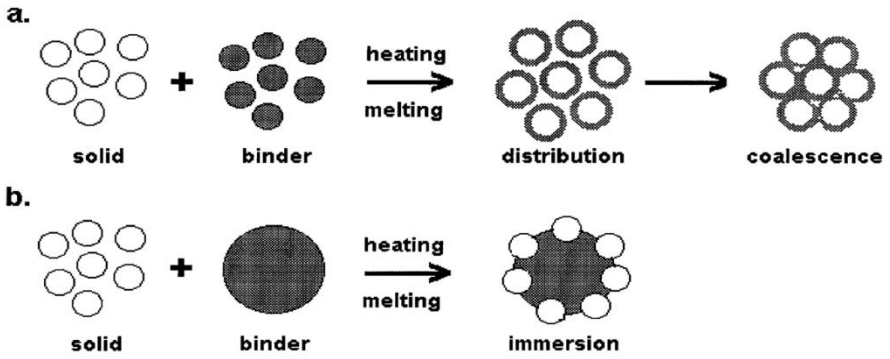

Figure 2.4 Agglomerate formation mechanisms in melt granulation (a) Distribution (b) Immersion. (Schæfer, 2001).

2.5.3.2 Coalescence

This step is to enhance the successful fusion of nuclei with the remaining surface liquid (Iveson, 2001). This will give a plastic texture to the nuclei and allow the deformation of the nuclei surface for coalescence as well as promoting the rounding of granulation (Halle et al., 2013).

2.5.3.3 Attrition and Breakage

Attrition and breakage refer to the phenomenon of granulation breakdown that is solidified by tray-cooling to room temperature (Tan et al., 2006). Consequently,

breakage has an essential role in affecting the resultant properties of the melt granulation during the granulation phase (Halle et al., 2013).

2.5.4 Factors affecting melt granulation

Several factors listed here and explained below, may affect melt granulation:

- Processing variables;
- Equipment variables;
- Formulation variables;
- Binder.

2.5.4.1 Processing variables

During the granulation process, increasing mixing time or speed leads to enhanced agglomerates growth by squeezing the molten binding liquid from the agglomerated core to the surfaces (Heng and Wong, 2007). This leads to an increase in the degree of liquid saturation of agglomerates and their tendency to grow by binary coalescence following the collision between two or more plastically deformable surfaces (Schaefer et al., 1992, Eliasen et al., 1998). The deformable surfaces can be rounded to form spherical pellets via intra-agglomerate rearrangement of particles by the continuous stirring of the impeller (Halle et al., 2013).

2.5.4.2 Equipment variables

The influence of the intensity of shearing forces is marked, especially in a high shear mixer (Schæfer et al., 1993, Rahmanian et al., 2008). It promotes a more even distribution of molten binding liquid allowing the size distribution of melt agglomerates to narrow (Halle et al., 2013). Shear is dependent on the geometry of the impeller blade, processing chamber design and their relative dimensions (Heng et al., 1999). Two factors may have an important effect on the flow pattern of the processing material: the construction of both the impeller blade and the processing chamber. Also the flow behaviour is related to mechanical force distribution, homogeneity of melt agglomeration and the size and shape of formed agglomerates (Halle et al., 2013).

2.5.4.3 Formulation variable

Multiple physical and mechanical variables have a great influence on the formulation process (Schaefer et al., 1992). Particle shape and density, particle size and size distribution are considered as the main variables (Schæfer and Mathiesen, 1996). The influence of each variable on the melt agglomerate process is complex and interdependent (Halle et al., 2013). The desirable particle size for a successful agglomeration process ranges between 20-25mm (Schaefer et al., 1992), as less binding saturation is required.

2.5.4.4 Binder

The molten binder viscosity, surface tension and specific volume significantly influence the increasing growth of melt agglomerates (Schæfer and Mathiesen, 1996). This influence is affected by product temperature, mixing speed and physicochemical properties of the fine solid particles (Halle et al., 2013).

According to what has been mentioned before, it is clear that melt granulation technology represents an efficient pathway for the manufacture of various drug delivery systems. This technique is beneficial in improving the dissolution characteristics of a poor water-soluble drug by improving the dissolution rate and bioavailability of the drug by forming a solid dispersion or solid solution. The melt granulation is an economic and less time-consuming technique (Halle et al., 2013).

2.6 Powder Flowability

The word ‘flow’ means a continuous, smooth movement. Powder flowability is defined as the ability of powder and granules to fall or flow under their own influence (or self-weight) (Jaeda, 2009). Powder flow behaviour is multidimensional and depends on various powder characteristics (Bodhmage, 2006). Multiple tests are required to predict powder and granules flowability and are never expressed as a single value or index. Slight changes in the measurement conditions and equipment’s position give different values of the parameters. In fact, flowability is not an inherent material property but a combination of the physical properties of the

particulate matter and the design of mechanical components that make up the handling and feeding system (Prescott and Barnum, 2000, Aole et al., 2012).

Flowability of bulk solids is influenced by single particle properties, particularly particle size, particle shape, particle size distribution, surface texture, and surface energy (Juliano and Barbosa-Cánovas, 2010). Moreover, operating conditions such as chemical composition, moisture content, friction, bulk charging and vessel geometry also have marked influences (Antony and Sultan, 2007, Emery et al., 2009). However, powder flow behaviour is hard to predict (Ganesan et al., 2008). Powder cohesivity depends on particle size; with small particle size of less than 100μm, the cohesive surface forces, i.e. electrostatic, capillary and van der Waals interaction, become more significant (Sandler and Wilson, 2010). Particle shape is another important factor because for non-spherical particles the cohesivity increases. Also, surface areas increase with small particle size and that enhances the cohesivity (Hou and Sun, 2008).

Why flowability is important?

Good powder flow behaviour is very important in many aspects of pharmaceutical industries, in particular during formulation development and production processes (Jaeda, 2009). It indicates what type of granulation and compression may be used. In addition, success or failure of product manufacturing, in terms of weight and content uniformity, relies on powder flowability (Prescott and Barnum, 2000). For instance, during the tableting process, a non-uniform flow of granules might alter the tablet weight and consequently affect the active pharmaceutical content. In high scale production requiring tableting at high press capacity, an improper granulation method sometimes leads to press shutdown. The flowability trend of granules and powders has a great influence on the integrity and quality of the finished product in multiple engineering industries in general and in the pharmaceutical industry in particular.

There are five common methods for testing powder flow (Usp, 2010) as summarised below:

- Angle of repose;
- Hausner Ratio;
- Flow rate through an orifice;
- Ball indentation;
- Shear cell.

All these methods have different procedures and techniques of measurement using multiple devices and instruments, and are able to provide an adequate and complete characterisation of flow properties and behaviour. At least two methods are used concurrently to evaluate the powder flow behaviour as no industry relies on a single test.

2.6.1 Angle of repose

Angle of repose is the angle α formed between the horizontal and the surface of the pile at a predetermined height h (Eq. 2.1) due to interparticulate resistance of movement between particles, as seen in Figure 2.5. Test results are dependent upon the method being employed. Prime difficulties during the experiment are the segregation of material and consolidation or aeration of the powder as the cone is formed. Regardless of its difficulties, the method is still used in the pharmaceutical industry (Usp, 2010).

The angle of repose provides a reliable, quick and simple method to measure the flowability of different powders. Freely flowing powders have lower angles of repose; however, higher angles indicate a poor flowing and cohesive material (Bodhmage, 2006).

The angle of repose can be determined by:

$$\tan(\alpha) = \frac{\text{height}}{0.5 \text{ base}} \tag{2.1}$$

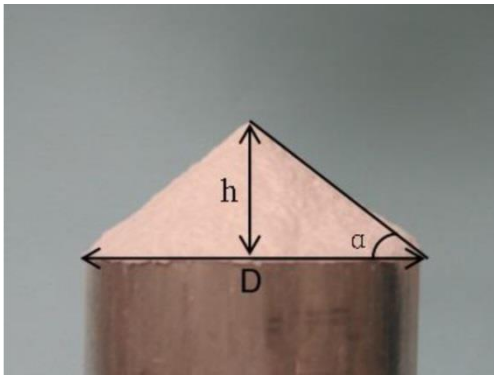

Figure 2.5 The definition of (poured) angle of repose (Armstrong, 2011).

Angle of repose can be further classified into (Emery, 2008, Jaeda, 2009, Usp, 2010, Armstrong, 2011, Lumay et al., 2012):

- Static angle of repose

  Two important variables can be used to determine the static angle of repose: Firstly, the height of the "funnel" through which the powder passes relatively to the base, or the height may be varied as the pile forms;

  Secondly, the base upon which the pile forms may be of a fixed diameter or the diameter of the powder cone may be allowed to vary as the pile forms.
- Drained angle of repose is measured by draining excess powder from a container over a fixed diameter base after which a pile formation drained angle of repose can be determined.
- Dynamic angle of repose is determined by filling a cylinder with a flat and clear cover and rotating it at a specified speed. Two angles will be determined. Firstly, the dynamic angle of repose is that which is formed by the flowing powder relative to the horizontal; secondly, the internal angle of kinetic friction is defined by the plane separating those particles sliding down the top layer of the powder and those particles that are rotating with the roughened surface of the drum.

Carr classified powders according to their flowability using the angle of repose (Riley et al., 1978). Table 2.3 summarises the powder flow ability qualitatively using angle of repose values. It is still used consistently in engineering industries.

If the range is between 40 and 50, that means the flow is still acceptable. When the angle of repose is more than 50, the flow is hardly acceptable for manufacturing.

Table 2.3 Flow properties and corresponding angles of repose (Usp, 2010).

Flow property	Angle of repose
Excellent	25 - 30
Good	31 - 35
Fair- aid not needed	36 - 40
Passable- may hang up	41 - 45
Poor- must agitate, vibrate	46 - 55
Very poor	56 - 65
Very, very poor	>66

2.6.2 Compressibility Index and Hausner Ratio

Both the Compressibility Index and Hausner Ratio are considered to be simple, fast, cheap, easy and popular methods for predicting the characteristics of powder flow. However, they have no strong theoretical basis (Abdullah and Geldart, 1999). The Compressibility Index has been proposed as an indirect measure of bulk density, size and shape, surface area, moisture content, and cohesiveness of materials because all of these can influence the observed Compressibility Index (Schulze, 2008, Usp, 2010).

The Compressibility Index and Hausner Ratio can be calculated using the following equation (Schulze, 2008);

$$\text{Compressibility Index (I)} = 100\ \left(\frac{V_b - V_t}{V_b}\right) \tag{2.2}$$

$$\text{Hausner Ratio} = \frac{V_b}{V_t} \tag{2.3}$$

Where:

I is Carr's index

V_b is the solid bulk density

V_t is the solid tapped density

Table 4 summarises the generally accepted values of both the Compressibility Index and the Hausner Ratio, both of which are unitless.

Table 2.4 Scale of flowability by Compressibility Index and Hausner Ratio (Abdullah and Geldart, 1999)

Compressibility Index	Flow character	Hausner Ratio
≥10	Excellent	1.00-1.11
11-15	Good	1.12-1.18
16-20	Fair	1.19-1.25
21-25	Passable	1.26-1.34
26-31	Poor	1.35-1.45
32-37	Very poor	1.46-1.59
>38	Very, very poor	>1.60

The Compressibility Index and Hausner Ratio are not intrinsic properties of the powder but depend on the methodology employed. In fact, there are four important considerations affecting the determination of (V_b) and (V_t) (Usp, 2010):

- The cylinder's diameter;
- The number of times that the powder is tapped to achieve the tapped density;
- The material's mass used in the test;
- Rotation of the sample during tapping.

2.6.3 Flow through an orifice method

This method for determining the flow rate can be classified based on three experimental variables (Usp, 2010):

- The container type used to contain the powder. Commonly used containers are cylinders, funnels, and hoppers;
- The orifice diameter and shape are critical factors in determining the powder flow rate. Moreover, the orifice diameter should be six times larger than the diameter of the particles;

- The method of measuring the powder flow rate can be either a continuous measurement by using an electronic balance with recording device (strip chart recorder, computer) or it can be measured in discrete samples, such as measuring the time it takes a certain amount of powder to pass through the orifice to the nearest tenth of a second.

Since the flow rate is strongly dependent on the measuring method, there is no general scale.

It is more appropriate to use a hopper as the container because it better represents flow in an industrial state. In addition, the flow will be influenced by the powder wall friction coefficient, which differs from one material to another (Schulze, 2008).

At the cylinder opening, a flat-faced bottom plate can be used to offer more flexible powder-flow measurements by allowing varied orifice diameters. The more effective way to measure the flow rate is by using a continuous measurement with an electronic balance, rather than discrete measurements (Usp, 2010).

2.6.4 Ball indentation method

A new and novel method used to assess the cohesive powder flowability is by using a small amount of the material powder (Wang et al., 2008). This method is very efficient, especially when the amount of material powder need for testing is very small, such as in the evaluation of pharmaceutical active ingredients – in particular, radioactive materials and crude drugs, as the risk of radiation and the cost are very high respectively (Das et al., 2010, Pasha et al., 2013). In addition, the small scale of loosely compacted powders and their bulk behaviour is hardly likely to be assessed using high compression levels.

Ball indentation procedure:

Powder is consolidated in a cylindrical die, and then indented by spherical indenter with no sharp edge. The cycle of depth and load must be recorded.

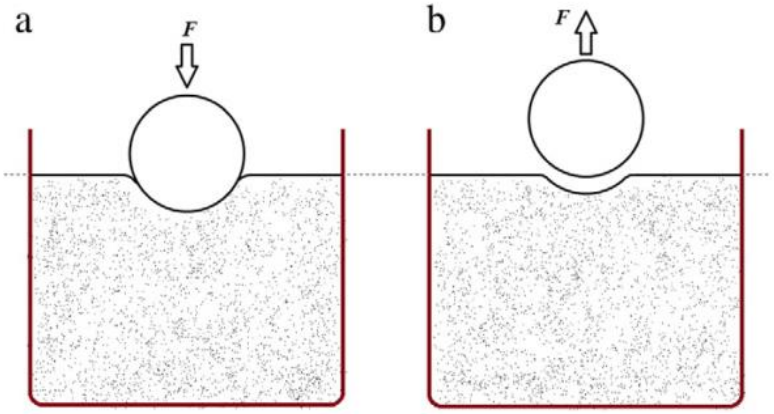

Figure 2.6 The ball indentation cycle (a) loading (b) unloading (Pasha et al., 2013).

The curve of the powder bed allows the powder to be sheared and a smooth transience from elastic to plastic behaviour, while some elastic recovery might occur through unload, as shown in Figure 2.6 (Hassanpour and Ghadiri, 2007, Pasha et al., 2013). Flow stress following a certain extent of strain can be represented by hardness (Tabor, 2000). The hardness (H) is the ratio of maximum indentation load (F) to the spherical cap of the impression area.

$$H = \frac{F}{A} \tag{2.4}$$

$$A = \pi(dh - h^2). \tag{2.5}$$

Where d is the diameter of the spherical indenter and h is the final depth, as shown in Figure 2.7.

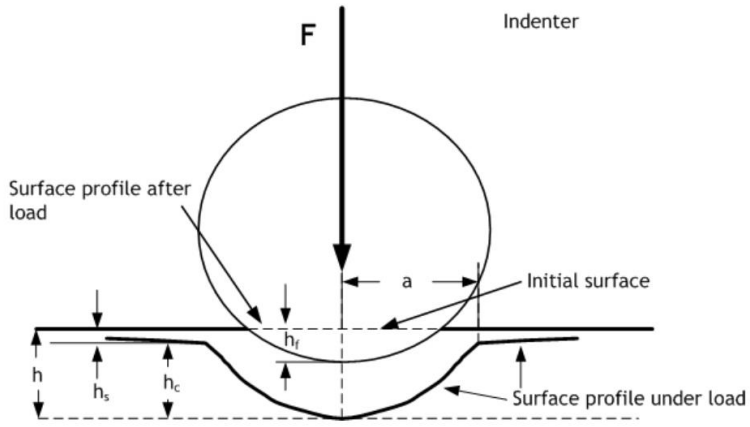

Figure 2.7 All variables are needed for hardness calculation (Hassanpour and Ghadiri, 2007).

Measuring powder flowability using the ball indentation technique is based on a constraint factor, for instance, the ratio between powder bed hardness and plastic yield stress. Increasing indenter diameter leads to a higher constraint factor due to the wall effects (Pasha et al., 2013).

2.6.5 Shear cell method

In 1960, Jenike introduced the first shear tester, which was designed for powder technology (Schulze, 2006). Up-to-date shear testers are compared to the Jenike shear tester. Although the Jenike shear tester is internationally known, it has disadvantages such as time-consuming due to operator's skills, measurement error due to manual preconcolidation and steady state flow can be hardly tested due to limited shear displacement (Schulze, 2008). In 1992, Schulze developed the ring shear tester (Schulze, 2006).

Shear cell methodology has been used extensively in the study of pharmaceutical powders. A wide variety of parameters can be achieved from these methods, including the yield loci representing the shear stress/shear strain relationship, the angle of internal friction, the unconfined yield strength, the tensile strength, and a variety of derived parameters such as the flow factor and other flowability indicators. Shear cell has many configurations and test methods that afford plenty of data to be analysed to determine the flow properties. In addition, the methods have been successfully used to design hoppers and bins.

2.6.5.1 Methods of shear cell tester

There are three types of shear cell: cylindrical, plate-type and annular (Schwedes and Schulze, 1990). The annular shear cell was used in this research. The annular cell is designed to use less material compared to other cells, though the design has a disadvantage which is that the powder bed is not sheared; equally, the material in the inner area being sheared is less than the material on the outside of the annulus. Despite the advantages and disadvantages of the shear cells, the methodology has a great degree of experimental control.

Schulze shear testers are direct shear testers with rotational displacement, and have many advantages (Schulze, 2008, Jaeda, 2009):

- They are internationally recognised in measuring the flow properties of cohesive bulk solids;
- They are fully automated and therefore not difficult to operate and their operation is not time-consuming;
- They require significant amounts of material and a well-trained operator.

Ring shear is connected to the RST-control 95 software and the flow properties of bulk solids can be measured (Schulze, 2005c, Schulze, 2005b). The parameters that describe the flow properties can be determined from the yield locus and they are listed below (Schulze, 2006, Schulze, 2008, Emery, 2008, Jaeda, 2009)

1- Flowability test: This is performed by measuring a yield locus, followed by constructing Mohr circles, as shown in Figure 2.8. From the Mohr circle analysis, both the consolidation stress σ_1 and unconfined yield strength σ_c are obtained. The flowability factor ff_c is defined as the ratio of consolidation stress σ_1 to unconfined yield strength σ_c and calculated from (Eq. 2.6):

$$ff_c = \frac{\sigma_1}{\sigma_c} \tag{2.6}$$

Used to characterise flowability numerically, the flow property test was the most important aspect of this study, since the flowability ff_c is the most significant consideration in quality control, comparative tests and product development.

2- Time consolidation test: Generally the strength of a bulk solid will increase when stored at rest. This effect can be determined as follows: the time consolidation test is performed by consolidating (pre shearing) a sample of bulk solid and storing it at a consolidation stress for a certain period of time and then shearing the bulk solid sample.

3- Wall friction test: The friction of the wall of the bin or silo and bulk solid is an important parameter. Ring shear can be prepared with a wall friction cell

to measure the wall friction. In this study the measurement of wall yield locus and angle of internal friction were performed.

4- Compressibility test: The sample is loaded by gradually increasing the vertical normal stress (uniaxial compression) without shearing. The mean bulk density in the shear cell can be calculated from the weight and the measured height of the bulk solid sample for each normal load.

5- Attrition test: Basically, this test is to assess the particle breakage and production of fine (Ghadiri et al., 2000). The attrition test helps to evaluate particle breakage and fine generation by crushing the bulk solid. The ring shear tester can only be used to evaluate bulk solids with well-defined normal stress for a certain shear displacement (Schulze, 2008). For evaluation, the amount of fine can be determined by using an appropriate sieve before and after the test. Alternatively, particle size distribution measurements can be carried out before and after shearing (Schulze, 2006).

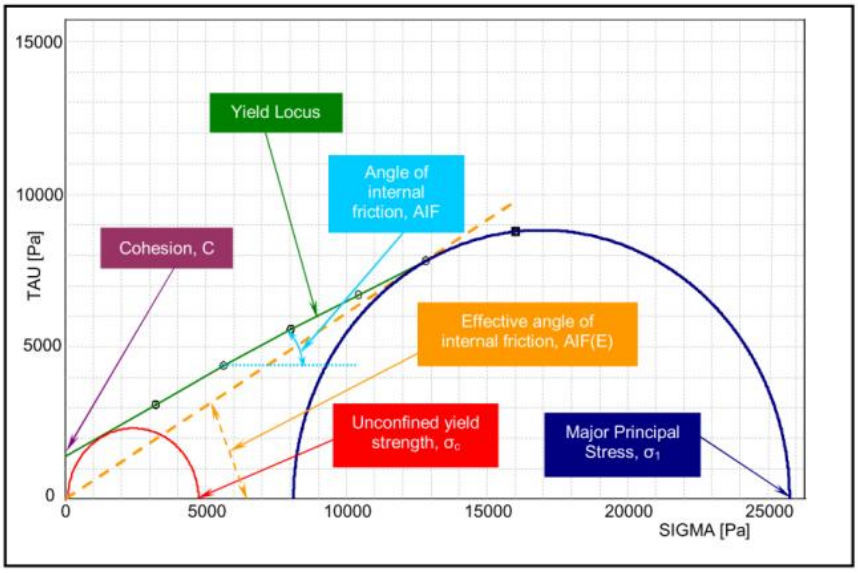

Figure 2.8 Graphical description of the yield locus and the parameters derived from the fitting of Mohr Circles to the σ/τ data set (Armstrong, 2011).

Shear stress

The Mohr circle is defined by two principal stresses and is always located on the σ axis, as shown in Figure 2.8. Each Mohr circle has two point intersections with the σ axis. The normal stresses defined through these points of intersection are called the principal stresses; the larger circle is called the major principal stress and designated as σ_1, and the smaller circle called the minor principal circle is designated as σ_2 (Schulze, 2008). The yield locus is represented by the incipient points (points of tangency) of Mohr's circles at steady state flow and from that line the angle of internal friction (slope of the effective yield locus) can be determined, while the effective angle of internal friction is represented by the slope of linearized yield locus which is a straight line tangent to both Mohr circles. In addition, cohesion can be determined when the yield locus intersects with the y-axis (shear stress) at the normal stress equal to zero.

2.6.5.2 Types of Schulze ring shear testers

Schulze ring shear testers are available into two models, RST-01.Pc and RST-XS. During 1992, ring shear tester model RST-01.01 was developed by Schulze (Schulze, 2008), and after five years, in 1997, a new version RST-01.pc, as seen in Figure 2.9, connected to a personal computer and was controlled by RST control 95 (Schulze, 2005a). It is available as stainless steel and aluminium cells with a capacity range of powder from 85ml to 900ml. The software is enabled to measure and calculate many parameters automatically including yield loci, wall yield loci, time consolidation, etc. (Schulze 2002-2005b; Schulze 2005).

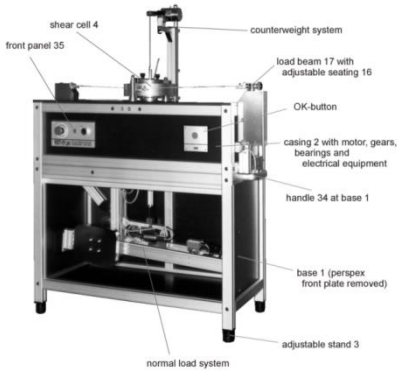

Figure 2.9 Ring Shear Tester RST-01.pc (computer-controlled)(Schulze, 2005a).

The second model of Schulze's ring shear tester was introduced to the industrial market during 2002. This model is small computer-controlled ring shear tester having a three cells volume ranging from (9-70 ml) and known as (RST-XS), as shown in Figure 2.10. (Schulze, 2006). Table 2.5 summarises the specifications of this model. In my research project, a 30 ml stainless steel cell has been used due to its advantages over the others. The operational test procedure of both models is similar and will be explained in the next paragraph.

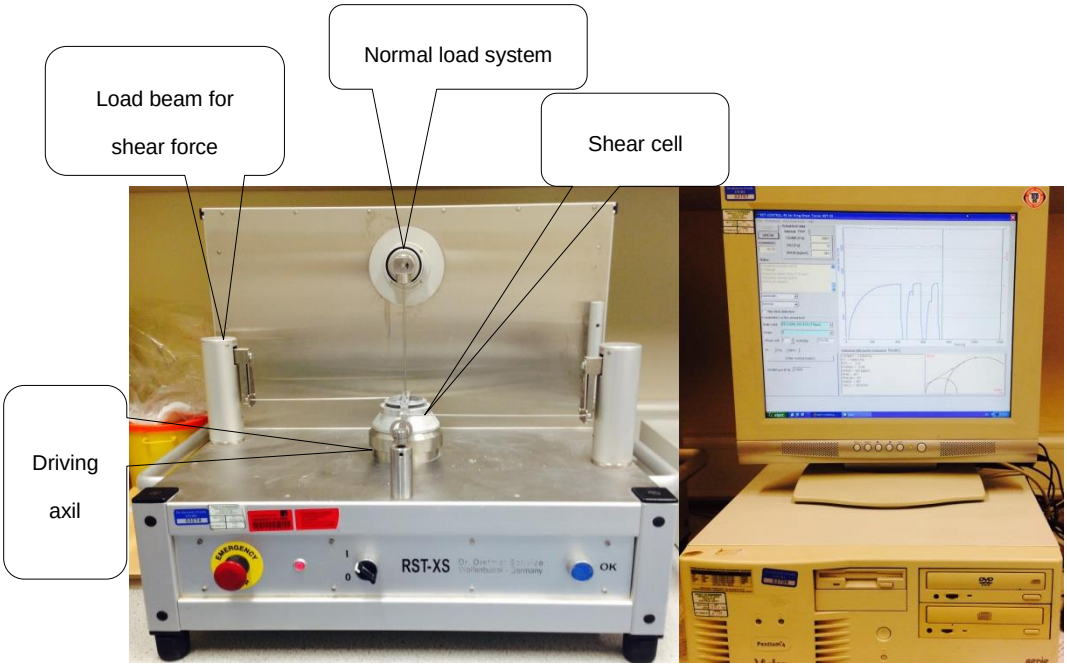

Figure 2.10 Ring Shear Tester RST-XS (computer-controlled).

Table 2.5 RST-XS specification.

	RST-SX
Cell volume	30ml
Shear area	2412.75mm
Driven section	Shear cell base
Consolidation load	Dead weight
Pre-shear	Single
Order of shear test	Low-High
Control method	Custom program on separate dedicated PC or on remote PC
Length of test	700-800 seconds
Weighting of sample	Needs a separate balance
Post processing	Custom program on instrument PC or on remote PC

Figure 2.11 shows a ring shear cell tester annular cell. Firstly, the annular cell is filled gently with a powder sample, covered carefully with an annular lid and mounted on the apparatus. The annular lid is connected to the cross-beam over the sample. During the shear and in order to prevent the bulk solid from sliding, the lid has a number of bars protruding into the sample. A normal force FN through the hanger (downward) is applied to the sample and represents the vertical stress σ. Also, FA acts on the cross-beam to counterweight all the connected parts to the lid. Then the cell is rotated clockwise and the sample is sheared with the speed of 1.5mm/min. The lid is connected with two tie rods to prevent the cell from rotation. The shear stress of the bulk solid can be calculated using F1 and F2 values measured through the rods. The aim of a shear test is to measure the yield locus of a well-defined consolidated bulk solid.

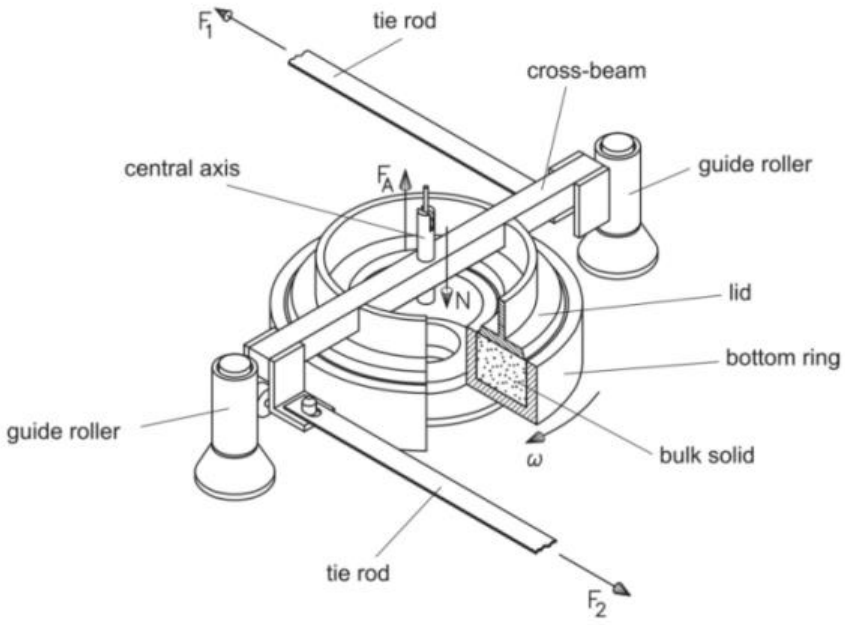

Figure 2.11 Shear cell of Ring Shear Tester RST-01.01

In order to measure the yield locus, the operational procedure of the ring shear tester consists of two main stages, as shown in Figure 2.12. The first stage is known as the pre-shear step and it is conducted to consolidate the sample by shearing the bulk under a normal stress σ_{pre} until constant pre-shear stress τ_{pre} is obtained. Reaching this stage means both shear resistance and bulk density will not increase further. Therefore the bulk solid sample is sheared at constant σ constant τ and constant bulk density and this stage is known as steady state flow. In a later stage the shear force minimised to zero value.

The second stage is called the shearing phase, where the normal stress is reduced to a level less than pre-shear in order to give the maximum shear stress τ_{sh}. The shear stress τ_{sh} may be called τ_{if} at the incipient point. At τ_{if} the consolidation of the sample fails which reflects that the consolidated sample starts to flow. Under different normal stress, several incipient flow points are used to draw σ and τ diagrams to measure the yield locus, as shown in Figures 2.12 and 2.13.

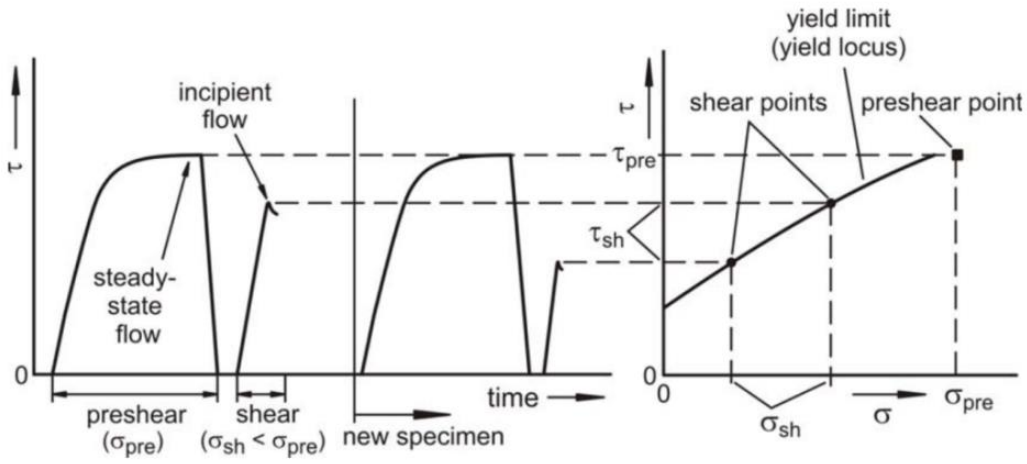

Figure 2.12 Plot of shear stress vs. time; yield locus (Schulze, 2006)

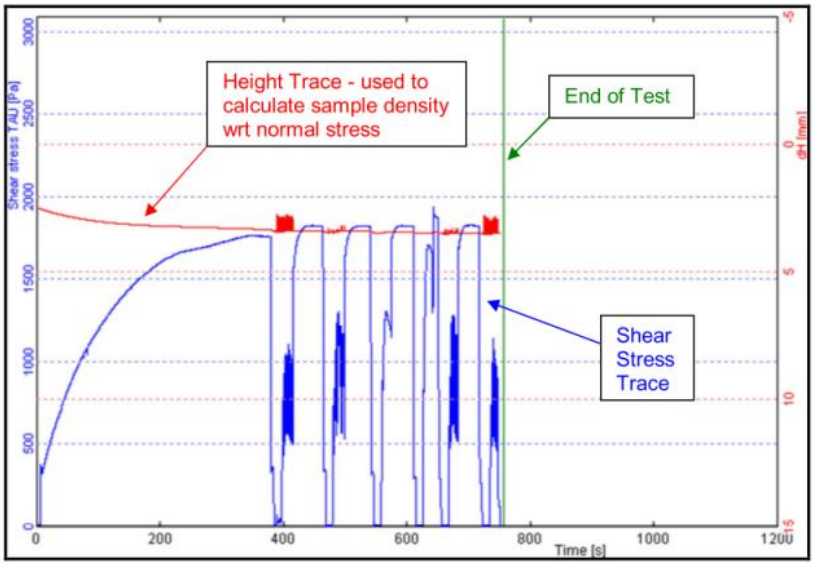

Figure 2.13 Screenshot of RST-XS performing a shear test. The blue trace shows the shear stress progress (left), the red trace shows the height of the lid (right), while the green line indicates the end of the test (Armstrong, 2011).

Flow properties, including unconfined yield strength, cohesiveness, angle of internal friction, consolidation stress, and bulk density, can all be measured with a ring shear cell tester. The flowability (ff_c) is the most important aspect of quality control, product improvement and comparative testing. The values of ff_c can be obtained by drawing the Mohr circle, as shown in Figure 2.8. The consolidation stress σ_1 is the major principal stress of the large Mohr circle and the minor principal stress

σ_2 equals 0, while the small Mohr circle which passes through the origin represents the unconfined yield strength σ_c.

ff_c ratio uses (σ_1 and σ_c) (Eq. 2.6) to obtain the flowability numerically. The flowability ratio is used to categorise the flow behaviour of bulk solids, according to Jenike's (1967) powder classification, as shown below in Figure 2.14:

$ff_c < 1$ not flowing
$1 < ff_c < 2$ very cohesive
$2 < ff_c < 4$ cohesive
$4 < ff_c < 10$ easy flowing
$10 < ff_c$ free flowing

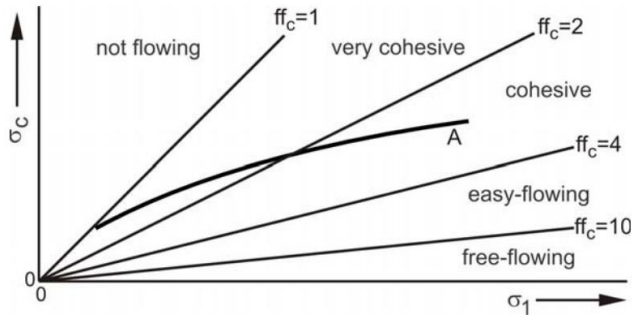

Figure 2.14 Flow function and line of constant flowability (Schulze, 2006).

The ring shear cell tester can be used to measure the wall friction which reflects the friction between the surfaces of the boundaries (silos and bins) and the bulk solids. Special cells need to be used to measure wall friction, as shown in Figure 2.15.Two pairs of variable can be determined using this test, including angle of wall friction φ_x and wall friction coefficient μ, both are essential factors for silo and hopper designing, as will be discussed in Chapter 4. Angle of wall friction φ_x is defined as the slope of a line running through the origin of the (σ_w , τ_w) plot as illustrated in Figure 2.16. The coefficient of wall friction is the ratio of wall shear stress τ_w to wall normal stress σ_w (Schulze, 2008); the higher the friction coefficient, the higher the wall friction.

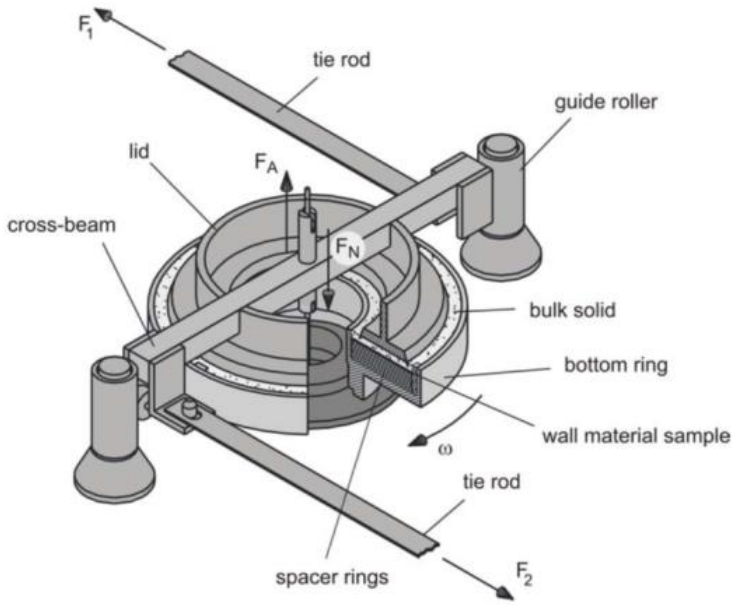

Figure 2.15 The shear cell for wall friction test (Schulze, 2006)

The principle of wall friction measurement is similar to the yield locus test; when the sample is placed in the cell and the vertical normal stress acts on the sample, the effect between the bulk solid and the wall material is called wall normal stress σ_{w1}. The shear process occurs when the bulk solid shifts against the wall with fixed velocity. The wall normal stress σ_{w1} is the highest, after which the stress value starts to decrease gradually. When shearing starts, the wall shear stress τ_w increases over time until it reaches a constant stress τ_{w1}, known as applied normal stress and called steady state. The wall normal stress and wall shear stress then start to decrease, as shown in Figure 2.16, to achieve the steady state again, after which the test is completed. Several pairs of value (σ_w, τ_w) are used to measure the wall friction through the plotting points, as shown in Figure 2.16.

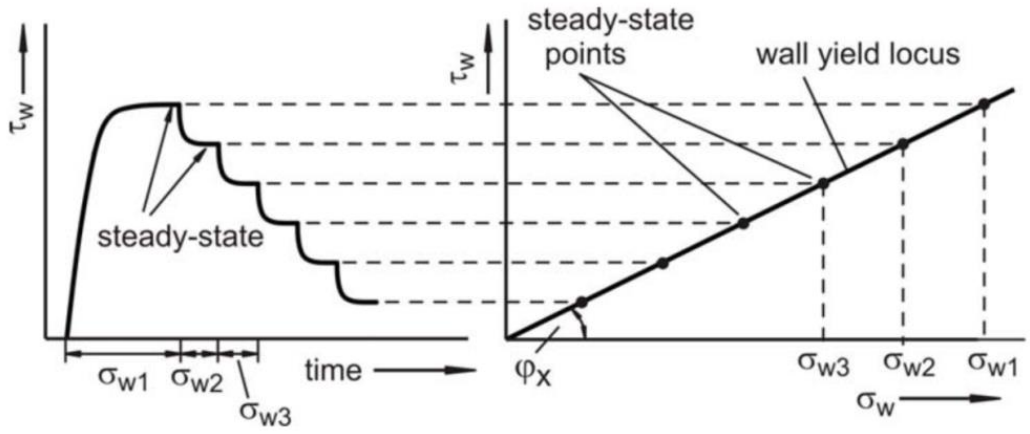

Figure 2.16 Wall shear stress in a wall friction test and (σ_w,τ_w) diagram (Schulze, 2006).

From the plot, two parameters can be measured: angle of wall friction and wall friction coefficient. There is a positive correlation between the wall friction and angle of wall friction. The wall yield locus has two trends; firstly, if the slope is running through the origin that indicates the pair (σ_w , τ_w) has the same value in each point of the line and the angle of wall friction is identical with the wall friction coefficient; secondly, if the line is not running through the origin that indicates a different angle of wall friction and wall friction coefficient for each point, and both are dependent on wall normal stress. In other words, each point on the line has a wall friction angle and wall friction coefficient which indicate the bulk solid is cohesive (Schulze, 2006). Although, ring shear has many advantages it still has limitations.

2.6.5.3 Limitations and disadvantages of the RST-XS ring shear cell tester

There are two practical disadvantages of using the RST-XS. Firstly the sample cell has to be overfilled with powder which means it can prove quite messy as shown in Figure 2.17. Secondly, the cell needs to be weighed on a separate balance as there is no self-balancing procedure.

The main practical limitation for RST-XS is related to applied loads and particle size. At low load, 2kPa or below, mainly with large particle size, the tester seems unable to control the force which is applied to the test cell due to an inability to

respond fast enough to the extremely rapid dilation that happens at the failure point of incipient of flow (Armstrong, 2011).

Figure 2.17 Filling of the RST-XS Shear Cell (reproduced from the Schulze web site http://www.dietmar-schulze.de).

2.6.5.4 Hoppers and silos design

The ring shear tester is used for designing both silo and hopper. In designing processes, the material properties must be known. The material properties are bulk density ρ_b (which characterises the internal friction of the bulk solid), effective angle of internal friction φ_e, angle of wall friction φ_x and unconfined yield strength σ_c (Schulze, 2008). The angle of wall friction and the unconfined yield strength are the most important properties, and are considered during mass flow hopper slope design and arching formation, respectively (Schulze, 2008). The flow properties are based on the major consolidation stress σ_1 measured by the ring shear cell tester (Schulze, 2005a).

Bulk solid flow under gravity can be distinguished by either mass or funnel flow to avoid any flow problems during silo designing. Silo design for mass flow is the most practical flow to avoid many flow problems, for instance, ratholes, flooding and segregation during filling (Prescott and Barnum, 2000). Arching tendency remains a problem in mass flow silos due to interlocking and wedging of particles (Schulze, 2005a). This problem can be avoided by designing the diameter of the conical hopper circular outlet to be at least 6-10 times larger than the maximum particle size. For wedge-shaped hoppers, the width of the rectangular outlet must be at least 3-7 times larger than the maximum particle size (Schulze, 2008).

For more than five decades, Jenike (Schulze, 2008) developed hopper and silo design methods, and until now, his method is still the most efficient. Two geometrical shapes, the conical and wedge-shaped hoppers, were investigated extensively (Schulze, 2008). Jenike designed two mass flow diagrams for each based on the effective angle of internal friction. In Figure 2.18, the angle of wall friction φ_x represented on the Y axis has been plotted versus the slope of the hopper from vertical Θ_c and Θ_p for conical and wedge-shaped hoppers respectively. Θ_c is defined as the inclination of the conical hopper wall to the vertical, while Θ_p is the inclination of the wall of the wedge-shaped hopper wall to the vertical.

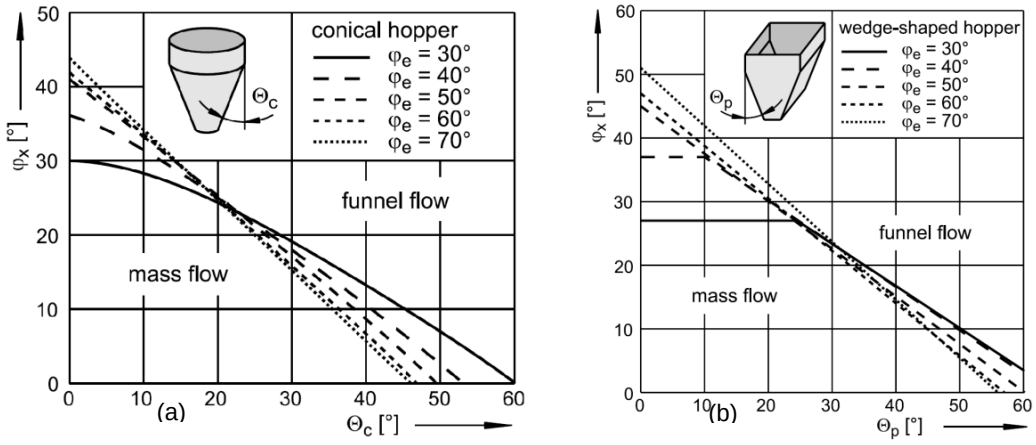

Figure 2.18 (a) mass flow diagram (conical hopper), (b) mass flow diagram (wedge-shaped hopper) (Schulze, 2008).

The funnel flow area is separated from the mass flow area by mass flow boundaries. From all given parameters, Θ_c and Θ_p can be easily determined from the mass flow boundaries and the values need to be subtracted to 2° to 3° as a safety margin. Subsequently, the minimum outlet size can be calculated to avoid arching. Major principal stress σ_1 and the unconfined yield locus, σ_c can be obtained from the yield locus. The major principal stress σ_1' (bearing stress) needs to be calculated (Eq. 2.7). From an engineering point of view, this stress is comparable to road arch bridge stress that carries only its own weight and neglects the weight above (Schulze, 2008). Similarly to that, if an arch is formed in the cohesive powder flow through a silo or hopper, the arch carries its own weight and the bulk cohesive powder weight is shifted to hopper or silo walls. A recent tomographic study conducted by Albaraki et al. (2013) at static conditions showed that the distribution of major principal stress

inside hopper geometry has a great influence on granular material flow; the lower the internal hopper angle, the better the uniform flow.

The stress in a such case is represented by major principal stress supporting a stable cohesive powder arch. In general, if σ_c is smaller than σ_1' then the bulk solid will flow.

$$\sigma_1' = \frac{\sigma_1}{\sigma_c} \tag{2.7}$$

Flow factor ff is different from the flow function that obtained from the yield locus. The flow factor ff is dependent on the flow properties (φ_x and φ_e) and the hopper shape. Jenike provided diagrams for an easy determination of the flow factor. Each of the diagrams is valid for single hopper geometry (i.e. conical and wedge-shaped) and a fixed value of the effective angle of internal friction, φ_e, being different from one diagram to another in steps of 10°. The solid curves represent constant values of ff. For values in between and φ_e values which are not multiples of 10°, the flow factor values must be obtained by interpolation. The mass flow boundary is also plotted in each diagram (dashed curve) (Schulze, 2008)

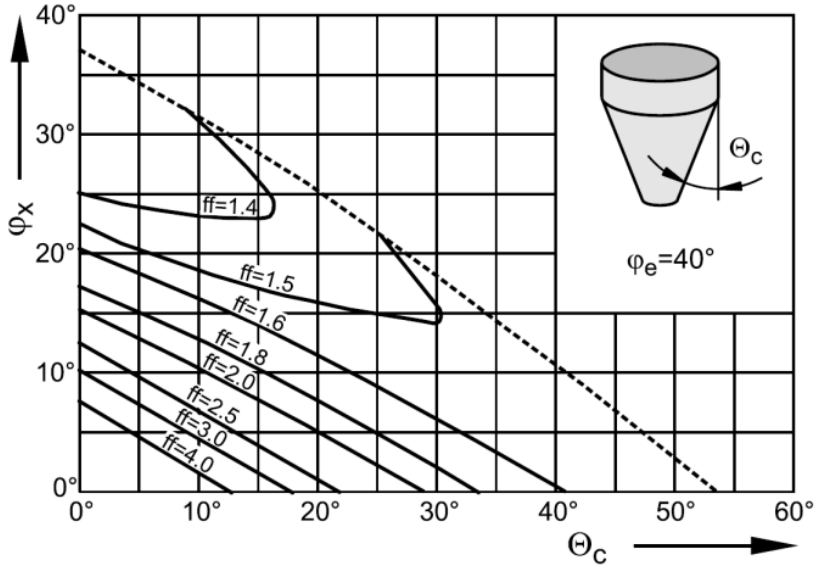

Figure 2.19 Flow factor ff, for conical hopper and $\varphi_e = 40°$ (Schulze, 2008).

The critical outlet dimensions can be determined by using a flow function plot as shown in Figure 2.20.

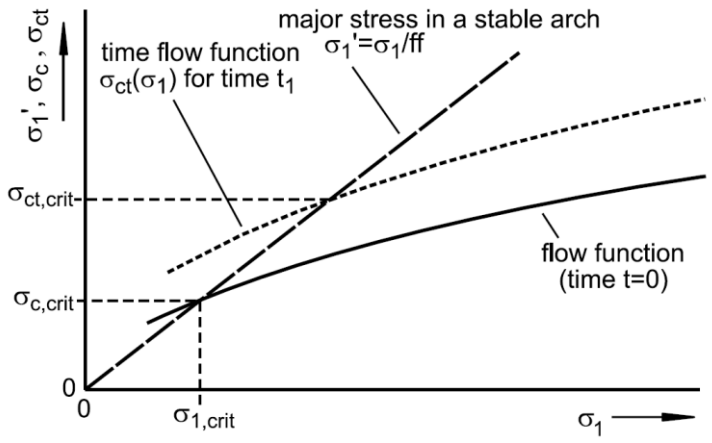

Figure 2.20 Flow function plot.

The critical outlet dimensions required to avoid arching are determined by the σ_1, σ_c plot. Bearing stress or the major principal stress in the arch can be σ_1', is plotted and is proportional to σ_1 (Eq.2.8).

$$\sigma_1{}' = \frac{\sigma_1}{ff} \tag{2.8}$$

The intersection point of the flow function plot with the major principal stress in the arch $\sigma_1{}'$ gives two coordinates, known as crit; they are unconfined yield strength $\sigma_{c,crit}$, and major principal stress $\sigma_{1,crit}$.

The critical outlet width for wedge-shaped hopper b_{crit} can be calculated by (Eq. 2.9):

$$b_{crit} = H(\Theta_P)\frac{\sigma_{c,crit}}{gP_{b,crit}} \tag{2.9}$$

Where g is acceleration due to gravity (9.81m/s^2).

And critical outlet diameter for conical hopper can be calculated by (Eq. 2.10):

$$d_{crit} = H(\Theta_c)\frac{\sigma_{c,crit}}{gP_{b,crit}} \tag{2.10}$$

$\rho_{b,crit}$ can be calculated by drawing the plot of ρ_b versus σ_1 similar to the flow function plot. Wall inclination of conical $H(\Theta_c)$ or wedge-shaped $H(\Theta_p)$ can be obtained from the plot in Figure 2.21.

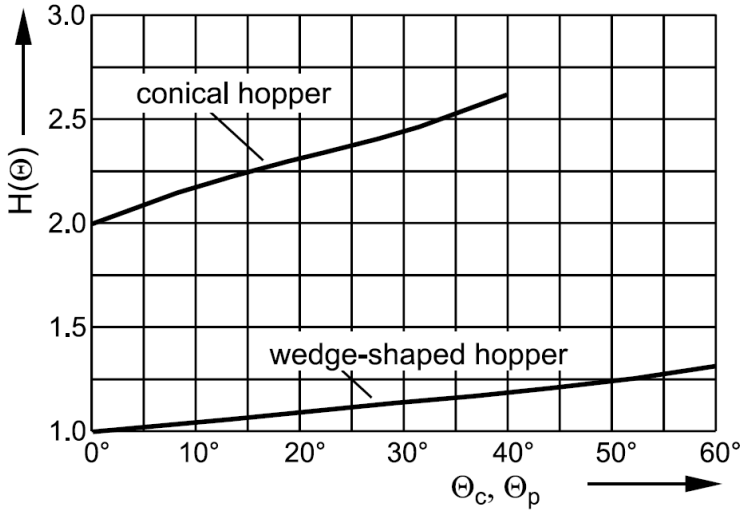

Figure 2.21 Function H(Θ) (Schulze, 2008).

2.7 **Particle Image Velocimetry (PIV)**

The term Particle Image Velocimetry (PIV) has appeared extensively in the literature over the last three decades (Adrian, 2005). However, the idea of PIV is older (Willert et al., 2007). The basic concept is observing small pattern movement on a flowing stream surface to determine the velocity field. Observation being qualitative, the concept was later developed to be quantitative by introducing electronic devices to the experiment. This had a great impact in the fluid dynamics field.

Generally, the PIV system is divided into different subsystems: optical lenses, laser light source, camera and computer, as seen in Figure 2.22. One of the experimental set-ups is based on adding tracer particles to the flow stream and the light is illuminated once or twice within a very short period of time. The light will be scattered by the particles and recorded by camera in single frame or multi-frame series. The particle image displacement between the light pulses must be determined (Willert et al., 2007).

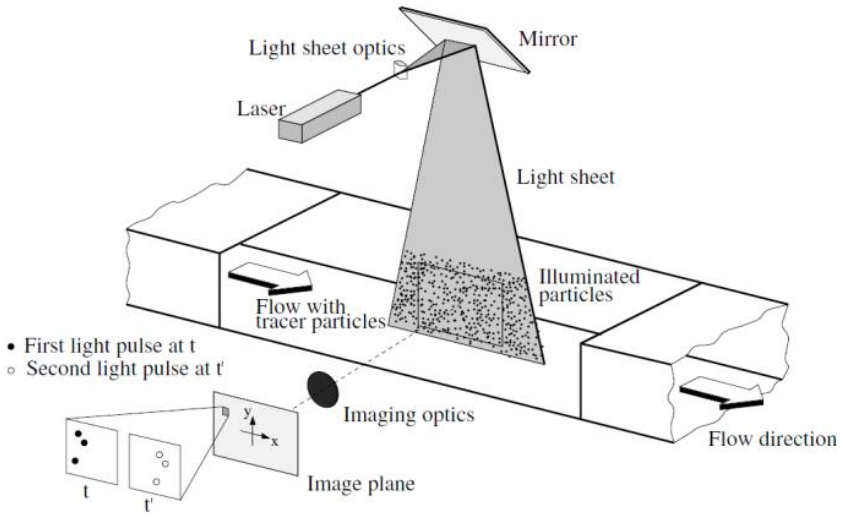

Figure 2.22 Experimental set-up for Particle Image Velocimetry (Willert et al., 2007).

In the mid-1990s (Westerweel, 1997), one of the most important developments in PIV, which made it an easier and therefore more popular technique, was moving from photographic to videographic recording with images becoming digitalised (Keane et al., 1995). The technique led to improved accuracy of interrogation due to high resolution digital images. Moreover, new video cameras – interline transfer cameras – have led to the development of DPIV (Adrian, 2005). The camera holds two images recorded in rapid succession by transferring the first image recorded by each pixel and storing it on the computer, and then recording a second image.

This technology has speeded up the interrogation process and automated the vector clean-up process. In addition, the computer and software have made it possible to analyse huge numbers of digital images.

Nowadays, the modern PIV is widely used because it is considered a very accurate method for the quantitative measurement of velocity.

PIV has been used in the fluid dynamic efficiency encouraging many scientists to use it in different disciplines – one of the recent applications of the DPIV being in determining granular material flow (Sielamowicz et al., 2006, Albaraki and Antony, 2014).

2.7.1 Granular material flow measurement using DPIV

Granular flow behaviour is very complex. Various factors can affect the flow, in particular, particle size, particle shape, particle size distribution, humidity, temperature and vessel geometry (Ganesan et al., 2008, Emery et al., 2009).

Two geometry vessels are used for powder storage, which are hopper and bin. The hopper has a conical shape while the bin has a cylindrical or rectangular shape. The flow pattern is classified as mass flow which is described as first in, first out; the second type is funnel flow which is described as last in, first out.

Studying the flow behaviour inside the hopper and silo is important, especially in the pharmaceutical industry, as flow will be adversely affected when they are not designed properly. The most common flow problems occurring inside hoppers and bins are either arching or "ratholing". Arching, or bridging, forms just above the outlet and prevents the granules from being discharged. The arch could be interlocking or cohesive. An interlocking arch occurs when the particles are large compared to the hopper outlet; when the particles pack together and obstruct the hopper outlet, this is called cohesive arching (Ulissi et al., 2009).

The flow of granular materials inside the hopper and bins has a velocity profile. Many applications have been used to determine the velocity profile, one of the most efficient applications being DPIV. Researchers were able to measure the velocity magnitude contours, velocity distribution and vector field (Sielamowicz et al., 2005).

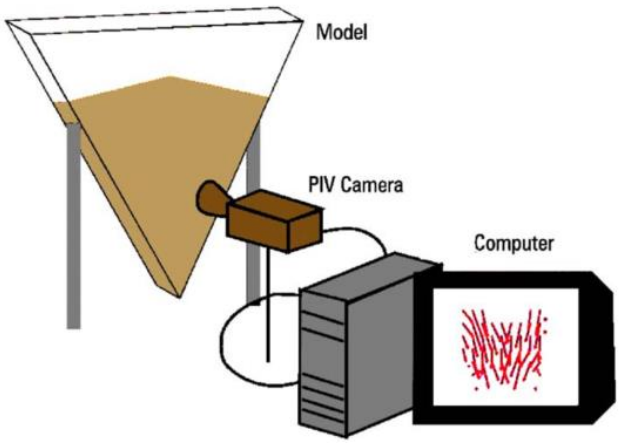

Figure 2.23 Measuring granular flow using digital particle image velocimetry (Sielamowicz et al., 2006).

Measuring the granular flow by using the PIV was a useful technique and an applicable tool; for example (Lueptow et al., 2000) measured the particle displacement velocities of granular flow by using dark particles and a mixture of lights. DPIV was used by (Sielamowicz et al., 2005), as shown in Figure 2.23, to measure the velocity vector field in the flowing zone and the technique appeared to be a useful and quantitative diagnostic tool. Also, DPIV can quantify flow region, shear zone, radial velocity field and measure transient variation. It is considered to be an accurate technique to obtain velocity gradients inside the flowing zones (Sielamowicz et al., 2006).

2.8 **Conclusions**

In pharmaceutical industries, powder must have a reliable and consistence flow out of hoppers and feeders without excessive overflow and dust generation. Poor powder flow properties may reduce reproducibility and cause financial losses during industrial processes. One of the most important approaches to improving the powder flow properties is particle size enlargement (i.e. granulation) (Hou and Sun, 2008), although, controlling particle size is not sufficient to improve the flow properties. Another approach is increasing binding ratios to improve the flow properties to accommodate the materials which have a hygroscopic nature. Both approaches can be used to improve the flow properties. There are many methods and instruments that are used to study the flow properties; however, the empirical method i.e. angle of repose, bulk and tapped density, Carr's index and Hausner Ratio are not reliable. The ring shear tester (RST-XS) is a recent instrument used to characterize the powder flow properties. It is connected to software to obtain automated results. Flow properties characterized by the ring shear tester have a clear physical meaning and are independent of scale. Data obtained in laboratory can be reliably used to design optimum equipment to handle large scale powders (Schulze, 2008).

Flow behaviour is dependent on powder flow behaviour and the geometries used to handle, store or process the materials. For instance, some materials have mass flow in one hopper and funnel flow in another. Recently, DPIV has been employed in the

industry to quantify the flow region, shear zone, radial velocity field and measure transient variation. This recent technique is an accurate technique used to visualize the mean resultant velocity vector to determine the flow trend inside the geometries (Sielamowicz et al., 2005).

In the following chapter, the materials used for the granulation methods of granules and grains that were prepared in this research work are presented.

Chapter 3 Materials and Methods

3.1 Introduction

For my research project and due to their wide applications in pharmaceutical industries, simplicity and cost effectiveness, wet and melt granulation methods have been used to prepare the granules. Each technique has a different mechanism and method of preparation and this gives a good opportunity to compare the results. Starch has been selected as the starting material for granulation due to its physical and mechanical properties and modification possibilities. In addition, it is commonly used in the pharmaceutical industries for different purposes.

The influence of the granulation technique on the physiomechanical properties, micro and macro mechanical properties and flow behaviour of the prepared granules has been evaluated using ring shear tester RST-XS. This tester has been used during this research as it is the most recently available apparatus to evaluate powders' and granules' flow trends and has many advantages over the other shear testers. The selected particle size ranges (45 - 710μm) are within the possible ranges to be used for ring shear tester RST-XS for yield locus and wall yield locus measurements.

DPIV has been implemented in the project as a dynamic non-invasive method to visualise and illustrate the granular flow trend and trajectories using two different internal angles (45° and 70°).

3.2 Materials

Corn starch and PEG 6000 were purchased from SIGMA-ALDRICH, UK. Both are used for granules preparation.

3.2.1 Physical properties of the materials

Physical properties for starch and polyethylene glycol (PEG 6000) are illustrated in Table 3.1. Both compounds are pharmaceutical excipients and used in pharmaceutical formulation. Starch in a concentration between 5-25% w/w is usually used as a wet binder to granulate cohesive powders in tablet manufacturing. Fine starch is used as the bulking agent, disintegrant and lubricant in solid dosage

form formulation. On the other hand, PEG 6000 is used as a tablet binder, disintegrant and melt binder in various ranges (Rowe et al., 2003).

Table 3.1 Physiochemical properties of corn starch and PEG 6000 (Zobel et al., 1988, Rowe et al., 2003).

	Starch	**PEG 6000**
Non-proprietary Names	Corn starch	Macrogol 6000
Description	White or whitish powder, fine, odourless, tasteless and has very small spherical or ovoid granules	White or off-white in colour, and comes as waxy flakes.
Density (bulk)	0.462 kg/m^3	1.15-1.21 kg/m^3
Particle size	2-23µm	181.4µm
Flowability	10.8-11.7 g/s , cohesive and has poor flow	Free-flowing
Moisture content	Hygroscopic	Not hygroscopic
Melting point	160-186°C	55-63°C
Application in Pharmaceutical formulation	Tablet binder and disintegrant.	Tablet binder and disintegrant
Safety	Non-toxic and non-irritant material	Non-toxic and non-irritant materials
State	Solid	Solid

3.3 **Methods**

Different methods were used in this chapter starting from granulation methods. Two common granulation methods (i.e. melt and wet) were applied for granules preparation. Three particle size ranges were selected from prepared granules and evaluated qualitatively using angle of repose, bulk and tapped density, Carr's index and Hausner Ratio. A ring shear cell tester was used to evaluate the granules qualitatively to assess flowability, yield locus and wall yield locus. Granular flow inside the hopper and silo were recorded using DPIV.

3.3.1 Granulation

Two different granulation methods (i.e. wet and melt) were used to prepare granules with different binding ratios.

3.3.2 Wet granulation

Starch paste was prepared in three different percentages (5%, 15% and 25%) and 400gm of each ratio has been prepared using distilled water as vehicle .This amount of base used to granulate sufficient quantities of the granules within the selected ranges for the required tests and evaluations. To prepare the paste, the required amounts (20gm, 60gm and 100gm) were accurately weighed as shown in Figure 3.1(a). The distilled water quantity was divided into two portions, 30% at 37°C and 70% boiled to 100°C. The starch powder dispersed gradually in the cold water with continuous mixing until the colour changed to white turbid suspension. The boiled water was added gradually to the white suspension with continuous mixing to obtain a more homogeneous and viscous mixture. In a later stage, the mixture was placed in a cold water bath for more cooling.

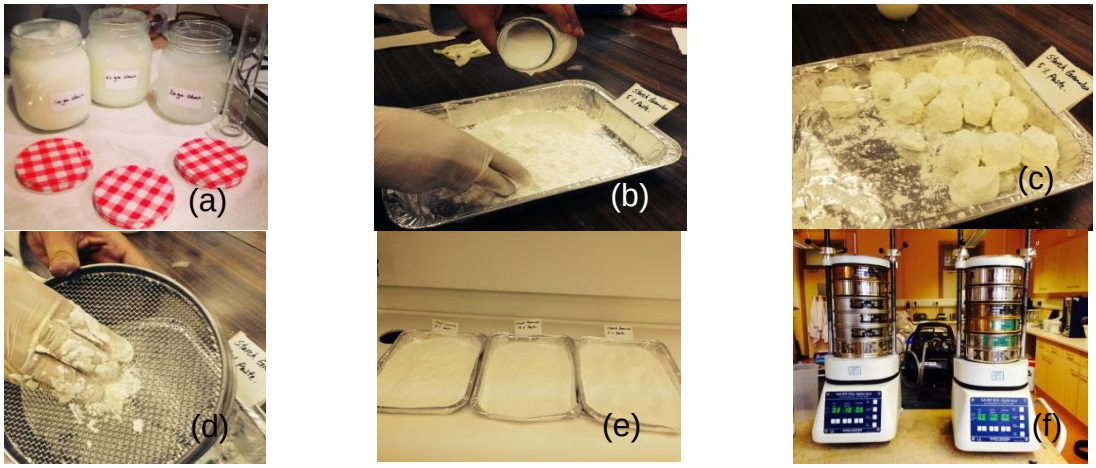

Figure 3.1 Wet granulation method for granules preparation (a) starch paste, (b) mixing starch with the paste, (c) starch mass, (d) granules formation by compresssing the mass through sieve, (e) drying granules and (f) automatic shaker.

The granules were prepared using a manual mixing method as the project is on a small laboratory scale (El-Say et al., 2010, Albaraki and Antony, 2014). A sufficient quantity of the starch paste was added to the raw material as shown in Figure 3.1(b).

The mixture was mixed continuously until a solid mass was obtained, as shown in Figure 3.1(c). The obtained bulk masses were compressed and passed through the sieve of 1.0mm for size uniformity and granulation, as shown in Figure 3.1(d). The granules were kept in the oven over night to dry at 60°C, as shown in Figure 3.1(e). The obtained dry granules were re-sieved through a series of sieves using an automated shaker to obtain the required granules ranges, as shown in Figure 3.1(f).

3.3.3 Melt granulation

Three different weights of PEG were used to prepare granules with three different binding ratios: 5% (5g of PEG/100g of starch), 15% (15g of PEG/100g of starch) and 25% (25g of PEG/100g starch) (Krycer et al., 1983). Starch powder and PEG 6000 were placed in a beaker and immersed in a thermostatically controlled water bath at 75ºC, where the melting point of PEG 6000 is 55-63ºC. Powder mixing was performed manually using a glass rod in a beaker until a dough mass was formed, followed by continuous stirring to produce fine homogeneous granules. The beaker was removed from the water bath and left to cool in an ice cooled bath with continuous mixing. All granules with different sizes were passed through a sieve of 1.0mm for size uniformity and re-sieved using the same procedure in the case of the wet granules to obtain similar ranges.

3.4 Ranges

In my research, the sieving technique was used since it is considered to be the simplest and probably the most commonly-used method in determining particle-size distribution and the technique met my requirements for all ranges used, i.e. 45-710µm.

Three ranges were selected to be studied, very fine granules (45-106µm), moderately coarse (250-355µm) and coarse granules (600-710µm). In between these ranges they have similar granular characteristics.

3.5 Static angle of repose

The angle of repose must be calculated on a fixed base, free from any vibration. The height of the funnel was fixed at a constant level in all the experiments. The granules were poured in small voids through a vibrating slide fixed above the funnel feeding outlet and fell on the wall of the funnel. The poured granules started to build up a symmetrical inverted cone-like shape until they reached the required height. As the funnel was moved, care was taken to prevent any vibration. The funnel height was maintained at approximately 2-4cm from the top of the powder pile as it formed, in order to minimise the impact of falling powder on the tip of the cone. This method would be considered inappropriate if the powder cannot successfully produce a symmetrical inverted cone. The height of the symmetrical pile and half the base was measured and recorded five times. Eq. 2.1 was used to calculate the value of the mean angle of repose α.

3.6 Compressibility Index and Hausner Ratio

The Compressibility Index or Carr's index is an indicator of any changes in the granular packing arrangement and considered to be one of the main factors to anticipate granular flow. Carr's index was simply calculated using the obtained values of the tapped and bulk densities according to Eq. 2.2. The results are shown in Tables 4.2 and 4.3.

The Hausner Ratio is another indirect indicator of granular materials flowability and simply calculated using the obtained values of tapped and bulk densities. The key border value of the Hausner Ratio is a value of 1.25. If the ratio is above 1.25 the flowability is poor and if it is less than that it is freely flowing. The Hausner Ratio can be calculated using Eq. 2.3.

3.7 Tapped and bulk densities

The tapped density test has been performed using tester Model AS 100. Preliminary tests have been conducted to determine the number of taps required to give fixed granules height. The test was conducted by accurately weighing of 25gm of granules poured gently and gradually through a funnel glass into a 100ml graduated glass

cylinder. The initial volume of the granules was measured and the value of the bulk density was calculated in units of kg/m^3. The cylinder was mounted on the tapped density tester and tapped up to 300 taps to exclude all air voids until a fixed height of the granules was obtained. The volume of the granules within the cylinder was measured and the tapped density was calculated in the same units. The procedure was repeated three times for each sample and the recorded tapped and bulk densities are the average of the three readings.

3.8 **Ring shear cell tester**

The Schulze ring shear tester RST-XS was used in this research to measure the yield locus and wall friction due to this tester's various advantages and extensive application for multiple industrial purposes.

3.8.1 Yield locus measurement

The granular flowability was measured using the RST-XS fully automated ring shear tester connected to a PC with RST-Control 95, and the annular cell was $30cm^3$. More details about this model have been explained in Chapter 2.

The annular cell was filled with granules and the excess amount was removed gently as shown in Figure 2.17, then the weight was recorded for every sample before the measurement. During the test, four normal loads were selected (5, 9, 13 and 17kPa). First, a normal load of pre-shear was adjusted at 5kPa; under this load the sample was consolidated and kept at steady state and the shearing occurred at 4, 3, 2 and 1kPa. Second, a normal load of pre-shear was adjusted at 9kPa; under this load the sample was also consolidated and kept at steady state and the shearing occurred at 7, 5, 3 and 1kPa. The third normal load of pre-shear was adjusted at 13kPa, under this load the sample was again consolidated and kept at steady state and the shearing occurred at 10, 7, 4 and 1kPa. The final normal load of pre-shear was adjusted at 17kPa, under this load the sample was still consolidated and kept at steady state and the shearing occurred at 13, 9, 5 and 1kPa.

From the test, the normal stress σ and obtained shear stresses τ with determined incipient flow are plotted as (σ, τ) in the diagram. The yield locus was obtained from

constructing Mohr's circle analysis. The flowability function ff_c was defined as the ratio of the consolidation stress σ_1 to the unconfined yield strength σ_c and calculated automatically by the software. In a later stage ff_c was used to determine the flow behaviour of the granules.

The system was adjusted on the recommended standard settings according to the apparatus manual. The slip-stick was turned off during the whole test and the shear velocity mode was set to normal mode. Every test was repeated three times and one reading was selected.

3.8.2 Wall yield locus

The wall friction test against Perspex boundaries was conducted using the annular cell. The Perspex circular disc was placed inside the cell and weighed as initial weight, the cell was reweighted after powder filling and the obtained values were fed into the software.

The granular sample over the Perspex ring was covered by the lid and mounted onto the apparatus. Five wall normal stresses were selected (10, 8, 6, 4 and 2kPa). During the test the normal wall load of pre-shear was adjusted at 10kPa. Under this load the sample was consolidated and kept at steady state and the wall shearing occurred at selected wall normal stresses.

At the end of the test, five points of the wall yield locus at five different wall normal stresses were obtained. The first point represents the greatest wall normal stress and the last one the lowest. After plotting the wall yield locus diagram using (τ_w, σ_w) values, multiple parameters can be obtained through the line that crosses all points. The main parameters include the angle of wall friction φ_x and the coefficient of the wall friction μ. φ_x is the slope of a line running through the origin and μ is the ratio of wall shear stress τ_w to wall normal stress σ_w.

The system was adjusted on a 25% setting and the slip-stick mode was turned on during the whole test and the shear velocity mode was set to normal mode. Every test was repeated three times and one reading was selected.

3.9 **Differential Scanning Calorimetry (DSC)**

DSC was used to measure the temperature and heat flow associated with the transitions as a function of time and temperature in a controlled atmosphere. Only one batch from each sample (In-house and Contractor) was tested. The experiments were carried out using a DSC 1 (Mettler Toledo, UK), equipped with an intra-cooler system in order to assist the cooling of the system. A mass of 6.3mg was weighed for the In-house sample and 6.1mg for the Contractor sample in a 40µl sealed aluminium crucible and placed in the DSC sample chamber. The experiments were carried out by heating up the sample from 0 to 500°C at 3°C/minutes under nitrogen purge gas at 50ml/minute (constant flow rate). Mettler Star® software was used for programming the system and data processing.

3.10 **Digital Particle Image Velocimetry**

The selected granular materials for the DPIV test were the granules containing PEG 25% and Starch 25%. Two particle size ranges were selected (250-355µm) and (600-710µm) prepared by both granulation techniques. The other ranges were excluded because the arch tendency is very high at different hopper and silo segments, as shown in Figure 3.2 a, b.

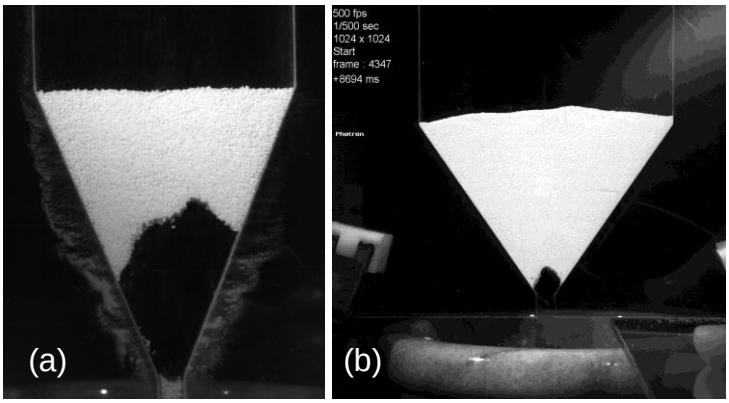

Figure 3.2 Arch formation with (a) PEG 15% granules (600-710µm), (b) Starch 5% granules (250-355µm).

Two different internal silo angles of 45° and 70° were used for the PIV study using one filling method. The study was conducted using a 2D set-up of laboratory scale dimensions using transparent Perspex sheets. Dimensions of both silos are shown in Figure 3.3. A high speed digital camera (photron fastcam viewer, model SA5) has been used to record the granular flow process at ambient room temperature at 500 frames per second, see Figure 3.4(a). Two fluorescent lamps have been used to illuminate the granular bed within the silo geometry, as shown in Figure 3.4(b). DynamicStudio V3.31 software platform (DSSP) from Dantec Dynamics was used for velocity vector analysis. Two transparent walls of Perspex sheet fixed with a wooden stand for two different angles, i.e. 45° and 70°, were taking place in between the Perspex sheet as seen in Figure 3.4(c).

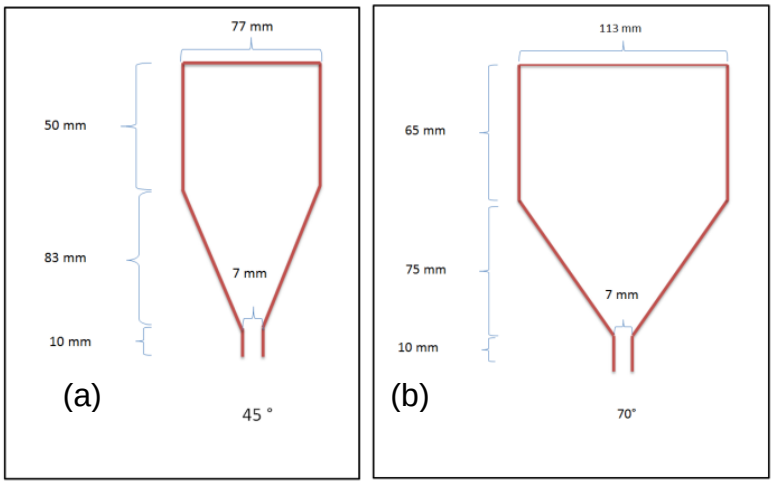

Figure 3.3 Dimensions of two geometric designs with two different angles 45º(a) and 70º(b).

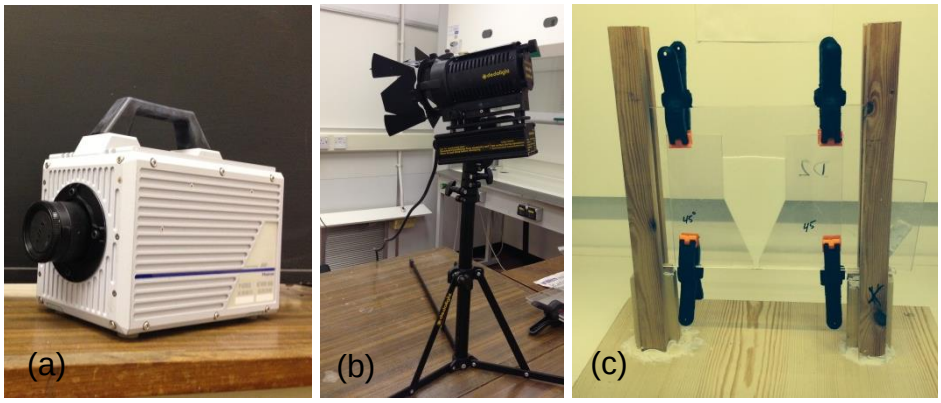

Figure 3.4 Experiments set-up (a) Speed camera. (b) Fluorescent lamp. (c) Wooden stand with perspex sheet.

Test procedure used:

The Perspex sheets were fixed with the selected angle and placed in the wooden stand. The outlet was closed to allow the granules to be filled inside the silo. The granules were filled slowly by using a small funnel until the required level was reached. The camera was turned on and focused on the silo. The lights were directed to the wooden stand to ensure the extent of the lights were sufficient for recording. The frame speed was selected from the software installed in the laptop. After recording, frames were saved for analysis. Fixed weights been used for each experiment. The outlet was opened immediately after starting recording.

Chapter 4 Results and discussion

4.1 Introduction

This chapter covers the physiomechanical properties for granules prepared by melt and wet granulation. Different qualitative results were obtained from angle of repose, bulk and tapped density, Carr's index and Hausner Ratio. Also, an SEM was used to compare the morphology of prepared granules while the DSC results indicated the effect of the binding ratio on melting points. Using the ring shear cell tester was an important quantitative method to measure flowability, cohesivity, wall friction and also for designing flow geometries. The flow trend was visualised inside the geometries using DPIV.

4.2 Physical and mechanical properties of the prepared granules

Physiomechanical properties for prepared granules by both granulation methods were analysed as follow.

4.2.1 Characterisation of granules prepared using wet granulation technique

The next paragraph will discuss the results obtained for the prepared granules including SEM and DSC.

4.2.1.1 Scanning electron microscope (SEM)

The SEM is a very useful and powerful qualitative or semi qualitative technique able to provide full details of particle morphologies due to its high potential resolution capability (Stern et al., 2004).

Starch is available commercially as white or whitish powder, depending on the source and manufacturing procedure. Under microscopic examination, raw starch granules are usually exerted as very small, spherical or ovoid granules, as shown clearly in Figure 4.1. Starch granules are semi crystalline granules composed of two main components, Amylose and Amylopectin and classified as porous material, as shown in Figure 4.1 (Rowe et al., 2003).

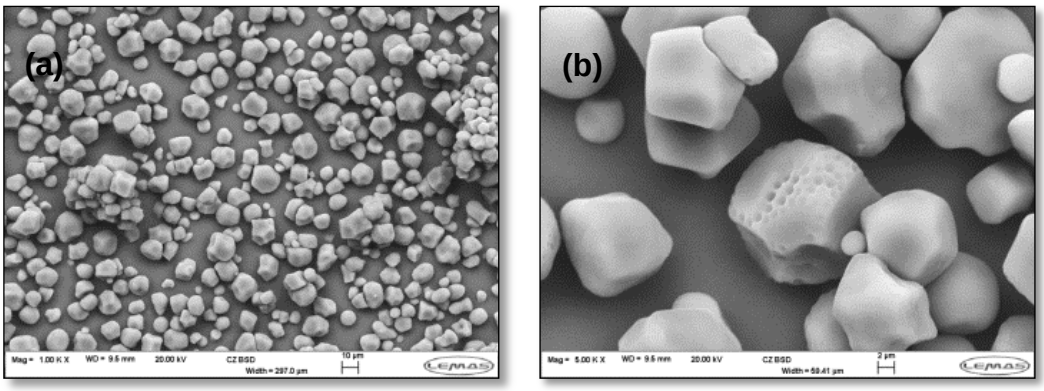

Figure 4.1 Images of the raw starch particles (a) at 10µm (b) at 2µm.

SEM examination of the wet granulated raw starch powder using 5%, 15% and 25% paste are shown in Figure 4.2 (a, b and c) respectively. The morphology of the starch granules shows that the granules have been become clumpier due to the effect of the percentage paste used.

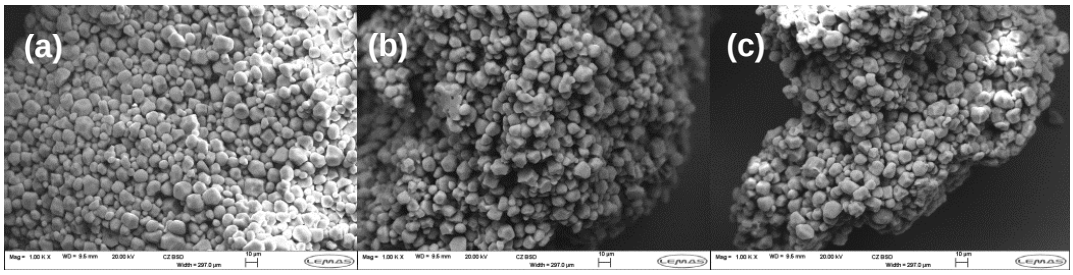

Figure 4.2 SEM images of the starch granules prepared by wet granulation technique using, (a) 5%, (b) 15% and (c) 25% starch paste.

Increasing binding ratios from 5% to 15% and up to 25% enhance the aggregation of the granules; the higher the binder ratio the more aggregated the granules. This is due to the fact that native starch powder is a polysaccharide compound consisting of 30% amylose and 70% amylopectin (Nguyen et al., 1998) and showing a high range of inter and intra granular-porosity (Sujka and Jamroz, 2010). Starch paste viscosity used for granulation purposes depends mainly on the amylose percentage within the paste. During the granulation process, amylose has the ability to form a film coat on the powder surfaces and forms a liquid bridge between contacting particles producing strong, dense granules (Rowe et al., 2003).

4.2.1.2 Differential scanning calorimetry DSC

The DSC has been conducted as a rapid and inexpensive method at this stage of research to investigate the effect of binding material inclusion on the melting point of the prepared granules. In the output results, any peak in the DSC thermogram curve is identified as a peak temperature, the onset and the offset temperature. In this experiment the peak shape was broad and not sharp enough; therefore the minimum peak temperature of the endothermic point of the peaks was used as a melting point of the samples.

The summary of the granules' DSC results prepared by the wet granulation technique using multiple starch paste concentrations is presented in Table 4.1. It can be seen clearly from the table that complete melting of the pure starch raw materials occurs at 140.77ºC, which is highly dependent on the crystal size and crystallinity of the sample, the onset temperature of melting starts at 127.97ºC and ends at 172.48ºC. In general, inclusion of starch paste shifts the onset to the right and the endset to the left. Increasing of starch paste concentrations from 15% and 25% gives marked changes in both the left and right shift due to the mixture crystallisation of the samples. For example, at binding ratio 15% starch paste, the melting point, onset and endset temperatures were 130.74ºC, 131.80ºC and 150.61ºC respectively. Increasing the binding ratio to 25% shifts the melting point, onset and endset temperatures to 130.52ºC, 135.04ºC and 155.44ºC respectively.

Table 4.1 Effect of starch paste inclusion on starch granules' melting points using DSC.

Sample Name	Onset Temp.	Endset Temp.	Peak Temp
Starch	127.97ºC	172.48ºC	140.77ºC
Starch 5%	129.07ºC	145.77ºC	130.28ºC
Starch 15%	131.80ºC	150.61ºC	130.74ºC
Starch 25%	135.04ºC	155.44ºC	130.52ºC

4.2.1.3 Physiomechanical properties

The physiomechanical properties of prepared granules using wet granulation have been evaluated by multiple tests including angle of repose, tapped density, Carr's index and Hausner Ratio and the results are illustrated in the Table 4.2. Values of

angle of repose for very fine granules using 5%, 15% and 25% of starch paste are 41.17°, 36.71° and 34.14° respectively. This indicates that increasing the binding ratio improves the value of angle of repose and consequently increases the flowability of the granules. Similarly, moderately coarse and coarse granules' angle of repose values are enhanced, and the values are 36.40°, 34.54° and 30.60° and 31.71°, 30.45° and 27.29° respectively at the same binding ratios.

In general, the obtained results indicate that increasing the binding ratio improves the angle of repose values in all granules ranges. For example, in the case of range (45-106μm) increasing the binding ratio from 5% to 15% improves the angle of repose by 10% and 7.5% respectively. Also the same improvement has been observed in the other ranges at the same binding ratio.

For granular bulk densities, there is a gradual increment in bulk density values among all ranges, either by increasing particle size or binding ratios. For instance, increasing the binding ratio for very fine granules from 5% to 15% increases bulk density by 4.4%, while coarse granules show 16.4% greater value than that obtained for very fine granules at the same binding ratio.

Values of the tapped densities were increased steadily with increasing binding ratio and particle size ranges. For example, tapped densities for very fine granules have been increased by 3% as the binding ratio increased from 15% to 25%, whereas coarse granules show an improvement of around 6% more than that obtained for very fine granules at 25% binding ratio.

The summarised results in Table 4.2 show that the wet granulation method improves granules' compressibility as observed through the marked decreases in Carr's index values. Increasing of both binding ratio and particle size ranges reduce the values significantly. The results indicate that increasing binding ratios from 5% to 15% for moderately coarse granules decreases Carr's index values by 7%, although increasing particle size ranges from very fine to coarse granules at 15% binding ratio decreases Carr's index value by 39%.

Similarly to the Carr's index, the values of the Hausner Ratio decreased with increasing binding ratio and granules ranges. For example, the values of the Hausner Ratio for very fine granules at binding ratio 5% and 15% were decreased by 3.4%, while they were decreased for very fine and coarse granules by 10% at 15% binding

ratio. This may indicate that the influence of particle size increases is higher than the increasing binding ratio.

Trend Table 4.3 summarises the physiomechanical properties for granules prepared by wet granulation. In general, the trend for angle of repose is decreased when particle size ranges and binding ratios are increased and the flowability is improved.

Bulk and tapped density are increased gradually by increased particle size ranges and binding ratios. Carr's index and Hausner Ratio are decreased by increasing particle size ranges and binding ratios for all prepared granules.

To conclude, the results indicate that the wet granulation method improves the granules' physiomechanical properties and flowability. This improvement can be observed clearly through the values of all evaluated parameters. Increasing binding ratio and particle size ranges shift the flow trend of granules from a passable flow trend at the very fine range with 5% binding ratio, to excellent flow trend at the coarse range with 25% binding ratio. In addition, concurrent steady increases of bulk and tapped densities' values with increasing particle size ranges and binding ratio mean that the granulation improves the packing arrangement of the granules and minimises inter-particles air voids. The larger the particle size at high binding ratio, the higher the dense particle size. Carr's index of very fine granules at 5%, 15% and 25% binding ratio has been shifted from passable to fair range, while coarse granules were in a good flow range in all binding ratios. This may indicate that the influence of particle size distribution on the flow properties is higher than the binding ratio. In respect of the Hausner Ratio, the higher binding ratios for all particle size ranges are less than 1.25 which indicates that the granules are freely flowing. Lower binding ratios of 5% and 15% were able to shift only coarse, and moderately coarse and coarse granules, respectively to freely flowing properties.

Table 4.2 Physiomechanical properties of granules prepared by wet granulation

Granulation method	Binding ratio	Granules Ranges [µm]	Angle of Repose (average)[°]	SD	Bulk Density (average)[kg/m^3]	SD	Tapped Density (average)[kg/m^3]	SD	Carr's Index	Hausner Ratio
Wet granulation (Starch)	5%	45-106	41.172	0.733	0.412	0.003	0.551	0.004	25.203	1.337
		250-355	36.4	0.664	0.441	0.004	0.556	0.004	20.653	1.26
		600-710	31.708	0.259	0.493	0.005	0.572	0.003	13.902	1.161
	15%	45-106	36.934	1.05	0.431	0.004	0.556	0.003	22.581	1.292
		250-355	34.545	1.055	0.459	0.007	0.568	0.006	19.167	1.237
		600-710	30.451	0.792	0.508	0.005	0.589	0.003	13.767	1.16
	25%	45-106	34.135	0.608	0.463	0.004	0.573	0.004	19.257	1.239
		250-355	30.602	0.69	0.495	0.004	0.597	0.005	17.101	1.206
		600-710	27.294	0.498	0.535	0.006	0.611	0.004	12.399	1.142

Table 4.3 Trend table for physiomechanical properties of granules prepared by wet granulation

Granulation method	Binding ratio	Granules ranges [µm]	Angle of Repose [°]	Bulk Density [kg/m^3]	Tapped density [kg/m^3]	Carr's Index	Hausner Ratio
Wet Granulation (starch)	5%	45-106	Passable-may hang up	0.412	0.551	Passable	Passable
		250-355	Fair-aid not needed	0.441 ↑	0.556 ↑	Fair	Passable
		600-710	Good	0.493 ↑↑	0.572 ↑↑	Good	Good
	15%	45-106	Fair-aid not needed	0.431	0.556	Passable	Passable
		250-355	Good	0.459 ↑	0.568 ↑	Fair	Fair
		600-710	Excellent	0.508 ↑↑	0.589 ↑↑	Good	Good
	25%	45-106	Good	0.463	0.573	Fair	Fair
		250-355	Excellent	0.495 ↑	0.597 ↑	Fair	Fair
		600-710	Excellent	0.535 ↑↑	0.611 ↑↑	Good	Good

4.2.2 Characterisation of prepared granules using melt granulation technique

4.2.2.1 Scanning electron microscope (SEM)

Polyethylene glycol PEG 6000 is available as white or off-white in colour and comes as waxy flakes, as shown clearly in Figure 4.3.

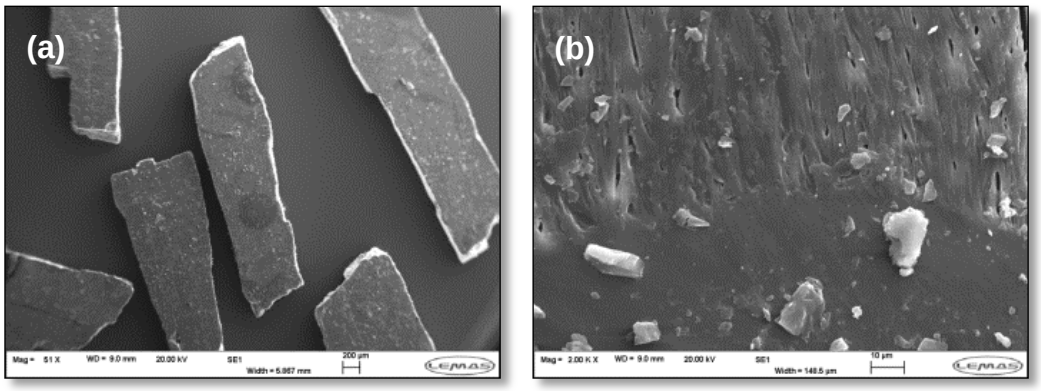

Figure 4.3 SEM images of PEG flakes at different magnification powers.

SEM examination of starch granules prepared by melt granulation technique using 5%, 15% and 25% PEG 6000 are shown in Figure 4.4 (a, b and c) respectively. Similarly to what has been observed previously for wet granulated granules, the morphology of the starch granules shows that the granules are aggregated, due to the effect of adding PEG 6000.

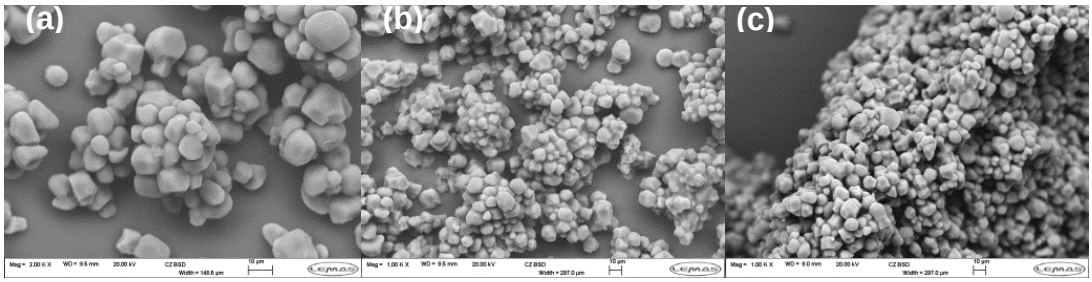

Figure 4.4 SEM images of the starch granules prepared by melt granulation technique using, (a) 5% , (b) 15% and (c) 25% PEG 6000.

The melting of PEG 6000 causes rapid initial agglomerate growth, leading to the creation of a large mean granule size and oversized agglomerates (Schæfer and

Mathiesen, 1996). This indicates that the distribution mechanism is the dominant method of nucleation. In general, raw PEG 6000 is available as moderate to large flakes, as shown in Figure 3.4; when melted, it produces large agglomerates showing a weak and loose structure that breaks down easily, especially at low binding concentration (Evrard et al., 1999). However, an increasing PEG binding ratio enhances powders' wettability and saturation leading to a greater smoothing of particulates surfaces (Ennis et al., 1991, Tardos et al., 1997). As a result, the coalescence mechanism dominates the agglomeration growth, leading to the formation of a semi spherical granule shape which has sufficient strength.

4.2.2.2 Differential scanning calorimetry (DSC)

Differential canning calorimetry (DSC 1 Mettler Toledo, UK), equipped with an intracooler system (Huber TC45), has been conducted in order to investigate the effect of binding material inclusion on the melting point of the prepared granules. Table 4.4 summarises the DSC results of granules prepared by melt granulation technique using PEG 6000. It is clear that the melting point of the pure PEG 6000 flakes occurs at 63.9ºC, the onset temperature starts at 59.39ºC and ends at 66.7ºC. In general, inclusion of PEG shifts the onset and endset to the left. Increasing the PEG concentrations to 15% and 25% produces minor shifting to the left of both sets. For example, at binding ratio 15% PEG the melting point, onset and endset temperatures were 56.15ºC, 53.96ºC and 57.54ºC respectively. Elevation of the binding ratio to 25% shifts the melting point, onset and endset temperatures to 55.92ºC, 57.44ºC and 53.36ºC respectively.

Table 4.4 Effect of PEG inclusion on starch granules melting points using DSC.

Sample Name	Onset Temp.	Endset Temp.	Peak Temp
PEG 6000	59.39 ºC	66.7 ºC	63.9 ºC
PEG 5%	56.64 ºC	58.79 ºC	57.86 ºC
PEG 15%	53.96 ºC	57.54 ºC	56.15 ºC
PEG 25%	53.36 ºC	57.44 ºC	55.92 ºC

4.2.2.3 Physiomechanical properties

Similarly to what has been conducted in the evaluation of granules prepared using the wet granulation method, the same procedures were applied here. The physiomechanical properties for prepared granules using melt granulation were evaluated by different tests including Angle of repose, Bulk and Tapped density, Carr's index and Hausner Ratio, as shown in Tables 4.5 and 4.6. The values of angle of repose of granules prepared by the different percentages of PEG, i.e. 5%, 15% and 25%, for very fine granules are 45.21°, 39.46° and 37.47° respectively. This reveals that increasing the binding ratio improves the values of angle of repose and increased flowability of the granules accordingly. Likewise, the angle of repose values for moderately coarse and coarse granules are 34.25° and 32.64° at 15% and 33.19° and 30.41° at 25% respectively; this indicates that the values of angle of repose are improved by increasing the binding ratio and flowability is enhanced. Overall, increasing particle size ranges at the same binding ratio improve the angle of repose in all ranges. For instance, for very fine granules, increasing the binding ratio from 5% to 15% improves the angle of repose values by 12.7% and 5% respectively, and that are reported with all ranges.

In bulk density, the values are gradually increased by increasing the binding ratio and particle size ranges. For example, for very fine granules, increasing the binding ratio from 5% to 15% increased the bulk density by 2.7%, whereas, for coarse granules it increased by 13.5% at same binding ratio of 25%.

For tapped densities results, the values were gradually increased with increasing particle size ranges and binding ratio. For instance, tapped densities values for very fine granules were increased by 3% as the binding ratio increased from 15% to 25%, while coarse granules values were improved by 4.6% at same binding ratio of 25%. Compressibility Index values, as shown in Tables 4.5 and 4.6, indicate that melt granulation has slightly improved the compressibility of prepared granules and this is clearly seen through the Carr's index values which decreased by increasing particle size and binding ratio. For example, increasing the binding ratio for moderately coarse granules from 5% to 15% decreased Carr's index values by 2.4%. However, Carr's index values are decreased by 9.7% by increasing the granules' particle size range from very fine to course at 15% binding ratio. Carr's index and

Hausner Ratio values are decreased in parallel with increasing binding ratio and particle size ranges. This is attributed to the concurrent decrease in both values of tapped and bulk densities. For example, the values of Hausner Ratio were decreased by 13.8% for very fine and coarse granules at the 5% binding ratio which might indicate that particle size has more influence on decreasing the Hausner Ratio than the binding ratio.

To sum up, and similarly to what has been observed previously for the wet granulation method, all the previous results indicate that there is a marked increase in the physiomechanical properties of granules prepared using the melt granulation method. The higher binding ratio granules of the large particle size are the most improved granules. This improvement can be observed through all the evaluated parameters.

The extent of improvements achieved by the melt granulation technique is less than that obtained by the wet granulation technique within all parameters. For example, coarse granules (600-710µm) at 25% binding ratio of melt and wet granulation methods show that angle of repose values are 30.41° and 27.29° respectively. According to Jenike's classification of angle of repose, the first angle of repose value is 30.41° and located at good flowability, while the second value is 27.29° and located in the excellent flow range. Likewise, the values of bulk and tapped densities which influence the values of Carr's index and Hausner Ratio showed a similar steady improvement. For instance, the values of bulk and tapped densities of coarse granules prepared by melt granulation are 0.51 kg/m^3 and 0.59 kg/m^3 respectively, while the values are 0.54 kg/m^3 and 0.61 kg/m^3 for the wet granulation method.

All the physiomechanical properties for the prepared granules have been illustrated in the trend table (Table 4.6). It is very obvious that the angle of repose is decreased by increasing the particle size ranges and binding ratios, which leads to improved flowability. Bulk and tapped density are increased gradually by increasing particle size ranges and binding ratios. For Carr's index and Hausner Ratio, they have different trends as they decreased when binding ratios and particle size ranges are increased.

The previous results provide evidence that the wet granulation method improved the physiomechanical properties of granules more than that obtained using the melt granulation method.

Table 4.5 Physiomechanical properties of granules prepared by melt granulation

Granulation method	Binding ratio	Granules Ranges [µm]	Angle of Repose (average)[°]	SD	Bulk Density (average)[kg/m^3]	SD	Tapped Density (average)[kg/m^3]	SD	Carr's Index	Hausner Ratio
Melt granulation (PEG)	5%	45-106	45.206	0.805	0.403	0.003	0.545	0.004	26.184	1.355
		250-355	41.269	0.931	0.435	0.004	0.554	0.004	21.458	1.273
		600-710	35.516	0.633	0.487	0.004	0.568	0.005	14.379	1.168
	15%	45-106	39.462	0.322	0.414	0.003	0.548	0.003	24.414	1.323
		250-355	34.248	0.625	0.442	0.005	0.559	0.005	20.939	1.265
		600-710	32.638	0.461	0.498	0.006	0.583	0.005	14.545	1.17
	25%	45-106	37.467	0.845	0.441	0.003	0.565	0.004	22.048	1.283
		250-355	33.185	0.863	0.466	0.005	0.582	0.004	19.848	1.248
		600-710	30.406	0.928	0.51	0.007	0.592	0.003	13.846	1.161

Table 4.6 Trend table for Physiomechanical properties of granules prepares by melt granulation

Granulation method	Binding ratio	Granules ranges [µm]	Angle of Repose [°]	Bulk Density [kg/m^3]	Tapped density [kg/m^3]	Carr's Index	Hausner Ratio
Melt Granulation (PEG)	5%	45-106	Passable-may hang up	0.403	0.545	Poor	Poor
		250-355	Passable-may hang up	0.435 ↑	0.554 ↑	Passable	Passable
		600-710	Good	0.487 ↑↑	0.568 ↑↑	Good	Good
	15%	45-106	Fair-aid not needed	0.414	0.548	Passable	Passable
		250-355	Good	0.442 ↑	0.559 ↑	Fair	Passable
		600-710	Good	0.489 ↑↑	0.583 ↑↑	Good	Good
	25%	45-106	Fair-aid not needed	0.441	0.565	Passable	Passable
		250-355	Good	0.466 ↑	0.582 ↑	Fair	Fair
		600-710	Good	0.51 ↑↑	0.592 ↑↑	Good	Good

4.3 Evaluation of granular materials' flowability using ring shear cell tester (RST-XS)

Ring shear data analysis for flowability ratio ff_c can be obtained from plotting the unconfined yield strength f_c or σ_c versus major consolidating stress or major principal stress σ_1. The powders' and granules' flow regions, according to Jenike's classifications, are divided into four ranges, see Figure 2.14. The grey dotted lines plot from left to right which represent the four ff_c values 1, 2, 4 and 10 respectively. Three different ranges of granules prepared by two granulation methods were selected for evaluation; very fine granules (45-106µm), moderately coarse granules (250-355µm) and coarse granules (600-710µm).

4.3.1 Evaluation of binding efficiency of PEG 5% and starch 5%

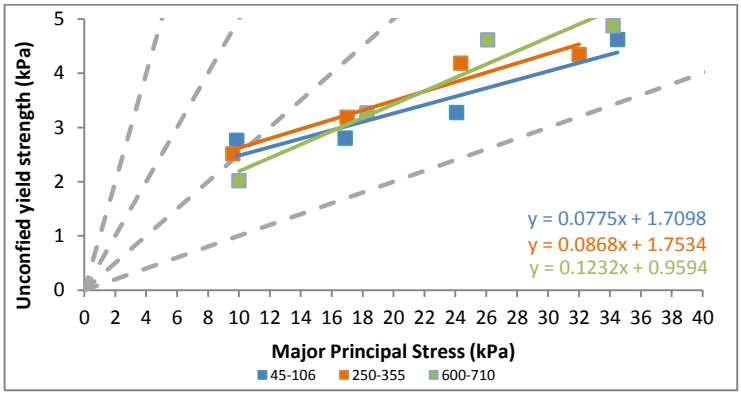

Figure 4.5. Unconfined yield strength σ_c vs. major principal stress σ_1 of PEG 5% granules at three particle size ranges.

Figure 4.5 shows the influence of increasing major principal stress on granular materials' flowability for the starch granules prepared by melt granulation using 5% PEG. Increasing the stress leads to marked increases in flowability of PEG 5% granules, especially for very fine and moderately coarse granules. The flow function ff_c values are 3.6 and 3.8 at 5kPa for very fine and moderately coarse granules respectively; more details are shown in Table A.1. At this force magnitude, both ranges are located at cohesive range (2-4); increasing the major principal stress to 17kPa shifts ff_c values to 7.5 and 7.4 which are located in easy flowing ranges and the flowability improves by $\approx 108\%$ and 94% respectively. The coarse granules

remain within easy flowing range at all shearing loads from 5 to 17kPa. At 5kPa the coarse granules have an ff_c value equal to 5 and show a marked improvement in flowability by around $\approx 40\%$ as the shear force increased to 17kPa.

Extrapolations of the data plots with Y axis represent the values of unconfined yield strength at zero major principal stress. Extra care should be taken during extrapolation to minimise the error (Marjanović and Jones, 1996, Gijón-Arreortúa and Tecante, 2014). The unconfined yield strength represents the stress needed to induce the failure of compacted powder. These magnitudes are 1.7098kPa, 1.7534kPa and 0.9594kPa for very fine, moderately coarse and coarse granules respectively. Large values indicate that granules are more compressible due to the high adhesive force between particles.

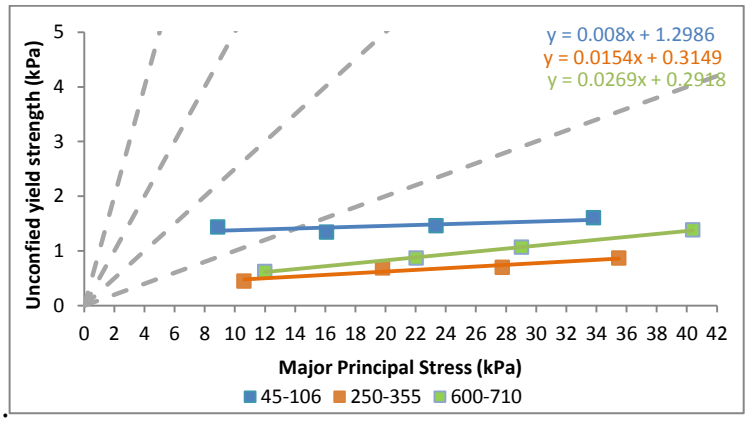

Figure 4.6. Unconfined yield strength, σ_c vs. major principal stress, σ_1 of Starch 5% granules for three particle size ranges.

Figure 4.6 shows the influence of increasing major principal stress on granules flowability prepared by the wet granulation method using 5% starch paste. Increasing the major principal stress leads to marked increases in flowability of granules. For example, at 5kPa the value of ff_c for very fine granules is 6.2 which is located within easy flowing range (4-10); increasing the major principal stress to 17kPa shifts the granular materials' flow trend to free flowing range (> 10) and the flowability is improved by $\approx 238\%$. More data are available in Table A.2.

Both moderately coarse and coarse granules are located in the free flowing range and ff_c values are 24 and 19.1 at 5kPa respectively as shown in Table A.2. Altering

major principal stress to 17kPa makes a considerable improvement in granules flowability by around $\approx 70\%$ and 51% respectively.

The plot also shows the unconfined yield strength value at zero principal stress. These values are 1.2986kPa, 0.3149kPa and 0.2918kPa for very fine, moderately coarse and coarse granules respectively. The value for very fine granules is larger compared to the values of moderately coarse and coarse granules. Large value indicates that granules' compressibility is greatly influenced by inter-particle cohesive forces (Li et al., 2004).

4.3.2 Evaluation of binding efficiency of PEG 15% and starch 15%

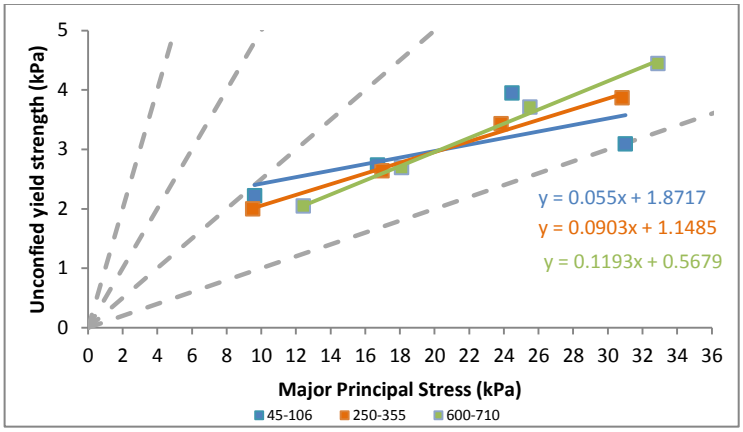

Figure 4.7 Unconfined yield strength σ_c vs. major principal stress σ_1 of PEG 15% granules at three particle size ranges.

Figure 4.7 shows the flowability behaviour of granules prepared by the melt granulation method using 15% PEG. Increasing major principal stress leads to marked increases in flowability of PEG 15% granules, especially for very fine granules. The flow function ff_c at 5kPa is 4.3 and located in the easy flowing range; increasing major principal stress to 17kPa leads to a marked increase in ff_c value reaching 10 which locates it at the borderline of the free flowing range. This increment of major principal magnitude shifts the flowability towards the free flowing range and the flowability is significantly increased up to $\approx 132\%$.

Table A.3 summarises the values of σ_1, σ_c and ff_c for all granules' ranges prepared using the melt granulation method. The results show that moderately coarse and

coarse granules ff_c values at 5kPa are 4.8 and 6.1 respectively. Both ff_c values are located in the easy flowing range. Increasing the major principal stress improves their flowability up to ≈ 66% and ≈ 21% respectively within the easy flowing range. Unconfined yield strength values at zero major principal stress are illustrated in Figure 4.7 as (m) on the extrapolated line equation. The σ_c values are 1.8717kPa, 1.1485kPa and 0.5679kPa for very fine, moderately coarse and coarse granules respectively. The larger σ_c value indicates the more compressible granules character due to inter-particle adhesive force. Large particle size exerts less adhesive forces and consequently less σ_c value.

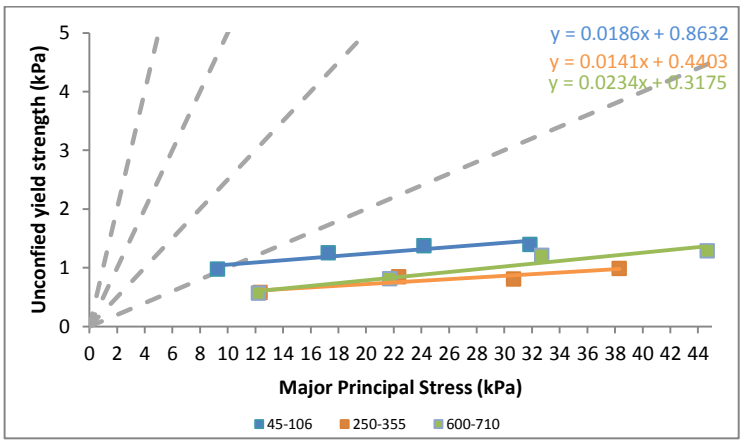

Figure 4.8 Unconfined yield strength σ_c vs. major principal stress σ_1 of starch 15% granules at three particle size ranges.

Figure 4.8 shows the flowability trend of granules prepared by the wet granulation technique using 15% starch paste. Elevation of major principal stress leads to a marked increase in flowability behaviour among all particle size ranges. At 5kPa, the very fine granules' flow function ff_c is 9.5 which is located in the easy flowing range. Increasing the major principal stress to 17kPa significantly improved the flowability of the granules and ff_c values reached 23 and almost around ≈ 142% improvement was achieved at 5kPa. The other two particle size ranges of moderately coarse and coarse granules' flow function values ff_c are 21 and 22 respectively at 5kPa. Increasing major principal stress to 17kPa improves their flow function by ≈ 85% and 59% respectively. Further details are available in Table A.4.

In addition, Figure 4.8 shows unconfined yield strength values at zero major principal stress for all particle size ranges. Their magnitudes are 0.8632kPa, 0.4403kPa and 0.3175kPa for very fine, moderately coarse and coarse granules respectively. These values are considered to be a reflection of the adhesive forces between particles which are decreased for an increase in particle size of the granules.

4.3.3 Evaluation of binding efficiency of PEG 25% and starch 25%

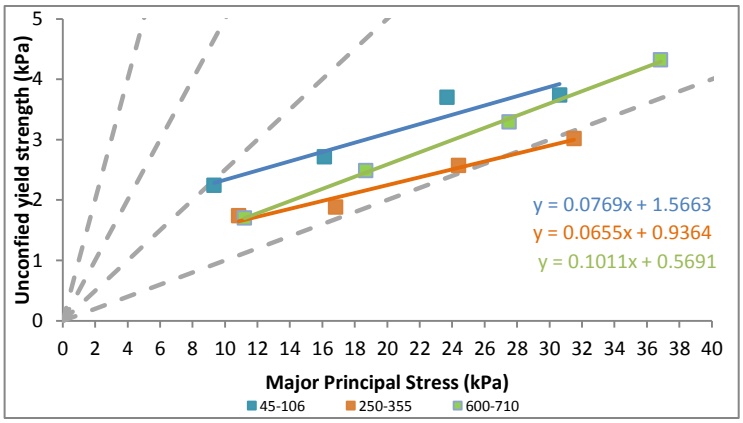

Figure 4.9 Unconfined yield strength σ_c vs. major principal stress σ_1 of PEG 25% granules at three particle size ranges.

Figure 4.9 illustrates the flow behaviour of multiple particle sized granules prepared by the melt granulation technique using 25% PEG as a binding ratio. It can clearly be seen that increasing the major principal stress leads to marked increases in granular flowability, especially for very fine and moderately coarse granules. At 5kPa load, their flow function ff_c values are 4.2 and 6.2 respectively and both are located in the easy flowing range. More details are available in Table A.5. The elevation of major principal stress to 17kPa obviously improves the granular flowability up to $\approx$ 95% and 67% respectively. In the case of moderately coarse granules, the ff_c is shifted from the easy flowing range at 5kPa to the freely flowing range at 17kPa. The coarse granules flow function values ff_c remains within the easy flowing range at both major principal loads. At 5kPa the flow function ff_c is 6.6 and 8.5 at 17kPa. Load elevation from 5kPa to 17kPa improves granular flowability of coarse granules by $\approx$ 28% within the same flow range.

Figure 4.9 also displays the magnitudes of unconfined yield strength values at zero major principal stress. These magnitudes are 1.5663kPa, 0.9364kPa and 0.5691kPa

respectively. The extents of these values are decreased by increasing the particle size of the granules.

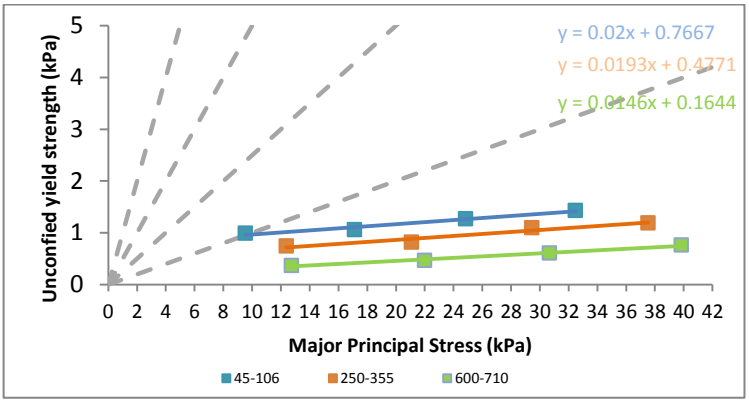

Figure 4.10 Unconfined yield strength σ_c vs. major principal stress σ_1 of Starch 25% granules at three particle size ranges .

Figure 4.10 demonstrates the flowability behaviour of granules prepared by the wet granulation technique using 25% starch paste. Increasing major principal stress leads to a marked increase in granular flowability. Flow function ff_c for very fine granules at 5kPa is 9.6 and located in the easy flowing range; increasing the major principal stress to 17kPa shifts the flowability to free flowing range and the flowability is significantly improved up to ≈ 139%. The flow function ff_c for both moderately coarse and coarse granules is 25 and 35 at 5kPa respectively and located in the free flowing range. Increasing the major principal stress to 17kPa improved their flowability to ≈ 28% and 50% respectively and remained within the freely flowing range. Additional information is available in Table A.6.

Additionally, Figure 4.10 displays the values of unconfined yield strength at zero major principal stress for all particle size ranges. The values are 0.7667kPa, 0.4771kPa and 0.1644kPa for very fine, moderately coarse and coarse granules respectively. It is very clear that the values are relatively low compared to the granules prepared using 25% PEG and across other starch and PEG binding ratios. This coarse range requires minimum unconfined yield strength to induce granular failure among all patches. This indicates that granules prepared using the wet granulation method at 25% starch paste has the most flowable patch.

To conclude, the previous results indicate that the granular flowability behaviour tends to increase by increasing the major principal stress. The influence of increasing major principal stress on granular flowability is more significant for very fine granules compared to moderately coarse and coarse granules.

In the case of the melt granulation technique, increasing the binding ratio from 5% to 15% for very fine granules at 5kPa improves the flowability by 19.4%. In contrast, increasing the binding ratio from 5% to 25% at the same load improves the flowability by around 17%. This may indicate that 15% PEG binding ratio is sufficient to improve the flowability behaviour to the required limit for this particular particle size range. On the other hand, increasing the binding ratio from 5% to 15%, 15% to 25% and 5% to 25%, for coarse granules at 5kPa improves the flowability trend by around 22%, 8.5% and 32% respectively. These results indicate that, at this particular particle size range, increasing the binding ratios to 25% improves the flowability higher than that observed at 15%.

In the case of very fine granules prepared by the wet granulation method altering binding ratios from 5% to 15%, 15% to 25% and 5% to 25% enhances granular flowability by 53.2%, 1% and 54.9% respectively at 5kPa. These results indicate that increasing the binding ratio by 15% or 25% has the same influence on granular flowability for this particular particle size range. The results of the coarse granules ranges indicates that the elevation of binding ratios from 5% to 15%, 15% to 25% and 5% to 25% improves the granular flowability by around 15%, 59% and 83% respectively at 5kPa.

In general, the unconfined yield strength at zero major principal stress is significantly influenced by the binding ratio and particle size ranges for both granulation techniques. Furthermore, the unconfined yield strength values for granules prepared by the wet granulation method are substantially lower than that prepared by the melt granulation for the same particle size ranges. This can be attributed to the high cohesive inter-particle forces on granules prepared using PEG binding ratio.

According to Jenike's flowability classification, starch granules in all particle size ranges are more flowable than their corresponding PEG granules. Figures 4.6, 4.8 and 4.10 display clearly that starch granules are located in the free flowing range

while PEG granules are located in the easy flowing range. The higher the binding ratio the more flowable the granules are for both granulation techniques.

4.4 Evaluation of granular materials' cohesivity using ring shear cell tester (RST-XS)

Granular material cohesivity can be evaluated using the ring shear tester by plotting the data of Yield locus plot. Figure 4.11shows the Yield locus plot; the X axis represents major principal stress σ_1 and the Y axis represents shear force τ. The applied shear forces during this test are 5, 4, 3, 2 and 1kPa. The extrapolated values of the plot at Y axis τ at zero major principal stress represent the granular materials' cohesivity (Schulze, 2008).

4.4.1 Evaluation of granular cohesivity of PEG 5% and Starch 5%

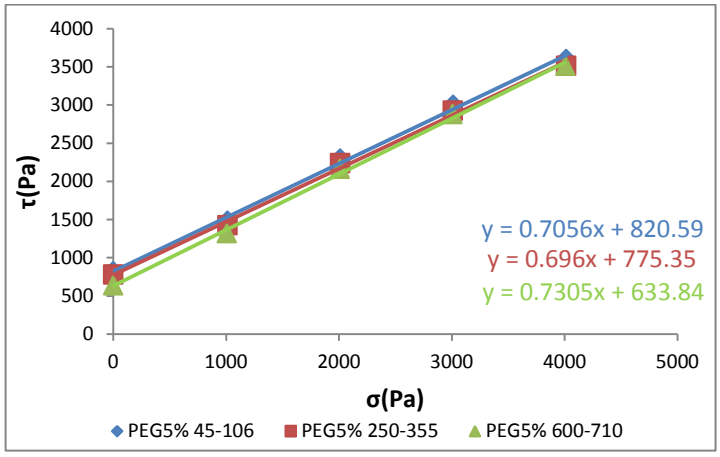

Figure 4.11 Yield locus plot for prepared granules by melt granulation method using PEG 5%.

Figure 4.11 shows the yield locus plot for the granules prepared by the melt granulation technique using 5% PEG. Extrapolated data on the Y axis indicate the magnitude of granules cohesivity at zero major principal stress and presented as (m) value in the equation. The magnitudes of granular cohesivity are 820.59 Pa, 775.35 Pa and 633.84 Pa for very fine, moderately coarse and coarse granules at 5kPa respectively. It is obvious that very fine granules have the highest value followed by moderately coarse and coarse granules. This might be attributed to the adhesive

forces between particles. The main inter-particle forces are van der Waals forces (Schulze, 2008)

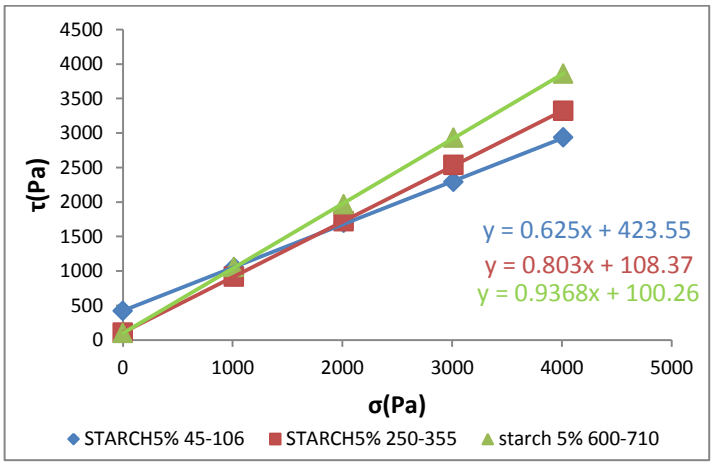

Figure 4.12 Yield locus plot for granules prepared using wet granulation method with 5% starch paste.

Figure 4.12 demonstrates the yield locus for the granules prepared using the wet granulation with 5% starch paste. The values of extrapolated data on the Y axis at zero major principal stress are 423.55 Pa, 108.37 Pa and 100.26 Pa for very fine, moderately coarse and coarse granules respectively. The obtained values from the equation are representing the cohesivity of the granules. It is clear that the cohesivity decreases by increasing the particle size ranges due to the less influence from inter-particle adhesive forces in this granules range.

4.4.2 Evaluation of granular cohesivity of PEG 15% and Starch 15%

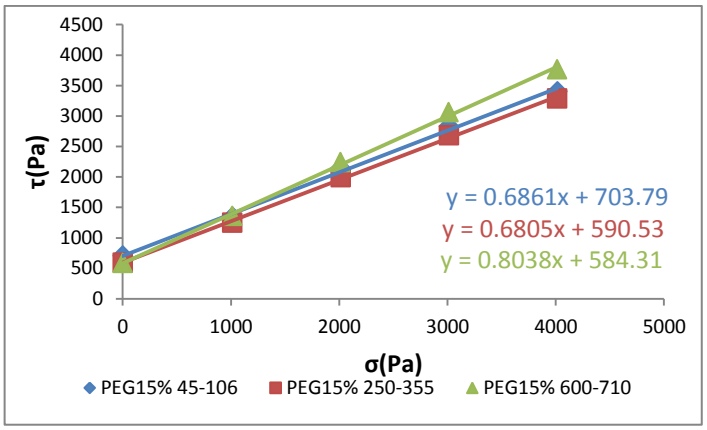

Figure 4.13 Yield locus plot of granules prepared by melt granulation method using PEG 15%.

Figure 4.13 shows the yield locus plot for the granules prepared by the melt granulation technique of using 15% PEG binding ratio. Extrapolated values on the Y axis indicate the granules cohesivity at zero principal stress. These obtained values are 703.79 Pa, 590.53 Pa and 584.31 Pa for very fine, moderately coarse and coarse granules respectively. It is noticeable that very fine granules have the highest value of the intercept and indicate their high cohesivity compared to other particle size ranges. The cohesivity value decreased with an increase in particle size ranges.

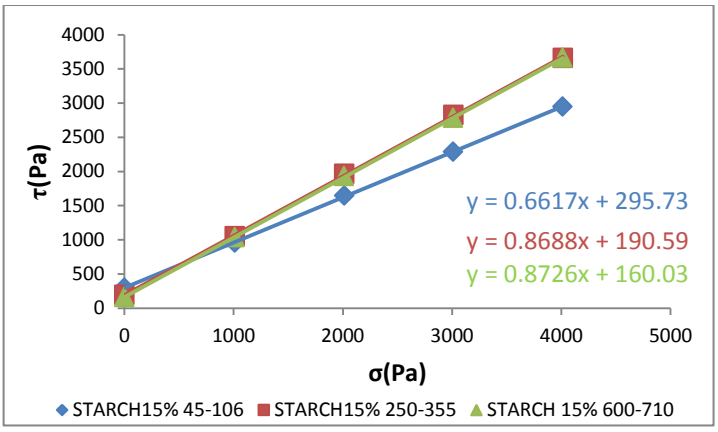

Figure 4.14 Yield locus plot of granules prepared using wet granulation with 15% starch paste.

Figure 4.14 shows the yield locus plot of prepared granules by wet granulation using starch 15% paste. The plot displays the extrapolated data of the Y axis at zero major principal stress. These values are 2.95.73 Pa, 190.59 Pa and 160.03 Pa for very fine, moderately coarse and coarse granules respectively. It is clear that the small particle size range showed more cohesivity compared to moderately coarse and coarse granules.

4.4.3 Evaluation of granular cohesivity of PEG 25% and Starch 25%

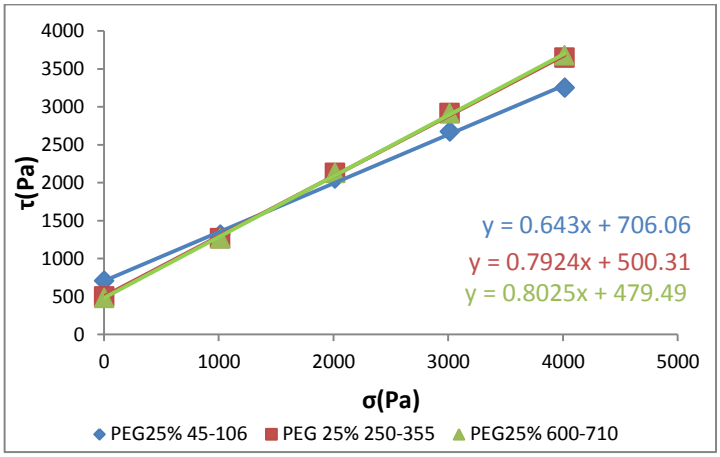

Figure 4.15 Yield locus plot of prepared granules by melt granulation using 25% PEG.

Figure 4.15 illustrates the yield locus plot for granules prepared using melt granulation with 25% PEG binding ratio. The extrapolated data of the Y axis at zero principal stress are shown in the plot and represent the granules cohesivity. The magnitudes are 706.06 Pa, 500.31 Pa and 479.49 Pa for very fine, moderately coarse and coarse granules respectively. It can be clearly seen that the cohesivity is high in small particle size due to the cohesive forces then it decreases by increasing the particle size ranges.

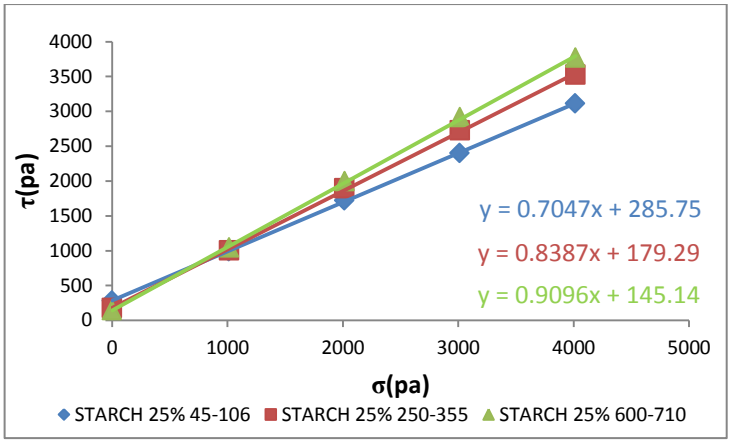

Figure 4.16 Yield locus of prepared granules using wet granulation with 25% starch paste.

Figure 4.16 shows the granules prepared by wet granulation using 25% starch paste.

The extrapolated data of the Y axis at zero major principal stress represent the granules cohesivity. The values of obtained values are 285.75 Pa, 179.29 Pa and 145.14 Pa for very fine, moderately coarse and coarse granules respectively. It is very clear that very fine granules are more cohesive compared to other particle size ranges, and that cohesivity is decreased by increasing the particle size of the granules.

To summarise, granular cohesivity is highly influenced in both granulation methods and particle size ranges. The smallest granular size is the most cohesive for all major principal stresses. Moreover, the cohesivity values are decreased in both granulation methods by increasing the binding ratio. In general, comparing the same particle size prepared using different granulation methods, the granules prepared using the melt granulation method are more cohesive than those obtained by wet granulation. This might give an indication that the wet granulation method is more efficient than the melt granulation method from a cohesivity point of view.

4.5 **Wall friction**

According the previous results and evaluations, it is clearly observed that the high binding ratio (25% PEG and 25% Starch) showed the best micromechanical properties and flowability trends, especially in the moderate and large particle size

ranges (250-355µm) and (600-710µm). Therefore, these four cases of granules have been selected for wall friction test, silo designing and dynamic flow evaluation using particle image velocimetry. More details about the rest of the formula are available in Table 4.7.

Wall friction yield against the Perspex wall has been conducted using RST-XS and the wall yield locus is plotted using normal vertical stress σ_w and τ_w. The values of the angle of wall friction φ_x (Eq. 4.11) and wall friction coefficient μ (Eq. 4.12) were determined using the wall yield locus plot. The effective angle of internal friction φ_e was obtained by yield locus.

$$\varphi_x = \arctan\left(\frac{\tau\omega}{\sigma\omega}\right) \tag{4.11}$$

$$\mu = \frac{\tau_w}{\sigma_w} \tag{4.12}$$

4.5.1 Evaluation of wall friction of granules prepared by melt granulation technique using 25% PEG at (250-355µm)

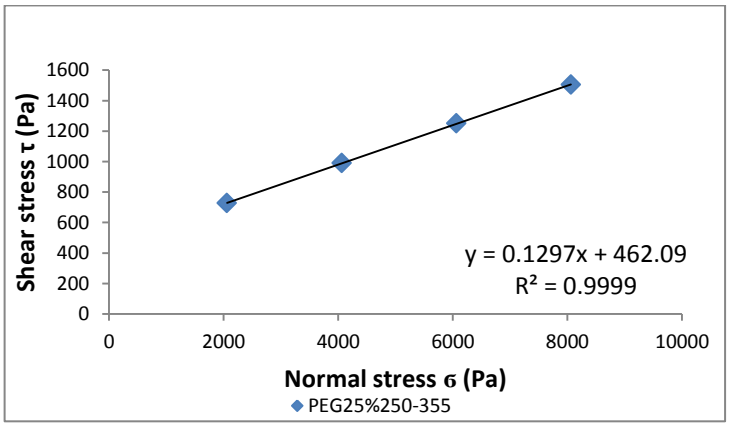

Figure 4.17 Wall yield locus of moderately coarse granules (250-355µm) using 25% PEG.

Figure 4.17 shows the wall yield locus plot for moderately coarse granules prepared using the melt granulation technique at 25% PEG binding ratio. At 5kPa normal stress, the angle of wall friction φ_x and wall friction coefficient μ values are 7.4° and 0.1297 respectively.

4.5.2 Evaluation of wall friction of granules prepared by melt granulation technique using 25% PEG at (600-710µm)

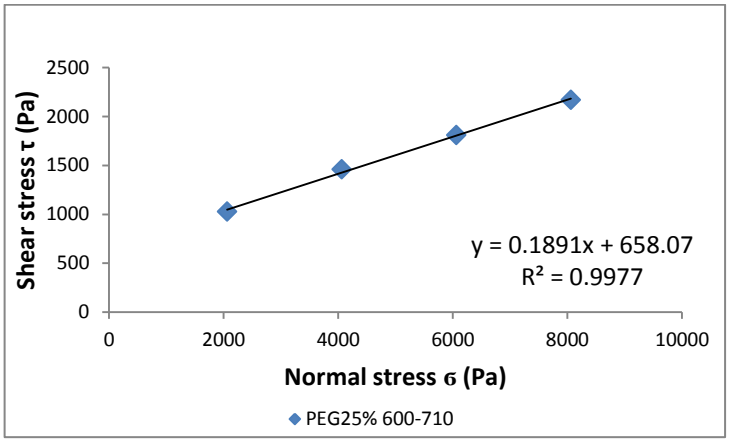

Figure 4.18 Wall yield locus of coarse granules (600-710µm) using 25% PEG.

Figure 4.18 illustrates the wall yield locus plot for coarse granules prepared by the melt granulation technique at 25% PEG binding ratio. At 5kPa normal stress, the angle of wall friction φ_x and wall friction coefficient µ values are 10.7° and 0.1891 respectively.

4.5.3 Evaluation of wall friction of granules prepared by wet granulation technique using 25% starch paste at (250-355µm)

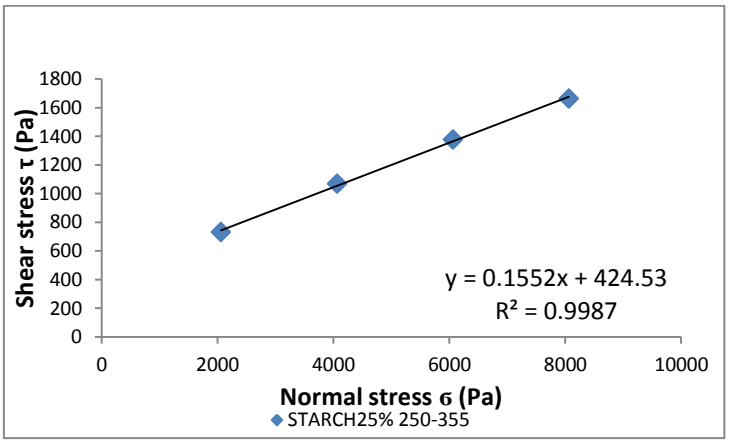

Figure 4.19 Wall yield locus of moderately coarse granules (250-355µm) using 25% starch.

Figure 4.19 shows the wall yield locus plot for moderately coarse granules prepared by wet granulation using 25% starch paste. At 5kPa normal stress, the angle of wall friction φ_x and wall friction coefficient μ values are 8.8° and 0.1552 respectively.

4.5.4 Evaluation of wall friction of granules prepared by wet granulation technique using 25% starch paste at (600-710μm)

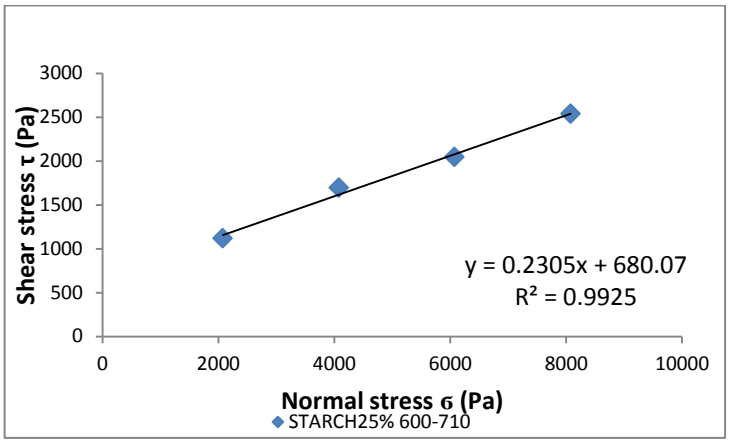

Figure 4.20 Wall yield locus of coarse granules (600-710μm) using 25% starch.

Figure 4.20 shows the wall yield locus plot for coarse granules prepared by wet granulation using 25% starch paste. At 5kPa normal stress, the angle of wall friction φ_x and wall friction coefficient μ values are 13° and 0.2305 respectively.

To conclude, the angle of wall friction and wall friction coefficient of both moderately coarse and coarse granules prepared by the wet granulation technique are higher than those obtained from the melt granulation granules. At 5kPa, the angle of wall friction and wall friction coefficient are 7.4° and 0.1297, and 10.7° and 0.189 respectively for moderately coarse and coarse granules prepared by the melt granulation technique. On the other hand, the values are 8.8° and 0.1552, and 13° and 0.2305 respectively for moderately coarse and coarse granules prepared by the wet granulation technique. This means that the friction between the granules and the boundaries' surfaces for granules prepared using the wet granulation technique is greater than that obtained by melt granulation granules. This could be attributed to the ability of PEG to smooth the granules' surfaces and decrease the friction.

More details about evaluated ranges are shown in Table 4.7.

Table 4.7 Wall yield locus results of all particle sizes granules prepared using both granulation techniques including φ_e[°].

Granulation method	Binding ratio	Particle size(µm)	φ_x^o	φ_e^o	ρ_b kg/m^3
MELT GRANULATION (PEG)	5%	45-106	14.4	44	422
		250-355	7.5	43	425
		600-710	9.2	42	461
	15%	45-106	10.8	41	428
		250-355	7.3	41	420
		600-710	10.1	43	446
	25%	45-106	12.8	40	431
		250-355	7.4	43	434
		600-710	10.7	43	449
WET GRANULATION (STARCH)	5%	45-106	9	36	420
		250-355	6.8	40	469
		600-710	10.1	44	485
	15%	45-106	10.2	36	428
		250-355	7.2	42	461
		600-710	11.1	42	492
	25%	45-106	9.8	38	434
		250-355	8.8	41	515
		600-710	13	43	521

4.6 Designing silo and hopper for the evaluated granule properties using data obtained from RST-XS

At this stage of my research and according to the previously obtained results, it is possible to predict the proper design of a silo and hopper suitable profile mass flow trend. Based on the previously obtained results from the evaluation of granular flowability, cohesivity and wall friction tests, two particle sizes were chosen from each granulation method; the selected ranges have the same binding ratios (25% PEG and 25% starch), the selected particle sizes are moderately coarse (250-355µm) and coarse (600-710mm) granules.

4.6.1 Designing of conical hopper and silo geometry for moderately coarse granules prepared by melt granulation technique using 25% PEG

The first step in designing a silo and hopper is to gather all the parameters needed for designing the process summarised in Table 4.8 for moderately coarse granules prepared by melt granulation using 25% PEG binding ratio.

Table 4.8 Yield locus results of moderately coarse granules PEG 25%.

YIELD LOCUS No.	σ_1 [Pa]	σ_c [Pa]	Pь [kg/m^3]	φe[°]
1	10835	1742	349	40
2	16821	1882	353	40
3	24390	2575	353	40
4	31508	3017	434	40

From the previous wall yield locus results, the angle of wall friction $\varphi_x = 7.4^o$ flow factor value ff depends on the values of both the internal angle of friction and the angle of wall friction. For this particular particle size range, the angle of wall friction is equal to 7.4° and the internal angle of friction is equal to 43º; as shown in Table 4.7, the value of ff obtained from the plotted diagram in Figure 4.21 equals 1.6.

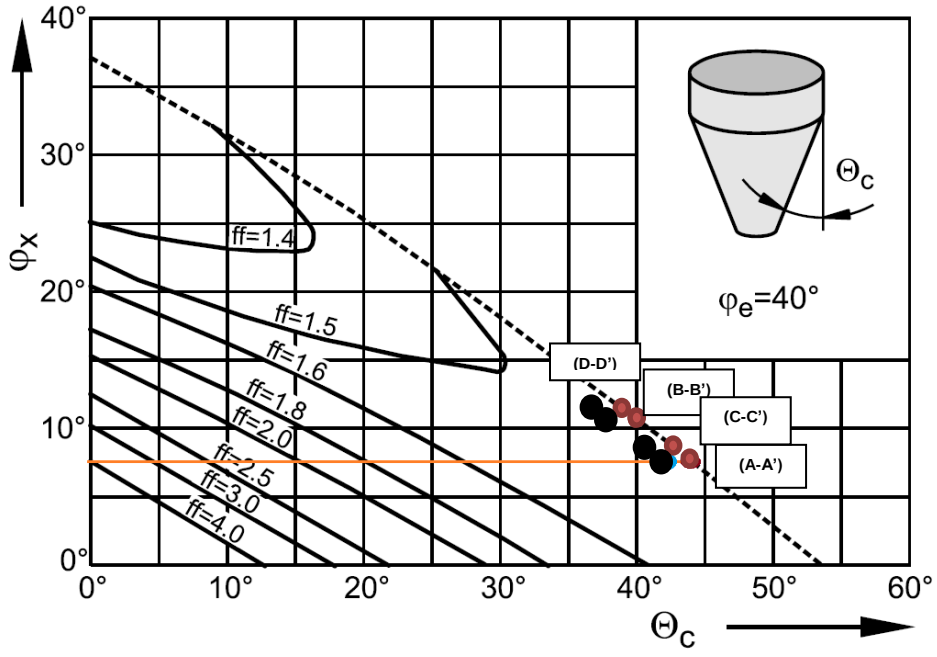

Figure 4.21 Flow factor diagram for conical hopper and $\varphi_e = 40°$ (Schulze, 2008).

To calculate hopper slope angle Θ_c that is able to give the mass flow trend, Figure 4.21 is used and the value of the inclined angle is $\Theta c = 44^o$ (A-A'). (A represents the point of intercept of φ_x value with the mass flow boundary for the conical hopper and A' represents the same point after reduction by safety margin). The value of the angle is located at the mass flow boundary (A), the value should be reduced by a safety margin of 2^o to 3^o (A') (Schulze, 2008). Thus the final hopper slope angle to produce mass flow trend is $\Theta_c = 42^o$. The next steps in the calculation of hopper and silo design are to determine the minimum outlet dimensions to avoid arch formation. This can be achieved by plotting unconfined yield strength σ_c, bulk density ρ_b and effective angle of internal friction φ_e against σ_1 axis using the same σ_1 unit as shown in Figure 4.22.

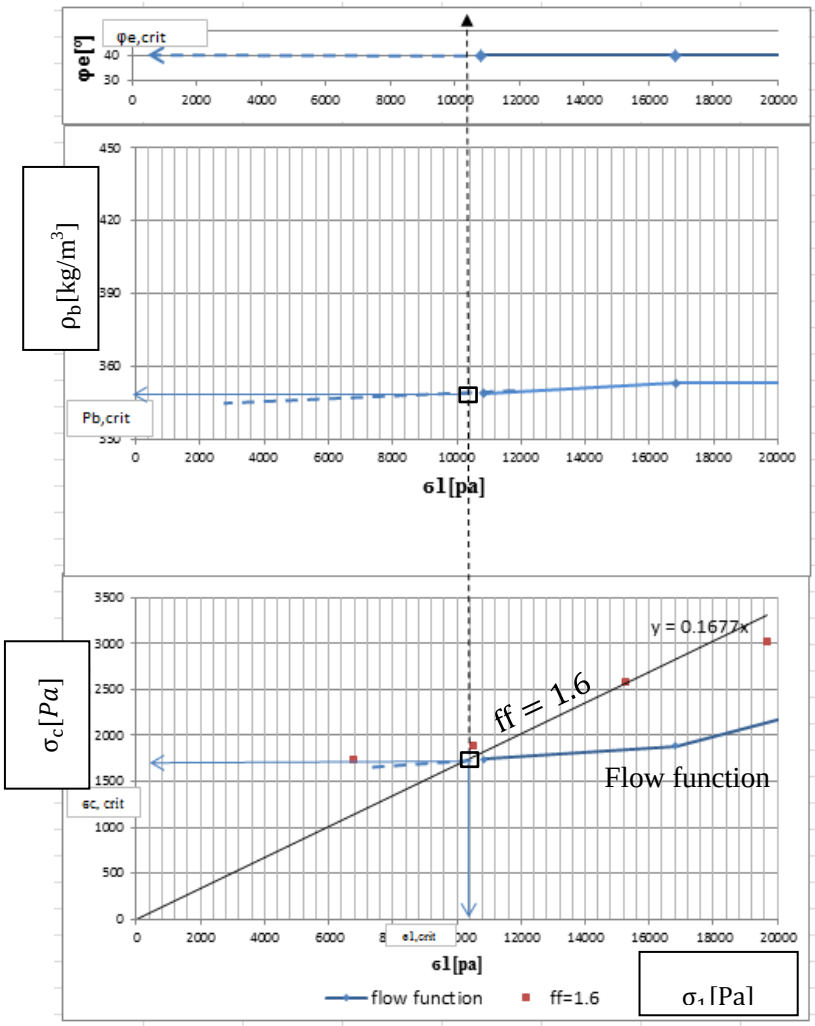

Figure 4.22 Diagram showing flow properties for the determination of minimum outlet dimension to avoid arching (black squares represent critical values according to the point of intersection of the flow function with the major principal stress in the arch σ_1').

From Figure 4.22, the listed critical parameters below can be obtained at the intersection point of the flow factor plot and the extrapolated yield locus plot. Bearing stress σ_1' is drawn by using (Eq. 2.8) and the line is passing the origin. The values of the parameters are;

$\sigma_{1,crit}$ = 10390 Pa.

$\sigma_{c,crit}$ = 1750 Pa.

$\rho_{b,crit}$ = 350 kg/m^3.

$H(\Theta_c)$ = 2.63. This value can be obtained from Figure 2.21.

Critical outlet dimensions can be calculated using (Eq. 2.10), as shown below.

$$d_{crit} = H(\Theta_c)\frac{\sigma_{c,crit}}{gP_{b,crit}} \quad (2.10)$$

$$d_{crit} = 2.63\frac{1750}{9.81\times350}$$

$$d_{crit} = 1.340 \text{ m.}$$

To obtain the mass flow for moderately coarse granules prepared by melt granulation using PEG 25% binding ratio, the best fit internal angle for a conical hopper is 96° with outlet diameter = 2.680m.

4.6.2 Designing of a wedge-shaped hopper and silo geometry for moderately coarse granules prepared by melt granulation technique using 25% PEG

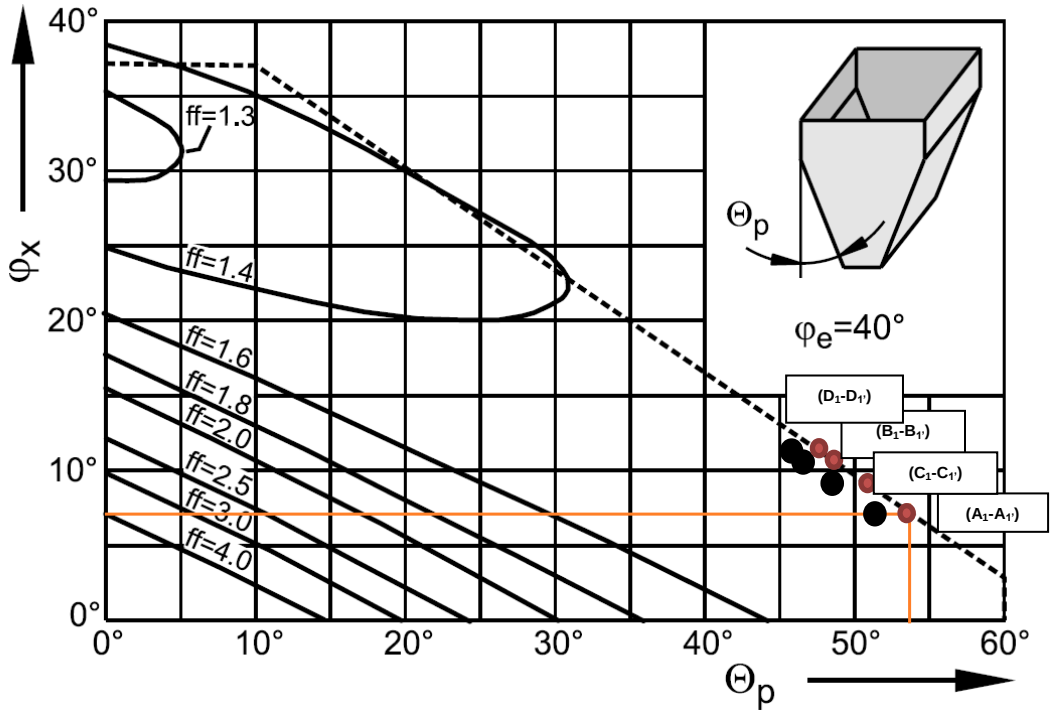

Figure 4.23 Flow factor diagram for wedge-shaped hopper and φ_e= 40° (Schulze, 2008).

To calculate the proper dimensions to produce mass flow trend for a wedge-shaped hopper, Figure 4.23 is used for a 40° internal angle of friction. The hopper slope

angle for a wedge-shaped hopper is Θ_p = 52° (A_1-$A_{1'}$). A_1 represents the intercept of φ_x value with the mass flow boundary of the wedge-shaped hopper and A_1' represents the point after reduction by safety margin. The flow factor is 1.6.

Since the ff=1.6 is similar to the previous calculation for the conical hopper, the critical parameters used for calculation are same as those obtained before. Bearing stress is drawing by using (Eq. 2.8) and the line is passing the origin.

To calculate the critical outlet dimensions for wedge-shape hopper (b_{crit}), (Eq. 2.9) and H(Θ_p) are used, as shown below;

H(Θ_p) = 1.2. This value has been obtained from Figure 2.21.

$$b_{crit} = H(\Theta_p) \frac{\sigma_{c,crit}}{gP_{b,crit}} \quad (2.9)$$

$$b_{crit} = 1.2 \frac{1750}{9.81 \times 350}$$

$$b_{crit} = 0.612 \text{ m.}$$

Since the b_{crit} value is the width of the wedge-shaped hopper, the hopper length must be at least three times the width of the hopper. So, the proper hopper dimension to produce mass flow trend for moderately coarse granules prepared by melt granulation technique using 25% PEG is equal to 0.612m (width) and 1.84m (length).

4.6.3 Designing of conical hopper and silo geometry for coarse granules prepared by melt granulation technique using 25% PEG

The value of the angle of wall friction which is obtained from the wall yield locus is $\varphi_x = 10.7°$ and the internal angle of friction equals 44°, as shown in Table 4.9.

The value of the hopper slope angle is Θc = 40º (B-B') and that can be obtained from Figure 4.21. It is located at the mass flow boundary. Therefore, that should be reduced, for a safety margin, to 38° and the flow factor is equal ff = 1.6.

Table 4.9 Yield locus results for coarse granules prepared using melt granulation by 25% PEG.

YIELD LOCUS No.	σ_1 [Pa]	σ_c [Pa]	Рь [kg/m^3]	φe[°]
1	11201	1701	349	44
2	18674	2488	441	44
3	27518	3293	447	44
4	36850	4323	449	44

All critical parameters can be obtained from Figure 4.24:
$\sigma_{1,crit}$ = 1200 Pa, $\sigma_{c,crit}$ = 600 Pa.

$\rho_{b,crit}$= 230 kg/m^3

$H(\Theta_c)$ = 2.65, this value has been obtained from Figure 2.21.

The minimum outlet dimension to avoid arching can be calculated as follows:

$$d_{crit} = H(\Theta_c)\frac{\sigma_{c,crit}}{gP_{b,crit}} \quad (2.10)$$

$$d_{crit} = 2.63\frac{600}{9.81 \times 230}$$

d_{crit} = 0.70 m.

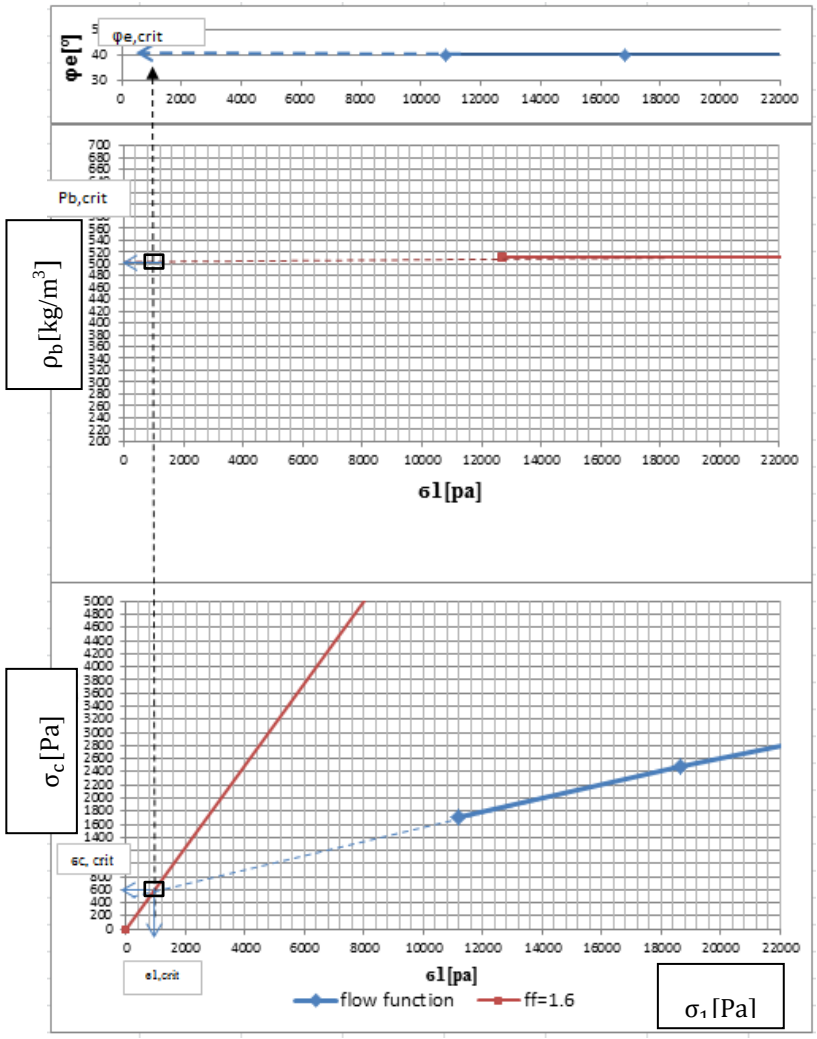

Figure 4.24 Diagram showing flow properties for the determination of minimum outlet dimension to avoid arching (black rectangles represent critical values according to the point of intersection of the flow function with the major principal stress in the arch σ_1').

From the above results, the best fit internal angle for coarse granules using PEG 25% to obtain the flow mass for a conical hopper is 104º, and the outlet dimension should be 1.40m.

4.6.4 Designing of a wedge-shaped hopper and silo geometry for coarse granules prepared by melt granulation technique using 25% PEG

All variables required to design a wedge-shaped hopper can be determined as follows:

The hopper slope angle is Θ_p = 49º (B_1-$B_{1'}$), and is reduced to 47º, because it is located at the mass flow boundary. The flow factor is ff = 1.6. Figure 4.23.

Conical and wedge-shaped hoppers have the same flow factor values and the critical parameters are the same as shown in Figure 4.24.

The next step is to use the equation for calculating b_{crit}.

$H(\Theta_p)$ = 1.2. This value has been obtained from Figure 2.21.

$$b_{crit} = H(\Theta_P)\frac{\sigma_{c,crit}}{gP_{b,crit}}$$

$$b_{crit} = 1.2\frac{600}{9.81 \times 230}$$

$$b_{crit} = 0.32 \text{ m}.$$

For a wedge-shaped hopper the best fit internal angle to obtain mass flow is 86º, and the outlet dimensions are: width 0.32m and length 0.98m.

4.6.5 Designing of conical hopper and silo geometry for moderately coarse granules prepared by wet granulation technique using 25% starch

The angle of wall friction is obtained from the wall yield locus and the value is φ_x = 8.8º and the internal angle of friction is φ_e = 42º as shown in Table 4.10.
the hopper slope angle Θ_c needs to be determined for the conical hopper with flow factor.

Table 4.10 Yield locus results for moderately coarse granules prepared using wet granulation method with 25% starch paste.

YIELD LOCUS No.	σ_1 [Pa]	σ_c [Pa]	Рь [kg/m^3]	φe[°]
1	12380	743	421	42
2	21095	815	423	42
3	29462	1099	440	42
4	37532	1187	515	42

From Figure 4.21, Θ_c = 41° (reduced by safety margin), and the ff = 1.6 (C-C').

The given data in Table 4.10 are required for plotting the yield locus to determine all the critical parameters, as shown in Figure 4.25

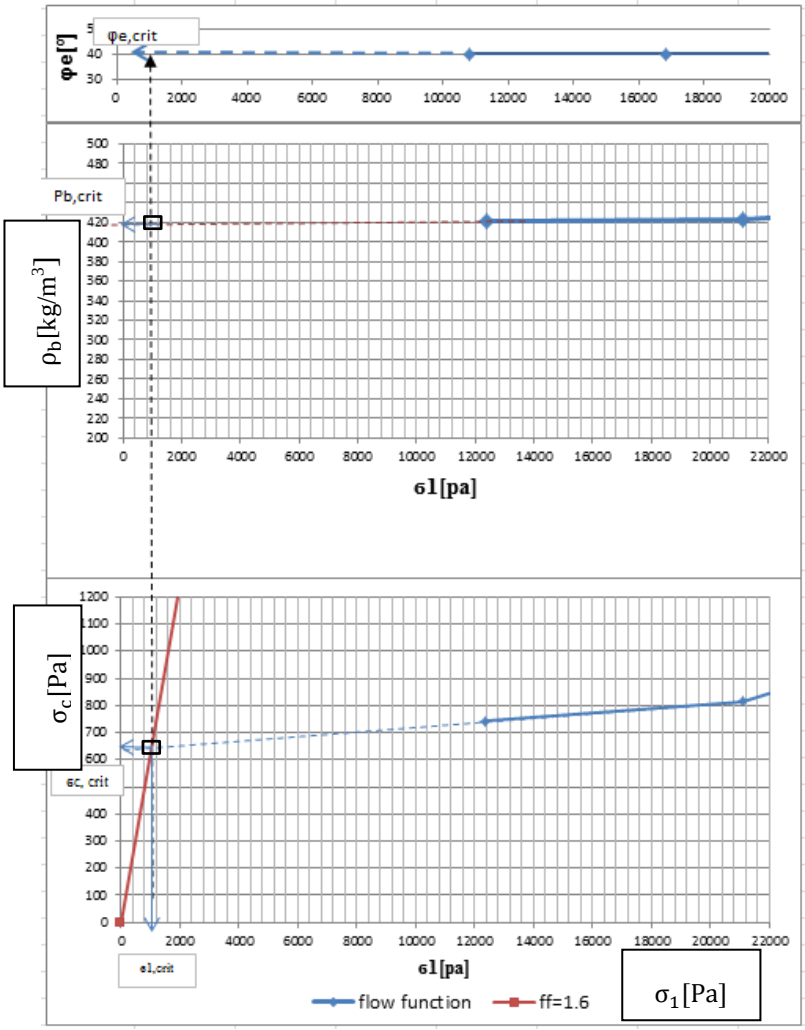

Figure 4.25 Diagram showing flow properties for the determinationof minimum outlet dimension to avoid arching (black rectangles represent critical values according to the point of intersection of the flow function with the major principal stress in the arch σ_1').

The obtained results from Figure 4.25 used to determine the outlet dimension for conical hopper are:

$\sigma_{1,crit}$ = 1000 Pa, and $\sigma_{c,crit}$ = 650 Pa.

$\rho_{b,crit}$ = 420 kg/m^3

$H(\Theta_c)$ = 2.65. This value has been obtained from Figure 2.21.

The minimum outlet dimensions to avoid arching can be calculated as follows:

$$d_{crit} = H(\Theta_c) \frac{\sigma_{c,crit}}{gP_{b,crit}} \quad (2.10)$$

$$d_{crit} = 2.63 \frac{1000}{9.81 \times 420}$$

$$d_{crit} = 0.64 \text{ m}$$

The best fit internal angle to obtain the mass flow for moderately coarse granules prepared by wet granulation using 25% starch paste, for the conical hopper is 98°, and the outlet dimension is 1.28 m.

4.6.6 Designing of wedge-shaped hopper and silo geometry for moderately coarse granules prepared by wet granulation technique using 25% starch

All parameters used to design the wedge-shaped hopper, such as angle of wall friction φ_x and internal angle of friction φ_e are (8.8° and 42°) respectively. The hopper slope angle Θ_p and flow factor can be determined from Figure 4.23.

Their values are Θ_p = 48° (reduced by safety margin), the value of flow factor is ff = 1.6. (C_1-$C_{1'}$) and $H(\Theta_p)$ = 1.2. This value has been obtained from Figure 2.21.

Critical parameters required to calculate the outlet dimension have the same values that are used for the conical hopper, as shown in Figure 4.25.

The next step is to calculate b_{crit}:

$$b_{crit} = H(\Theta_P) \frac{\sigma_{c,crit}}{gP_{b,crit}} \quad (2.9)$$

$$b_{crit} = 1.2 \frac{1000}{9.81 \times 420}$$

b_{crit} = 0.29 m.

For the wedge-shaped hopper, the best fit internal angle to obtain mass flow for the same particle size is 84° and the outlet dimensions are: width 0.29m and length 0.87m.

4.6.7 Designing of conical hopper and silo geometry for coarse granules prepared by wet granulation technique using 25% starch

The angle of wall friction obtained from the wall yield locus is φ_x= 13°. Internal angle of friction is φ_e = 40 as shown in Table 4.11.

Table 4.11 Yield locus results for coarse granules prepared using wet granulation method with 25% starch paste.

YIELD LOCUS No.	σ1 [Pa]	σc [Pa]	Ρь [kg/m^3]	φe[°]
1	12742	376	510	40
2	22002	467	512	40
3	30670	607	512	40
4	39854	759	521	40

The hopper slope angle Θ_c for the conical hopper and flow factor can be determined from Figure 4.21. These values are Θ_c = 37º (D-D') (reduced by safety margin) and the flow factor is ff = 1.6.

The above mentioned data in Table 4.11 are used to plot Figure 4.26 to determine the critical data needed to calculate the critical outlet dimensions.

The critical parameters obtained from Figure 4.26 are:

$\sigma_{1,crit}$= 500 Pa,

$\rho_{b,crit}$ = 505 kg/m^3,

$\sigma_{c,crit}$ = 250 Pa

H(Θ_c) = 2.65. This value has been obtained from Figure 2.21.

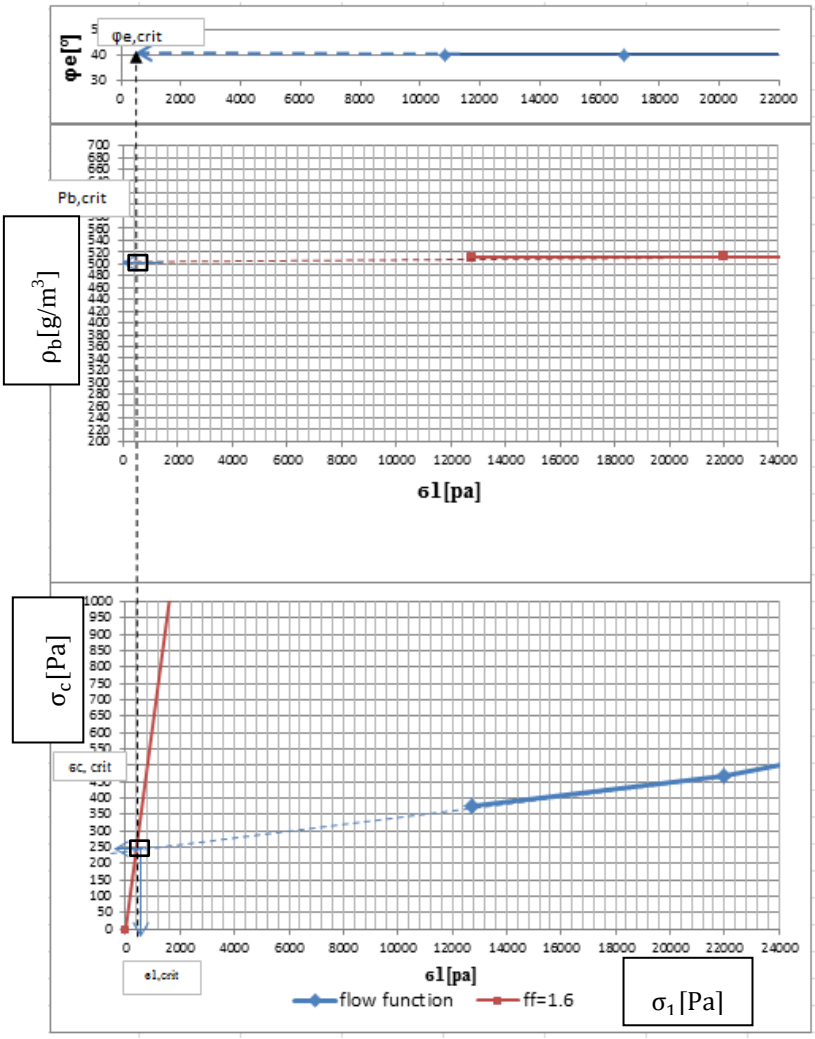

Figure 4.26 Diagram showing flow properties for the determination of minimum outlet dimension to avoid arching (black rectangles represent critical values according to the point of intersection of the flow function with the major principal stress in the arch σ_1').

The minimum outlet dimensions to avoid arching can be calculated as follows:

$$d_{crit} = H(\Theta_c)\frac{\sigma_{c,crit}}{gP_{b,crit}} \qquad (2.10)$$

$$d_{crit} = 2.63\frac{250}{9.81\times505}$$

$$d_{crit} = 0.133 \text{ m.}$$

For this particular particle size using the conical hopper, the best fit internal angle to obtain the mass flow is 106°, and the outlet diameter is 0.266m.

4.6.8 Designing of wedge-shaped hopper and silo geometry for coarse granules prepared by wet granulation technique using 25% starch

Similarly to those values obtained from the previous calculation for designing the conical hopper, the same values were used to calculate the dimensions for the wedge-shaped hopper.

The slope of the hopper angle is Θ_p =46° (D_1-$D_{1'}$) (reduced by safety margin), the flow factor is $ff = 1.6$. as shown in Figure 4.23 and $H(\Theta_p)$ = 1.2. This value has been obtained from Figure 2.21.

The critical parameters are obtained from Figure 4.26, used for the conical hopper, and also used for the wedge-shaped hopper.

The critical dimensions for the wedge-shaped hopper can be calculated as follows:

$$b_{crit} = H(\Theta_P)\frac{\sigma_{c,crit}}{gP_{b,crit}} \quad (2.9)$$

$$b_{crit} = 1.2\frac{250}{9.81 \times 505}$$

$$b_{crit} = 0.06$$

For the same particle size the best fit internal angle for the wedge-shaped hopper to obtain mass flow is 88°, and the outlet dimensions are: width 0.06m and length 0.18m.

All calculated dimensions are illustrated in Table 4.12.

Table 4.12 Calculated internal angles and outlet dimensions of conical and wedge-shaped hoppers.

Granules	Conical hopper			Wedge-shaped hopper			
	Θ_c[°]	Internal angle of hopper [°]	d_{crit} [m]	Θ_p[°]	Internal angle of hopper[°]	b_{crit}(width)[m]	Length ($3\times b_{crit}$)[m]
PEG 25% (250-355)	**42**	**96**	**1.34**	**52**	**76**	**0.612**	**1.84**
PEG 25% (600-710)	**38**	**104**	**0.7**	**47**	**98**	**0.32**	**0.98**
Starch 25% (250-355)	**41**	**98**	**0.64**	**48**	**84**	**0.29**	**0.87**
Starch 25% (600-710)	**37**	**106**	**0.13**	**46**	**88**	**0.06**	**0.18**

In conclusion, the summarised results in Table 4.12 show that the required internal angle of the wedge-shaped hopper to obtain a mass flow trend for both moderately coarse and coarse granules prepared by melt and wet granulation techniques is less than that required for the conical hopper. In addition, the required internal angle for the conical hopper design is less in the case of the melt granulation technique than that for wet granulation technique over the same granules range. On the other hand, the outlet dimensions are opposite to that. This might indicate that an arching tendency is more likely in the case of granules prepared by melt granulation than in that prepared by the wet granulation technique.

4.7 **Conclusion**

In the case of applying the melt granulation method, the results indicate that using PEG 6000 at 5% and 15% binding ratios form agglomerates having irregular, deformable and elongated shapes due to continuous formation and breakage mechanisms as shown in Fig. (B.1 and B.2). These characteristics may influence negatively the granular materials flowability because of the increasing interlocking tendency. This phenomenon will be investigated qualitatively in Chapter five using DPIV. Raising the binding ratio to 25% was sufficient to counteract agglomerate breakage and produce granules having a good flow trend, as shown in Fig. B.3.

The results in Tables A.1, A.3. and A.5 show clearly that using 25% PEG 6000 lowers the unconfined yield strength (σ_c) along all particle size ranges and at all consolidation stress levels. For example, at 5 kPa, the σ_c and ff_c for coarse granules at 25% binding ratio were 1.701 and 6.6 compared to 2.012 and 2.042 and 5 and 6.1 for 5% and 15% respectively. This indicates that increasing the PEG binding ratio dramatically increases the granular flow.

In the case of applying the wet granulation method, the obtained results indicate that using 15% and 25% starch paste was able to produce less porous granules having sufficient strength compared to that obtained in the case of 5%, as shown in Fig. 3.2 (b). However, the ring shear cell tester results show that the ff_c and σ_c values of granules prepared using 5% starch paste were 19.1 and 0.627 respectively and these values are much better than those obtained in the case of 25% PEG. Increasing the binding ratio to 15% and 25% is sufficient to produce granules showing excellent

flow trend, as shown in Tables A.4 and A.6. This could be attributed to the high viscosity of the granulating pastes and domination of the coalescence method for agglomeration.

Moreover, the obtained results prove that using 15% and 25% starch paste lowers the unconfined yield strength (σ_c) along most particle size ranges and at all consolidation stress levels. For example; at 5 kPa, the σ_c and ff_c for coarse granules at 15% and 25% binding ratio were 0.568 and 0.367 and 22 and 35 respectively comparing to 0.6.27 and 19.1 in the case of 5% binding ratio. This indicates that increasing the starch paste concentration greatly influences the granules' flow trend.

The results prove that granules prepared by the melt granulation technique are more cohesive compared to those prepared by the wet granulation technique among all ranges. Wall yield locus results indicate that granules prepared by the melt granulation technique have a lower friction coefficient against the Perspex wall compared to that obtained by wet granulation method. This could be attributed to the surface smoothing effect of molten PEG 6000.

According to the hoppers and silos design fundamentals, moderately coarse and coarse granules require a smaller internal hopper angle for the wedge-shaped hopper than that required for the conical hopper shape for both granulation techniques.

Chapter 5 Evaluation of dynamic granular materials flow trends using DPIV

According to the previously obtained results using the ring shear cell tester (RST-XS) for multiple evaluation purposes and the micromechanical properties of the prepared granules, four cases of granules have been selected for the DPIV study. The aim of this part of the research project is to apply a non-destructive dynamic technique to investigate and visualise the influences of hopper internal angles on granular flow trends on granules prepared by two different granulation techniques. Two different internal hopper angles (45° and 70°) and two particle size ranges moderately coarse granules (250-355µm) and coarse granules (600-710µm) prepared by both granulation techniques at 25% binding ratio are used based on their mechanical properties ,as shown in Figure (3.2 a and b).

It was worth applying this study according to the previously calculated hopper angles and dimensions to visualise the mass flow trend. But unfortunately shortage of time allocated for the research project and lack of funds were the main limitations to using the available silo dimensions. This can be considered in future work.

5.1.1 Dynamic flow evaluation of moderately coarse granules prepared by wet granulation technique using 25% starch

The mean resultant velocity vectors map of moderately coarse granules prepared by the wet granulation technique using 25% starch paste inside (70°) a silo is shown in Figure 5.1. The general trend of the flow is a combination of both central and radial flow behaviour.

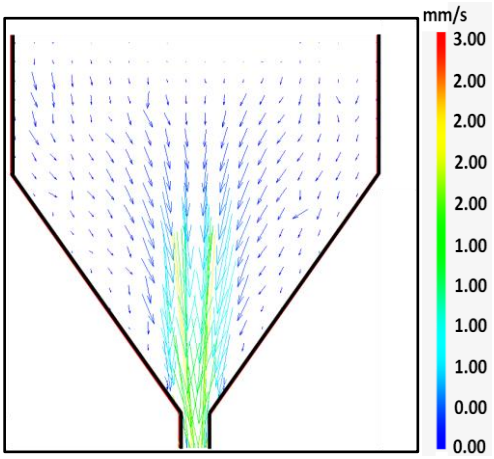

Figure 5.1 Mean resultant velocity vector map of moderately coarse granules prepared by wet granulation technique using 25% starch paste inside (70°) silo geometry.

The central zone of the silo shows vertical to almost vertical velocity vectors and the magnitude of the vectors are decreased upwards. As the granules become close to the boundaries, the velocity vectors' directions are changed to the inclined position.

In contrast, Figure 5.2 illustrates the mean resultant velocity vectors map of moderately coarse granules prepared by the wet granulation technique using 25% starch paste inside the (45°) silo. The general trend of the flow is close to being a mass flow trend in most of the silo segments. More vertical to almost vertical velocity vectors are available inside the hopper geometry compared to what have been observed in the (70°) silo, but few inclinations are observed close to the boundaries. Similarly to what has been observed in the (70º) silo, the higher velocity vectors are located close to the hopper outlet and the magnitude decreases in the high segments.

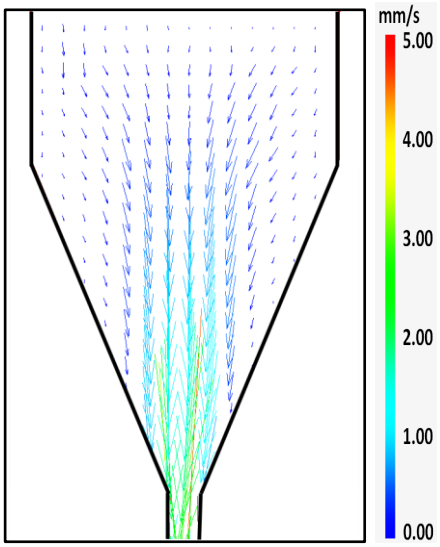

Figure 5.2 Mean resultant velocity vector map of moderately coarse granules prepared by wet granulation technique using 25% starch paste inside (45°) silo geometry.

5.1.2 Dynamic flow evaluation of moderately coarse granules prepared by melt granulation technique using 25% PEG

The obtained mean resultant velocity vectors map of the dynamic flow trend of moderately coarse granules prepared by melt granulation technique using 25% PEG inside the (70°) silo is shown in Figure 5.3.

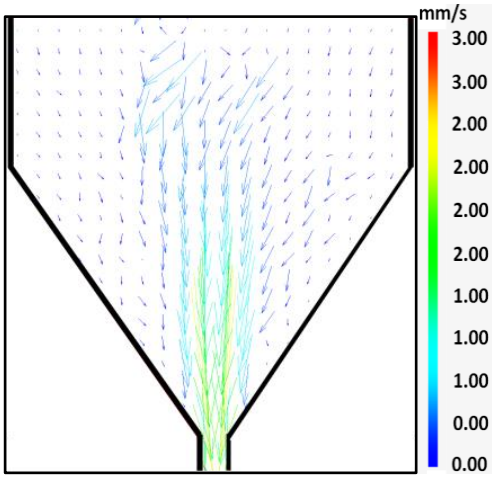

Figure 5.3 Mean resultant velocity vector map of moderately coarse granules prepared by melt granulation technique using 25% PEG inside (70°) silo geometry.

The map shows there is a clear asymmetric granular flow inside the silo compared to what has been observed for the same particle size in (70°) silo geometry using the wet granulation granules. This asymmetry might be attributed to the granules' cohesivity which alters the flow trend dramatically. In general, it is obvious that the flow trend is a combined radial and central flow trend. The velocity vectors away from and at the top of the central flow zone show multiple inclined vectors.

Similarly to what has been observed in the (70°) silo for the same particle size range, an asymmetrical flow trend is also observed in the (45°) silo, as is illustrated in Figure 5.4.

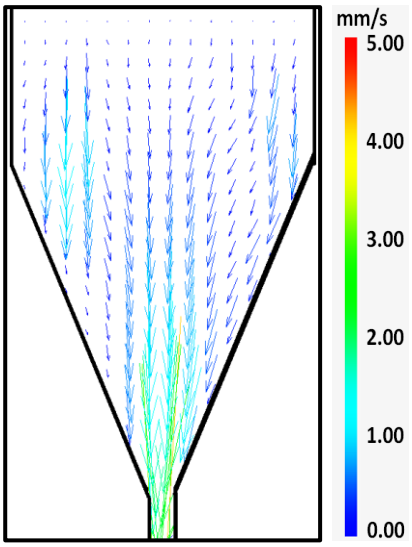

Figure 5.4 Mean resultant velocity vector map of moderately coarse granules prepared by melt granulation technique using 25% PEG inside (45°) silo geometry.

The silo shows almost vertical vectors in the central zone and segments close to the boundaries. The area next to the central zone shows some inclined vectors and also semi vertical. This complex trend of flow might be due to the cohesivity of the granules leading to obvious asymmetric flow behaviour.

5.1.3 Dynamic flow evaluation of coarse granules prepared by wet granulation technique using 25% starch

Figure 5.5 displays the mean resultant velocity vectors obtained through a dynamic flow of coarse granules prepared by the wet granulation technique using 25% starch paste inside (70º) silo geometry. Obviously, the map shows the symmetric flow trend of the granules in a combined trend of both central and radial flow. The central flow zone and the granules close to the silo boundaries are in a vertical direction. The granules close to the hopper boundaries are inclined identically to the hopper angle. The velocity is higher close to the silo outlet comparing to the other silo segments. The symmetric flow of this particle range might be attributed to the particle size distribution and negligible cohesivity between the granules.

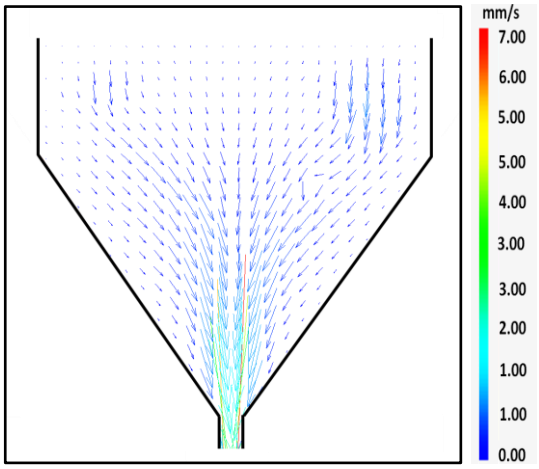

Figure 5.5 Mean resultant velocity vector map of coarse granules prepared by wet granulation technique using 25% starch inside (70°) silo geometry.

Figure 5.6 shows the mean resultant velocity vectors map and general flow trend of coarse granules prepared by wet granulation technique using 25% starch inside (45º) silo geometry. Unlike the flow trend in (70º) silo geometry, it is clear that the flow is uniform and close to being a mass flow trend. This good symmetrical granular flow can be attributed to the low inter-particle adhesive forces. Similarly to what has been achieved before, the higher velocity vectors region is obtained close to the outlet region.

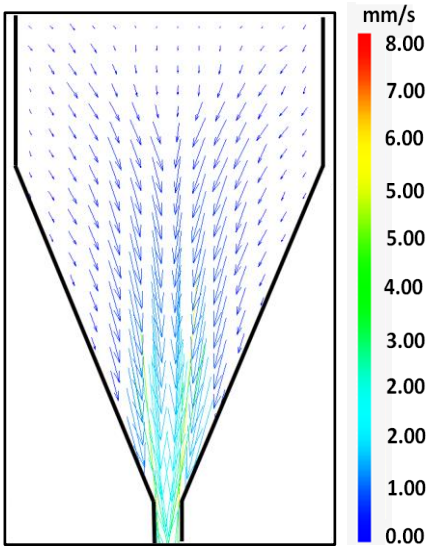

Figure 5.6 Mean resultant velocity vector map of coarse granules prepared by wet granulation technique using 25% starch inside (45°) silo geometry

5.1.4 Dynamic flow evaluation of coarse granules prepared by melt granulation technique using 25% PEG

The dynamic flow trend of coarse granules prepared by the melt granulation technique using 25% PEG is illustrated in Figure 5.7. Similarly to what has been observed for the coarse granules prepared by the wet granulation technique at the same silo geometries, the mean resultant velocity vector shows a good range of symmetrical flow trend.

The central zone of the flow and the boundaries close to the silo walls show vertical to almost vertical velocity vectors. The hopper boundaries show inclined velocity vectors towards the central zone.

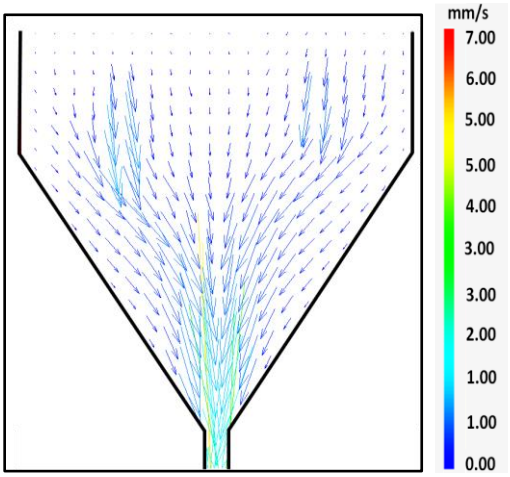

Figure 5.7 Mean resultant velocity vector map of coarse granules prepared by melt granulation technique using 25% PEG inside (70°) silo geometry.

Finally, Figure 5.8 shows the observed flow trend of coarse granules prepared by the melt granulation technique using 25% PEG inside (45°) silo geometry through displaying the spatial and temporal mean velocity vectors. The general trend of the flow within this geometry follows almost a mass flow trend. This is clear through the almost vertical direction of the vectors inside the silo in all silo segments. The region closer to the silo outlet indicates the higher velocity magnitude.

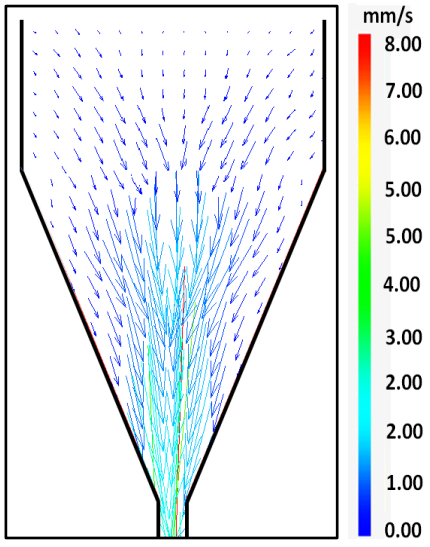

Figure 5.8 Mean resultant velocity vector map of coarse granules prepared by melt granulation technique using 25% PEG inside (45°) silo geometry.

To conclude, the obtained results indicate that both granulation methods and particle size ranges have a marked influence on the flow trend. The melt granulation technique using 25% PEG was unable to produce moderately coarse granules with symmetrical flow trend inside both (45°) and (70°) silo geometries. On the other hand, granules formulated using wet granulation technique for the same particle size range using 25% starch paste show a better symmetrical flow trend inside both silo geometries. This might be attributed to the high inter-particle adhesive forces between the granules in the case of melt granulation. In contrast, the obtained PIV results for the coarse granules ranges showed that both granulation methods were able to produce a symmetrical flow trend inside both silo geometries.

In addition, the results indicate that the silo angle has a great influence on the general flow trend of the granular material among all particle sizes. The smaller silo angle (45°) showed a general flow trend close to the mass flow behaviour, while the larger silo angle (70°) showed a combined flow trend that was both radial and central. This combined flow is similar to the funnel flow trend.

5.2 **Conclousion**

The DPIV results indicate that moderately coarse granules prepared by the melt granulation technique using 25% PEG were unable to show a symmetrical flow trend inside both (45º) and (70º) silo geometries. On the other hand the coarse granules ranges for both granulation techniques showed a symmetrical flow trend inside both silo geometries. The results also indicate that the silo angle has a great influence on the general flow trend of the granular material among all particle sizes.

Chapter 6 Conclusions and future work

6.1 Conclusion

Wet and melt granulation techniques have been successfully applied to prepare multiple granules ranges on a laboratory scale. Starch paste and PEG 6000 have been used as granulating agents in ratios of (5%, 15% and 25%) for wet and melt granulation methods respectively. the granules size ranged from (45-710 µm) and was subdivided into three subdivisions including very fine range (45-106 µm), moderately coarse range (250-355 µm) and coarse range (600-710 µm). The results indicate that binding ratios have a great influence on granular flowability in both methods.

In the case of melt granulation, using 25% PEG binding ratio was the minimum concentration able to produce satisfactory physio-micromechanical properties and proper flow tendency. In such cases, the distribution mechanism becomes the dominant method of nucleation which enhances powders' wettability and saturation. Concurrently the surface textures of the granules become smoother and granules show a semi spherical shape due to the high coalescence tendency.

On the other hand, the wet granulation method shows adequate physio-micromechanical properties and suitable flow ability for all binding ratios. However, 5% starch paste was not able to produce a sufficient coating of the granules due to its low paste amylose content that influenced its viscosity. Raising the binding ratios to 15% and 25% enhanced the paste viscosity and improved the film coating mechanism. These factors enhance the formation of inter-particle liquid bridges between contacting particles and produce strong, dense granules.

Moreover, these results have been proved quantitatively and qualitatively using ring shear cell tester and DPIV method. The unconfined yield strength values (σ_c) in the case of applying wet granulation were lower than those obtained in the case of the melt granulation technique. This indicates that the granular flow pattern is much better in the case of applying the wet granulation method. In addition, the flow factors' (ff_c) values obtained in the case of the wet granulation technique are much higher than those obtained by the melt granulation technique for all binding ratios.

The unconfined yield strength results at zero major principal stress show that granules prepared by the melt granulation technique are more cohesive compared to those prepared by the wet granulation technique among all ranges. Granular wall friction values of melt granulation granules were less than those obtained by the wet granulation due to PEG surface smoothing.

The DPIV results showed that the particle size distribution and internal hopper angle have a crucial influence on the nature of the granular flow behaviour. In general, the smaller the hopper angles, the better the flow pattern.

6.2 **Future work**

The use of recent apparatus (ring shear cell tester) to determine the granules characteristics coupled with the new visualising technology, such as DPIV, has been successfully applied. It is recommended that in future studies using these reliable methods could be carried out for assuring flow characterisation of different types of granules. The main areas of focus should be:

- Compare the experimental extrapolated data with the calculated results under low loads using a ring shear tester.
- Implement these granulation techniques to modify the release and dissolution of chemically or pharmaceutically active ingredients.
- Apply DPIV analysis to the calculated internal hopper angle and outlet dimensions, and evaluation of the flow key variables, such as particle size distribution, lubricants, roughness and outlet dimensions.
- Further investigation into the flow properties of granular materials inside the hopper and silo design using DEM for comparison with corresponding experimental results.

References:

Abdullah, E. & Geldart, D. 1999. The use of bulk density measurements as flowability indicators. *Powder Technology,* 102**,** 151-165.

Adrian, R. J. 2005. Twenty years of particle image velocimetry. *Experiments in Fluids,* 39**,** 159-169.

Agrawal, R. & Naveen, Y. 2011. Pharmaceutical processing–A review on wet granulation technology. *International J Pharmaceutical Frontier Research,* 1**,** 65-83.

Albaraki, S. & Antony, S. 2014. How does internal angle of hoppers affect granular flow? Experimental studies using Digital Particle Image Velocimetry. *Powder Technology*.

Albaraki, S., Antony, S. J. & Arowosola, C. B. Visualising shear stress distribution inside flow geometries containing pharmaceutical powder excipients using photo stress analysis tomography and DEM simulations. POWDERS AND GRAINS 2013: Proceedings of the 7th International Conference on Micromechanics of Granular Media, 2013. AIP Publishing, 706-709.

Albertini, B., Passerini, N., González-Rodríguez, M., Cavallari, C., Cini, M. & Rodriguez, L. 2008. Wet granulation as innovative and fast method to prepare controlled release granules based on an ion-exchange resin. *Journal of pharmaceutical sciences,* 97**,** 1313-1324.

Allen, T. 1990. Sieving. *Particle Size Measurement.* Springer Netherlands.

Andrews, G. P. 2007. Advances in solid dosage form manufacturing technology. *Philosophical Transactions of the Royal Society A: Mathematical, Physical and Engineering Sciences,* 365**,** 2935-2949.

Antony, S. 2007. Link between single-particle properties and macroscopic properties in particulate assemblies: role of structures within structures. *Philosophical Transactions of the Royal Society A: Mathematical, Physical and Engineering Sciences,* 365**,** 2879-2891.

Antony, S. & Sultan, M. 2007. Role of interparticle forces and interparticle friction on the bulk friction in charged granular media subjected to shearing. *Physical Review E,* 75**,** 031307.

Antony, S. J. 2000. Evolution of force distribution in three-dimensional granular media. *Physical Review E,* 63**,** 011302.

Aole, D., Jain, M. K. & Bruhis, M. 2012. New characterization methods for powder die fill process for producing powder metallurgical components. *Powder Technology,* 232**,** 7-17.

Armstrong, B. 2011. *The study of pharmaceutical powder mixing through improved flow property characterisation and tomographic imaging of blend content uniformity.* University of Birmingham.

Aulton, M. E. & Wells, T. 2002. *Pharmaceutics: The science of dosage form design*.

Bodhmage, A. 2006. *Correlation between physical properties and flowability indicators for fine powders.* University of Saskatchewan.

Breitenbach, J. 2002. Melt extrusion: from process to drug delivery technology. *European Journal of Pharmaceutics and Biopharmaceutics,* 54**,** 107-117.

Chan, L. W. & Heng, P. 2005. Drug substance and excipient characterization. *DRUGS AND THE PHARMACEUTICAL SCIENCES,* 154**,** 79.

Christensen, L., Johansen, H. & Schaefer, T. 1994. Moisture-activated dry granulation in a high shear mixer. *Drug development and industrial pharmacy,* 20**,** 2195-2213.

Das, G., Das, M., Ghosh, S., Dubey, P. & Ray, A. K. 2010. Effect of aging on mechanical properties of 6063 Al-alloy using instrumented ball indentation technique. *Materials Science and Engineering: A,* 527**,** 1590-1594.

Duran, J. 2000. *Sands, powders, and grains,* Springer, New York.

Edwards, D. 2010. Applications of capsule dosing techniques for use in dry powder inhalers. *Therapeutic Delivery,* 1**,** 195-201.

El-Say, K. M., Refaey, T. A., Samy, A. M. & Badawy, A. A. 2010. Comparative study among different techniques to improve the physical and technical properties prevailing to compression of poorly flowing and highly cohesive drug. *Int J of Pharm Sci Rev Res,* 4**,** 67-76.

Eliasen, H., Schæfer, T. & Gjelstrup Kristensen, H. 1998. Effects of binder rheology on melt agglomeration in a high shear mixer. *International journal of pharmaceutics,* 176**,** 73-83.

Emery, E. 2008. *Flow Properties of Selected Pharmaceutical Powders.* MSc of science Thesis (MSc,University of Saskatchewan), University of Saskatchewan.

Emery, E., Oliver, J., Pugsley, T., Sharma, J. & Zhou, J. 2009. Flowability of moist pharmaceutical powders. *Powder Technology,* 189**,** 409-415.

Ennis, B. & Litster, J. 1997. Particle size enlargement. *Perry's Chemical Engineers' Handbook. 7th edition, McGraw-Hill, New York***,** 20.56-20.89.

Ennis, B. J. 2005. Theory of granulation: an engineering perspective. *DRUGS AND THE PHARMACEUTICAL SCIENCES,* 154**,** 7.

Ennis, B. J., Tardos, G. & Pfeffer, R. 1991. A microlevel-based characterization of granulation phenomena. *Powder Technology,* 65**,** 257-272.

Evrard, B., Amighi, K., Beten, D., Delattre, L. & Moës, A. 1999. Influence of melting and rheological properties of fatty binders on the melt granulation process in a high-shear mixer. *Drug development and industrial pharmacy,* 25**,** 1177-1184.

Faure, A., York, P. & Rowe, R. 2001. Process control and scale-up of pharmaceutical wet granulation processes: a review. *European Journal of Pharmaceutics and Biopharmaceutics,* 52**,** 269-277.

Fitzpatrick, J., Barringer, S. & Iqbal, T. 2004. Flow property measurement of food powders and sensitivity of Jenike's hopper design methodology to the measured values. *Journal of Food Engineering,* 61**,** 399-405.

Freeman, R. The flowability of powders—an empirical approach. International Conference on Powder and Bulk Solids Handling (London, UK, 2000), 2000.

Ganesan, V., Rosentrater, K. A. & Muthukurnarappan, K. 2008. Flowability and handling characteristics of bulk solids and powders - a review with implications for DDGS. *Biosystems Engineering,* 101**,** 425-435.

Ghadiri, M., Ning, Z., Kenter, S. & Puik, E. 2000. Attrition of granular solids in a shear cell. *Chemical Engineering Science,* 55**,** 5445-5456.

Gijón-Arreortúa, I. & Tecante, A. 2014. Mixing time and power consumption during blending of cohesive food powders with a horizontal helical double-ribbon impeller. *Journal of Food Engineering*.

Gokhale, R. & Trivedi, N. R. 2010. Wet granulation in low-and high-shear mixers. *Handbook of Pharmaceutical Granulation Technology,* 3**,** 183-203.

Halle, P., D, Sakhare, R., S, Dadage, K., K & Birajdar, G., O 2013. A review on melt granulation technique.

Hampel, R., Heinrich, S., Mörl, L. & Peglow, M. Modeling and experimental analysis of superheated steam granulation. Proceedings of the 5th World Congress on Particle Technology, Orlando/Florida, 2006.

Hassanpour, A. & Ghadiri, M. 2007. Characterisation of flowability of loosely compacted cohesive powders by indentation. *Particle & Particle Systems Characterization,* 24**,** 117-123.

Hassanpour, A., Kwan, C. C., Ng, B. H., Rahmanian, N., Ding, Y. L., Antony, S. J., Jia, X. D. & Ghadiri, M. 2009. Effect of granulation scale-up on the strength of granules. *Powder Technology,* 189**,** 304-312.

Hassanpour, A., Pasha, M., Susana, L., Rahmanian, N., Santomaso, A. C. & Ghadiri, M. 2013. Analysis of seeded granulation in high shear granulators by discrete element method. *Powder Technology,* 238**,** 50-55.

Heinrich, S. & Mörl, L. 1999. Fluidized bed spray granulation—A new model for the description of particle wetting and of temperature and concentration distribution. *Chemical Engineering and Processing: Process Intensification,* 38**,** 635-663.

Heng, P., Wan, L. & Wong, T. 1999. Effect of off-bottom clearance on properties of pellets produced by melt pelletization. *Pharmaceutical development and technology,* 4**,** 27-33.

Heng, P. & Wong, T. W. 2003. Melt processes for oral solid dosage forms. *Encyclopedia of Pharmaceutical Technology***,** 1-6.

Heng, P. W. & Wong, T. W. 2007. Melt processes for oral solid dosage forms. *Encyclopedia of pharmaceutical technology,* 4**,** 2257-2261.

Hou, H. & Sun, C. C. 2008. Quantifying effects of particulate properties on powder flow properties using a ring shear tester. *Journal of pharmaceutical sciences,* 97**,** 4030-4039.

Iveson, S. M. 2001. Granule coalescence modelling: including the effects of bond strengthening and distributed impact separation forces. *Chemical engineering science,* 56**,** 2215-2220.

Iveson, S. M., Litster, J. D., Hapgood, K. & Ennis, B. J. 2001. Nucleation, growth and breakage phenomena in agitated wet granulation processes: a review. *Powder Technology,* 117**,** 3-39.

Jaeda, H. 2009. *The Use of a Ring Shear Tester to Evaluate the Flowability of Pharmaceutical Bulk Solids.* Heinrich-Heine-University.

Jaeger, H. M., Nagel, S. R. & Behringer, R. P. 1996. Granular solids, liquids, and gases. *Reviews of Modern Physics,* 68**,** 1259-1273.

Jenike, A. W. 1967. Quantitative design of mass-flow bins. *Powder Technology,* 1**,** 237-244.

Jillavenkatesa, A., Dapkunas, S. J. & Lin-Sien, H. L. 2001. *NIST recommended practice guide special publication 960-1 Particle size characterization*.

Juliano, P. & Barbosa-Cánovas, G. V. 2010. Food powders flowability characterization: theory, methods, and applications. *Annual review of food science and technology,* 1**,** 211-239.

Keane, R., Adrian, R. & Zhang, Y. 1995. Super-resolution particle imaging velocimetry. *Measurement Science and Technology,* 6**,** 754.

Kidokoro, M., Sasaki, K., Haramiishi, Y. & Matahira, N. 2003. Effect of crystallization behavior of polyethylene glycol 6000 on the properties of granules prepared by fluidized hot-melt granulation (FHMG). *Chemical & pharmaceutical bulletin,* 51**,** 487-493.

Kimura, G. 2012. *Design of pharmaceutical tablet formulation for a low water soluble drug.* PhD, University of Basel.

Kristensen, H. G. & Schaefer, T. 1987. Granulation: A review on pharmaceutical wet-granulation. *Drug Dev Ind Pharm,* 13**,** 803-872.

Krycer, I., Pope, D. G. & Hersey, J. A. 1983. An evaluation of tablet binding agents part I. Solution binders. *Powder Technology,* 34**,** 39-51.

Kunii, D. & Chisaki, T. 2007. *Rotary reactor engineering,* Elsevier.

Lee, K. T. 2013. *Continuous granulation of pharmaceutical powder using a twin screw granulator.* University of Birmingham.

Li, M., Wilkinson, D. & Patchigolla, K. 2005. Comparison of particle size distributions measured using different techniques. *Particulate science and technology,* 23**,** 265-284.

Li, Q., Rudolph, V., Weigl, B. & Earl, A. 2004. Interparticle van der Waals force in powder flowability and compactibility. *Int J Pharm,* 280**,** 77-93.

Lin, H.-L., Ho, H.-O., Chen, C.-C., Yeh, T.-S. & Sheu, M.-T. 2008. Process and formulation characterizations of the thermal adhesion granulation (TAG) process for improving granular properties. *International journal of pharmaceutics,* 357**,** 206-212.

Litster, J., Ennis, B. & Lian, L. 2004. *The science and engineering of granulation processes,* Springer.

Litster, J. D. 2003. Scaleup of wet granulation processes: science not art. *Powder Technology,* 130**,** 35-40.

Liu, L. X., Litster, J. D., Iveson, S. M. & Ennis, B. J. 2000. Coalescence of deformable granules in wet granulation processes. *AIChE Journal,* 46**,** 529-539.

Lueptow, R. M., Akonur, A. & Shinbrot, T. 2000. PIV for granular flows. *Experiments in Fluids,* 28**,** 183-186.

Lumay, G., Boschini, F., Traina, K., Bontempi, S., Remy, J. C., Cloots, R. & Vandewalle, N. 2012. Measuring the flowing properties of powders and grains. *Powder Technology,* 224**,** 19-27.

Marjanović, P. & Jones, M. 1996. Assessment of a new technique for measuring flow properties of powdered materials stored in hoppers. *Proceedings of the*

Institution of Mechanical Engineers, Part E: Journal of Process Mechanical Engineering, 210**,** 1-8.

Mittal, B. 1999. *Correlation Between Deposition Method, Powder Compression Response and Compact Quality.* Pennsylvania State University.

Miyamoto, Y., Ryu, A., Sugawara, S., Miyajima, M., Ogawa, S., Matsui, M., Takayama, K. & Nagai, T. 1998. Simultaneous optimization of wet granulation process involving factor of drug content dependency on granule size. *Drug development and industrial pharmacy,* 24**,** 1055-1065.

Newitt, D. & Conway-Jones, J. 1958. A contribution to the theory and practice of granulation. *Trans. Inst. Chem. Eng,* 36.

Nguyen, Q. D., Jensen, C. T. & Kristensen, P. G. 1998. Experimental and modelling studies of the flow properties of maize and waxy maize starch pastes. *Chemical Engineering Journal,* 70**,** 165-171.

Onoue, S., Sato, H., Ogawa, K., Kawabata, Y., Mizumoto, T., Yuminoki, K., Hashimoto, N. & Yamada, S. 2010. Improved dissolution and pharmacokinetic behavior of cyclosporine A using high-energy amorphous solid dispersion approach. *International Journal of Pharmaceutics,* 399**,** 94-101.

Pandeya, A. 2009. *Relating mechanical properties of dry and granulated pharmaceutical powder formulations with tablet quality parameters.* The Pennsylvania State University.

Parikh, D. M. 2009. *Handbook of Pharmaceutical Granulation Technology; NY,* Taylor & Francis.

Parikh, D. M. & Mogavero, M. 2005. Batch fluid bed granulation. *DRUGS AND THE PHARMACEUTICAL SCIENCES,* 154**,** 247.

Pasha, M., Hare, C., Hassanpour, A. & Ghadiri, M. 2013. Analysis of ball indentation on cohesive powder beds using distinct element modelling. *Powder Technology,* 233**,** 80-90.

Patel, S., Kaushal, A. & Bansal, A. 2007. Effect of Particle Size and Compression Force on Compaction Behavior and Derived Mathematical Parameters of Compressibility. *Pharmaceutical Research,* 24**,** 111-124.

Prescott, J., K, & Barnum, R., A, 2000. On powder flowability. *Pharmaceutical Technology,* 24**,** 60-84.

Qiu, Y., Chen, Y., Zhang, G. G., Liu, L. & Porter, W. 2009. *Developing solid oral dosage forms: pharmaceutical theory & practice,* Academic Press.

Radjai, F., Roux, S. & Moreau, J. J. 1999. Contact forces in a granular packing. *Chaos: An Interdisciplinary Journal of Nonlinear Science,* 9**,** 544-550.

Rahmanian, N., El Ganimi, T. & Ghadiri, M. 2013. Further investigations on the influence of scale-up of a high shear granulator on the granule properties. *Particuology,* 11**,** 627-635.

Rahmanian, N. & Ghadiri, M. 2011. Comment of the Cover Photograph Seeded Granulation. *Kona Powder and Particle Journal***,** 3-3.

Rahmanian, N. & Ghadiri, M. 2013. Strength and structure of granules produced in continuous granulators. *Powder Technology,* 233**,** 227-233.

Rahmanian, N., Ghadiri, M. & Jia, X. 2011. Seeded granulation. *Powder Technology,* 206**,** 53-62.

Rahmanian, N., Ng, B., Hassanpour, A., Ding, Y., Antony, J., Jia, X., Ghadiri, M., Van Der Wel, P., Krug-Polman, A., York, D., Bayly, A. & Tan, H. S. 2008. Scale-up of High-Shear Mixer Granulators. *KONA Powder and Particle Journal,* 26**,** 190-204.

Remington, J. P., Troy, D. B. & Beringer, P. 2006. *Remington: The science and practice of pharmacy*, Lippincott Williams & Wilkins.

Riley, G., Mann, S. & Jesse, R. Angle of repose of cohesive powders. International Conference of Powder Technology and Pharmacy, 1978. 1-9.

Rowe, R. C., Sheskey, P. J. & Weller, P. J. 2003. Handbook of pharmaceutical excipients. Pharmaceutical press London.

Saikh, M. a. A. 2013. A technical note on granulation technology: a way to optimise granules. *International Journal of Pharmaceutical Sciences & Research,* 4.

Sandler, N. & Lammens, R. F. 2011. Pneumatic dry granulation: potential to improve roller compaction technology in drug manufacture. *Expert opinion on drug delivery,* 8**,** 225-236.

Sandler, N. & Wilson, D. 2010. Prediction of granule packing and flow behavior based on particle size and shape analysis. *Journal of Pharmaceutical Sciences,* 99**,** 958-968.

Schæfer, T. 2001. Growth mechanisms in melt agglomeration in high shear mixers. *Powder Technology,* 117**,** 68-82.

Schaefer, T., Holm, P. & Gjelstrup Kristensen, H. 1992. Melt pelletization in a high shear mixer. I. Effects of process variables and binder. *Acta Pharmaceutica Nordica,* 4**,** 133-140.

Schæfer, T. & Mathiesen, C. 1996. Melt pelletization in a high shear mixer. IX. Effects of binder particle size. *International journal of pharmaceutics,* 139**,** 139-148.

Schæfer, T., Taagegaard, B., Thomsen, L. J. & Gjelstrup Kristensen, H. 1993. Melt pelletization in a high shear mixer. V. Effects of apparatus variables. *European Journal of Pharmaceutical Sciences,* 1**,** 133-141.

Schulze, D. 2005a. Flow properties testing with ring shear testers RST-01.01, RST-01. pc and RST-XS. *Schwedes+ Schulze Schüttguttechnik GmbH, Braunschweig*.

Schulze, D. 2005b. Ring Shear Tester RST-XS Operating Instructions.

Schulze, D. 2005c. RSV 95 Software for the evaluation of shear test data for Ring Shear Testers RST-01.01, RST-01.pc and RST-XS.

Schulze, D. 2006. Flow properties of powders and bulk solids. *Braunschweig/Wolfenbu ttel, Germany: University of Applied Sciences*.

Schulze, D. 2008. Powders and bulk solids Behaviour, Characterization, Storage and Flow.

Schwedes, J. & Schulze, D. 1990. Measurement of flow properties of bulk solids. *Powder Technology,* 61**,** 59-68.

Sheskey, P., Keary, C., Clark, D. & Balwinski, K. 2007. Scale-Up Trials of Foam Granulation Technology-High Shear. *Pharmaceutical technology,* 31**,** 94.

Shimoska, A., Nousou, I., Shirakawa, Y. & Hidaka, J. 2013. Effect of Particle Shape on Size Segregation of Particles. *CHEMICAL ENGINEERING,* 32.

Sielamowicz, I., Blonski, S. & Kowalewski, T. A. 2005. Optical technique DPIV in measurements of granular material flows, Part 1 of 3—plane hoppers. *Chemical Engineering Science,* 60**,** 589-598.

Sielamowicz, I., Błoñski, S. & Kowalewski, T. A. 2006. Digital particle image velocimetry (DPIV) technique in measurements of granular material flows, Part 2 of 3-converging hoppers. *Chemical Engineering Science,* 61**,** 5307-5317.

Skinner, T. 1862. The Granulation of Medicines. 1. [Accessed 09.05.2014].

Srivastava, S. & Mishra, G. 2010. Fluid bed technology: Overview and parameters for process selection. *International Journal of Pharmaceutical Sciences and Drug Research,* 2**,** 236-246.

Stern, L. A., Kirby, S. H., Circone, S. & Durham, W. B. 2004. Scanning electron microscopy investigations of laboratory-grown gas clathrate hydrates formed from melting ice, and comparison to natural hydrates. *American Mineralogist,* 89**,** 1162-1175.

Sujka, M. & Jamroz, J. 2010. Characteristics of pores in native and hydrolyzed starch granules. *Starch-Stärke,* 62**,** 229-235.

Tabor, D. 2000. The hardness of metals, 1951. Clarendon Press, Oxford.

Tan, H., Salman, A. & Hounslow, M. 2006. Kinetics of fluidised bed melt granulation I: the effect of process variables. *Chemical engineering science,* 61**,** 1585-1601.

Tang, P. & Puri, V. 2007. Segregation quantification of two-component particulate mixtures: Effect of particle size, density, shape, and surface texture. *Particulate Science and Technology,* 25**,** 571-588.

Tardos, G. I., Khan, M. I. & Mort, P. R. 1997. Critical parameters and limiting conditions in binder granulation of fine powders. *Powder Technology,* 94**,** 245-258.

Trivedi, N. R., Rajan, M. G., Johnson, J. R. & Shukla, A. J. 2007. Pharmaceutical approaches to preparing pelletized dosage forms using the extrusion-spheronization process. *Critical Reviews™ in Therapeutic Drug Carrier Systems,* 24.

Ulissi, F., Ippolito, I. & Calvo, A. 2009. PIV Technique applied to granular flows in hoppers. *Journal of Physics: Conference Series,* 166**,** 012004.

Usp. 2010. *USP29–NF24 ,<1174>,POWDER FLOW,Page 3017* [Online]. Available: http://www.pharmacopeia.cn/v29240/usp29nf24s0_c1174.html [Accessed 30 May. 2014]. [Accessed 30.05.2014.

Usp 2012. USP31–NF26 ,<811>, POWDER FINENESS,Page 339.

Walker, G. M., Andrews, G. & Jones, D. 2006. Effect of process parameters on the melt granulation of pharmaceutical powders. *Powder Technology,* 165**,** 161-166.

Wang, C., Hassanpour, A. & Ghadiri, M. 2008. Characterisation of flowability of cohesive powders by testing small quantities of weak compacts. *Particuology,* 6**,** 282-285.

Westerweel, J. 1997. Fundamentals of digital particle image velocimetry. *Measurement Science & Technology,* 8**,** 1379-1392.

Willert, C. E., Wereley, S. T. & Kompenhans, J. 2007. *Particle image velocimetry: a practical guide*, Springer.

Winterton, R. 1970. Van der Waals forces. *Contemporary Physics,* 11**,** 559-574.

Wisniewski, R. 1999. System for freeze granulation. Google Patents.

Zobel, H. F., Young, S. N. & Rocca, L. A. 1988. Starch Gelatinization - an X-Ray-Diffraction Study. *Cereal Chemistry,* 65**,** 443-446.

Appendix A The flowability values

A.1 The (ff_c) values obtained from RST-XS for PEG 5% granules

PEG 5% [µm]	shear force [kPa]	σ_1 [kPa]	σ_c [kPa]	ff_c
45-106	5	9.862	2.756	3.6
	9	16.885	2.801	6
	13	24.085	3.274	7.4
	17	34.503	4.618	7.5
250-355	5	9.618	2.512	3.8
	9	17.002	3.182	5.3
	13	24.359	4.183	5.8
	17	32.013	4.34	7.4
600-700	5	10.007	2.012	5
	9	18.293	3.266	5.6
	13	26.093	4.61	5.7
	17	34.212	4.868	7

A.2 The (ff_c) values obtained from RST-XS for starch 5% granules

Starch 5% [µm]	**shear force** [kPa]	σ_1 [kPa]	σ_c [kPa]	**ff_c**
45-106	5	8.87	1.44	6.2
	9	16.1	1.343	12
	13	23.359	1.459	16
	17	33.816	1.608	21
250-355	5	10.627	0.451	24
	9	19.811	0.686	29
	13	27.755	0.701	40
	17	35.493	0.868	41
600-700	5	12.006	0.627	19.1
	9	22.053	0.869	25
	13	29.044	1.069	27
	17	40.398	1.387	29

A.3 The ff_c values obtained from RST-XS for PEG 15% granules

PEG 15% [µm]	**shear force [kPa]**	**σ**1 [kPa]	**σ**c [kPa]	**ff**c
45-106	5	9.613	2.217	4.3
	9	16.711	2.732	6.1
	13	24.472	3.946	6.2
	17	31.013	3.091	10
250-355	5	9.507	1.995	4.8
	9	16.966	2.635	6.4
	13	23.852	3.43	7
	17	30.832	3.863	8
600-700	5	12.422	2.042	6.1
	9	18.096	2.689	6.7
	13	25.509	3.708	6.9
	17	32.891	4.44	7.4

A.4 The ff_c values obtained from RST-XS for Starch 15% granules.

Starch 15% [µm]	**shear force** [kPa]	**σ**1 [kPa]	**σ**c [kPa]	**ff**c
45-106	5	9.273	0.977	9.5
	9	17.269	1.254	13.8
	13	24.197	1.373	17.6
	17	31.847	1.396	23
250-355	5	12.348	0.578	21
	9	22.367	0.844	27
	13	30.663	0.806	38
	17	38.315	0.99	39
600-700	5	12.217	0.568	22
	9	21.713	0.811	27
	13	32.705	1.212	27
	17	44.67	1.289	35

A.5 The ff_c values obtained from RST-XS for PEG 25% granules.

PEG 25% [μm]	**shear force** [kPa]	σ_1 [kPa]	σ_C [kPa]	**ffc**
45-106	5	9.335	2.243	4.2
	9	16.125	2.716	5.9
	13	23.688	3.704	6.4
	17	30.629	3.738	8.2
250-355	5	10.835	1.742	6.2
	9	16.821	1.882	8.9
	13	24.39	2.575	9.5
	17	31.508	3.017	10.4
600-700	5	11.201	1.701	6.6
	9	18.674	2.488	7.5
	13	27.518	3.293	8.4
	17	36.85	4.323	8.5

A.6 The ff_c values obtained from RST-XS for Starch 25% granules

Starch 25% [μm]	**shear force** [kPa]	σ_1 [kPa]	σ_c [kPa]	**ff**$_c$
45-106	5	9.532	0.988	9.6
	9	17.127	1.06	16.1
	13	24.857	1.268	19.6
	17	32.476	1.428	23
250-355	5	12.38	0.743	25
	9	21.095	0.815	26
	13	29.462	1.099	27
	17	37.523	1.187	32
600-700	5	12.742	0.367	35
	9	22.002	0.465	47
	13	30.67	0.607	51
	17	39.854	0.759	53

Appendix B (SEM Images)

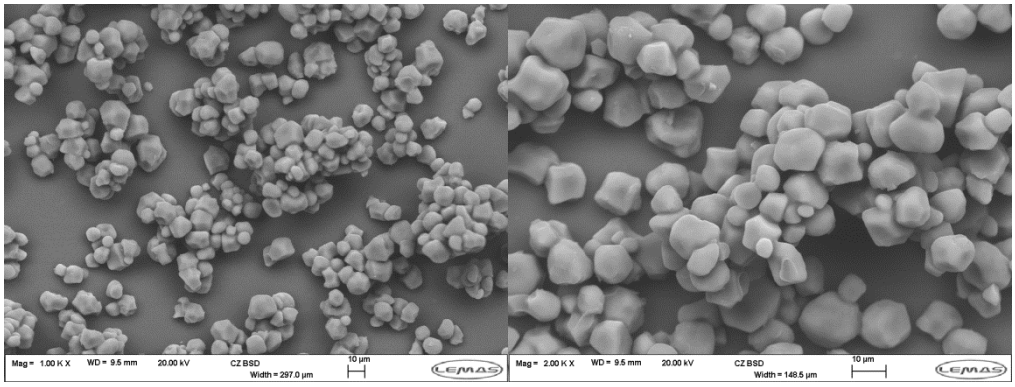

B.1 SEM images of PEG 6000 (5%) granules repared by melt granulation technique at 10 µm.

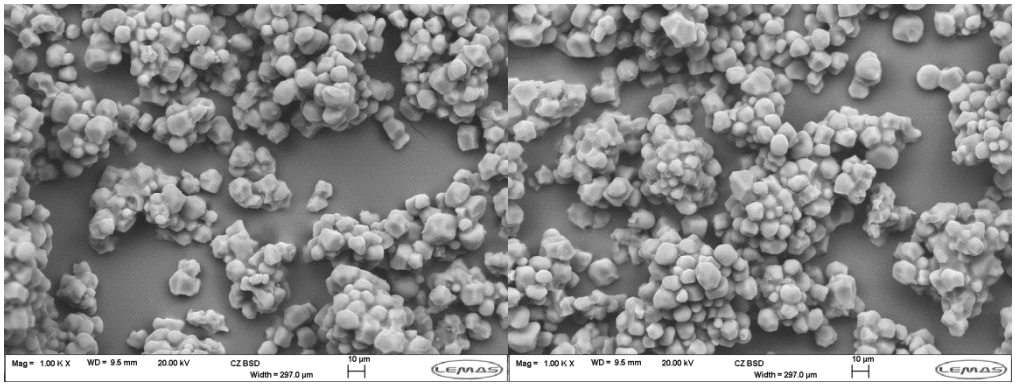

B.2 SEM images of PEG 6000 (15%) granules repared by melt granulation technique at 10 µm**.**

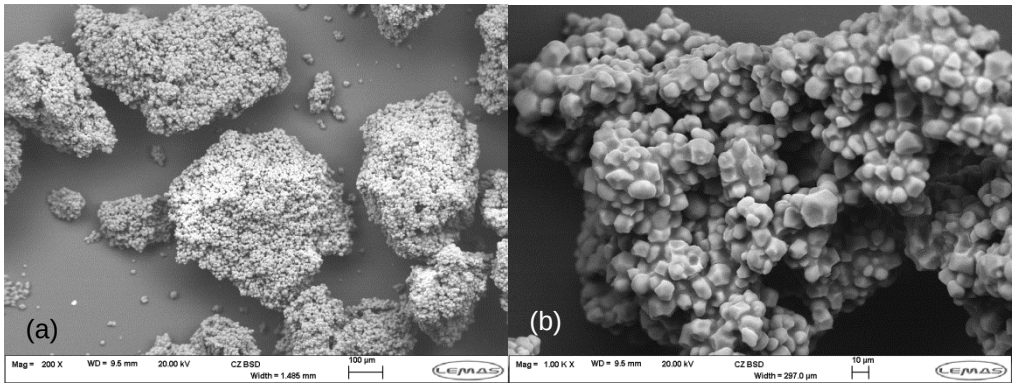

B.3 SEM images of PEG 6000 (25%) granules repared by melt granulation technique at 100 µm (a) and 10 µm (b).

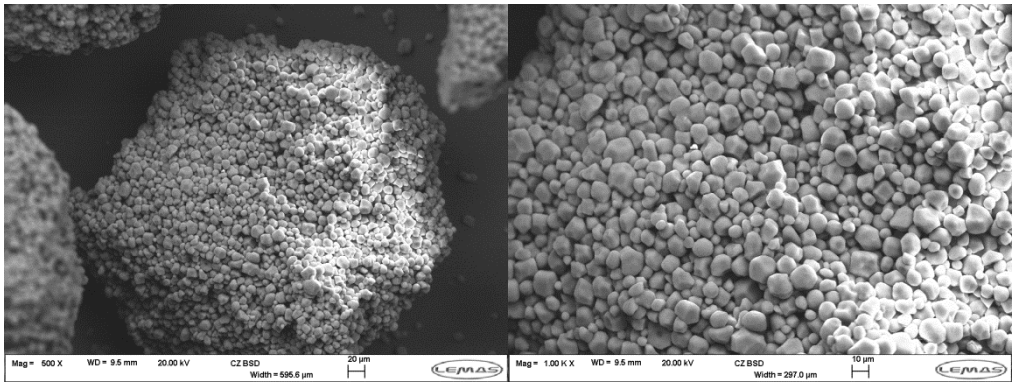

B.4 SEM images of granules prepared by wet granulation using starch paste (5%) 20 µm and 10 µm

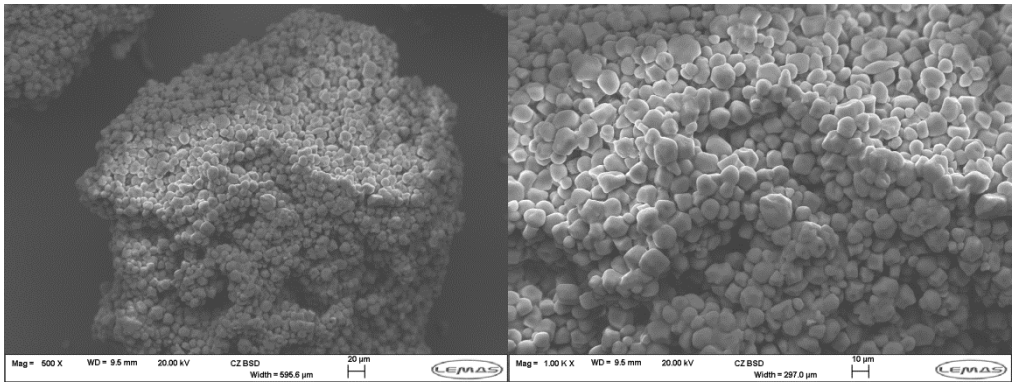

B.5 SEM images of granules prepared by wet granulation using starch paste (15%) 20 µm and 10 µm.

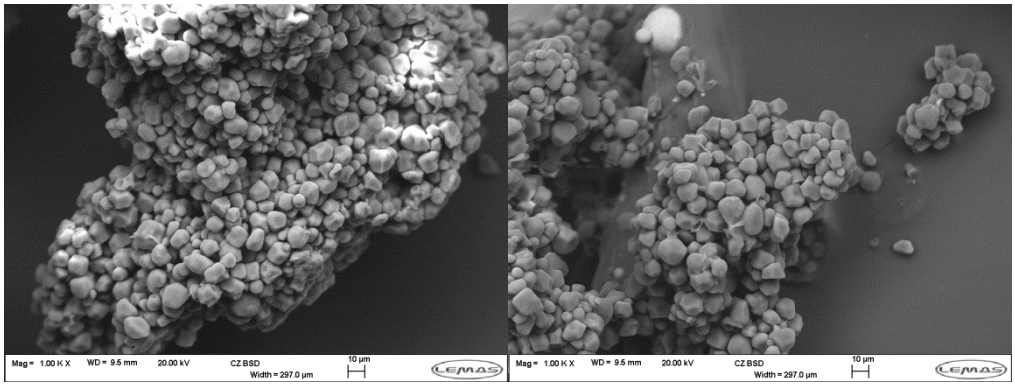

B.6 SEM images of granules prepared by wet granulation using starch paste (25%) 10 µm